

The University of Nottingham

UNITED KINGDOM · CHINA · MALAYSIA

MOLECULAR MECHANISMS OF MODERN AND ANCIENT PAGET'S DISEASE

Ana Navarro Martinez, MRes student

School of Life Sciences, University of Nottingham

Acknowledgements

I would like to express my deepest gratitude and appreciation to all the people who helped me through my MRes. A year very important for my life not only from a professional point of view, if not also personal.

Firstly, I would not have been able to complete my project without the insight, incredible and constant support of my supervisor, Prof. Robert Layfield, who showed confidence in me from the beginning. Thanks for his constant generosity and forgiveness. I hope I would be able to show my sincere gratitude. His ambition made me to give the best of me every day. His ideas and suggestions to the project made my work very interesting and challenged my way of thinking. I am so grateful for everything that I have learnt during this year, regardless of the difficulties and occasional setbacks of the work. Dr. Ian Kerr, thanks for his kindness and his continuous interest in the outgoing of the project.

Special thanks go to those who provided practical and technical support through the project, especially to Barry Shaw at the start of the project as well as to Daniel Scott, who have not stopped answering my questions, thanks for their patience. And Christopher Gell, thanks for his technical support on Delta-Vision imaging, advice, and tips.

I also express my gratitude to the Paget's Association, without their financial support I would not have been able to do this project, and especially the Michael Davie Research Foundation for their funding and support.

Finally, my gratitude and thanks go to my family, including my parents and my brother, for their tolerance, patience, financial support, and endless phone calls, it helped a lot. My aunt Luisa for her professional, and emotional support as well as for letting me to stay in her house during this year, and my partner, for his tolerance, patience, each skype and visit, he has been crucial for me.

Contents 2-4

Acknowledgements 1
Abstract 5

CHAPTER 1: Introduction 6-37

1.1. Introduction 6-7
1.2. Bone 7-12
1.2.1. Bone structure and cell types (osteoclasts and osteoblasts) 7-9
1.2.2. Bone remodelling 9
1.2.3. Bone in PDB 10
1.2.4. Signalling pathways in bone 10-12
1.2.4.1. Signalling in osteoclasts 11-12
1.3. Autophagy 12-16
1.3.1. Functions of autophagy 13-14
1.3.2. The process of autophagy 14-16
1.3.3. Regulation of autophagy 16
1.4. Paget's disease of bone 17-23
1.4.1. Definition 17
1.4.2. Origin 18-19
1.4.3. Geographic distribution 19
1.4.4. Symptoms 19-20
1.4.5. Diagnosis 20
1.4.6. Causes 21-23
1.4.6.1. Genetic factors 21-22
1.4.6.2. Environmental factors 22
1.4.6.3. Viruses and PDB 22-23
1.4.7. Treatment of PDB 23
1.5. The SQSTM1/p62 protein 23-35
1.5.1. Structure of the SQSTM1/p62 protein 24-29
1.5.1.1. PB1 Domain 25-26
1.5.1.2. ZZ finger 26
1.5.1.3. TF6-Binding Motif 26
1.5.1.4. PEST Sequences 26-27
1.5.1.5. LIR region 27
1.5.1.6. KIR region 27
1.5.1.7. UBA domain 28-28
1.5.1.7.1. Ubiquitin-mediated procesess 28-29
1.5.2. Biological functions of the SQSTM1/p62 protein 29-34
1.5.2.1. Functional Significance of the SQSTM1/p62 UBA Domain 30-33
1.5.2.1.1. SQSTM1/p62's role in RANKL-NF-κβ signalling in osteoclasts 30-32
1.5.2.1.2. SQSTM1/p62's role in autophagy in osteoclasts 32-34
1.5.3. SQSTM1/p62 and PDB: consequences of different disease-associated Mutations 34-35
1.6. Aims and objectives 36-37

CHAPTER 2: Methods 38-51

2.1. DNA techniques 38-40
2.1.1. Plasmids 38
2.1.2. Plasmid DNA preparation 38-39
2.1.3 Measurement of DNA concentration and purity 39
2.1.3 Storage of plasmid DNA 40
2.1.4 DNA Sequencing 40
2.2. Mammalian cell culture methods 40-42
2.2.1. Cell handling 40
2.2.2. Passaging cells 40
2.2.3. Thawing cells 40
2.2.4. Counting cells with a haemocytometer 40-41
2.2.5. Seeding cells 41
2.2.6. Transient transfection/co-transfection based on non-lipid based transfection reagent 41-42
2.2.7. Treatment of cells with H_2O_2 42
2.2.8. Scraping cells 42
2.3. Standard immunofluorescence method for DeltaVision microscopy 42-43
2.3.1. DeltaVision microscopy 43
2.4. Protein extractions from bone 43-44
2.4.1. Extraction A 43
2.4.2. Extraction B 44
2.4.3. TCA precipitation 44
2.4.4. Collagenase digestion 44
2.5. Western blotting and immunodetection techniques 45-47
2.5.1. Sodium dodecyl sulphate polyacrylamide-gel electrophoresis (SDS PAGE) 45-46
2.5.2. Coomassie blue staining of SDS PAGE gels 46
2.5.3. Silver staining of SDS PAGE gels 46
2.5.4. Western blotting 46
2.5.5. Ponceau S staining of nitrocellulose membranes 47
2.5.6. Immunodetection 47
2.5.7. Stripping membranes 47
2.6. General laboratory methods 47-51
2.6.1. Preparation of chemically competent bacterial cells 47-48
2.6.2. Oligonucleotide mutagenic primer preparation 48
2.6.3. Site-directed mutagenesis 48-49
2.6.4. Transformation of Plasmid DNA to XL10-Gold® competent cells 50
2.6.5. Protein expression 50
2.6.6. Bacterial storage 50
2.6.7. Measurement of protein concentration using the BCA assay 50-51
2.6.8. Preparation of Control/Glutathione/Ubiquitin/LC3B-Sepharose 51
2.6.9. Control/Glutathione/Ubiquitin/LC3B-Sepharose binding assay 51

CHAPTER 3: Disease mechanisms in 'modern' Paget's disease 52-71

3.1. Introduction 52-53
3.2. Results 53-68
3.2.1. Impact of F406V mutation on ubiquitin- and LC3B-binding properties of SQSTM1/p62 53-56
3.2.1.1. Generation of prokaryotic expression constructs for F406V mutant SQSTM1/p62 53-54

3.2.1.2. Effects of F406V mutation on ubiquitin- and LC3B-binding of SQSTM1/p62 54-56
3.2.2. Impact of PDB-associated SQSTM1/p62 mutations on cellular autophagy phenotypes 56-68
3.2.2.1. Generation of eukaryotic expression constructs for PDB mutant SQSTM1/p62 proteins 57
3.2.2.2. Cellular phenotypes of transfected His-FLAG-SQSTM1/p62 and F406V mutant in HEK293T cells 57-61
3.2.2.3. Optimisation of His-FLAG-tagged SQSTM1/p62 transfections for LC3B lipidation assays in HEK293T cells 62-63
3.2.2.4. Effects of expression of PDB-associated mutant SQSTM1/p62 on autophagy markers under conditions of oxidative stress in HEK293T cells 63-65
3.2.2.5. Effects of co-expression of PDB-associated mutant SQSTM1/p62 with TBK1 on autophagy markers in HEK293T cells 65-68
3.3. Discussion 68-71

CHAPTER 4: Disease mechanisms in 'ancient' Paget's disease 72-94

4.1. Introduction 72
4.2. Work leading up to the project 72-76
4.2.1. LC-MS/MS-based sequencing of ancient proteins from petrous bone 72-74
4.2.2. Identification of ancient SQSTM1/p62 protein in petrous bone sample by western blotting 75-76
4.3. Analyses of additional petrous bone samples from the Norton collection 76-81
4.3.1. SDS PAGE and silver stain analysis of ancient petrous bone extracts 77
4.3.2. Western blotting analysis of ancient petrous bone extracts 78
4.3.3. Epitope mapping of the rabbit SQSTM1/p62 antibody 79-81
4.4. Analyses of tooth samples from the Norton collection 82-89
4.4.1. Analysis of tooth SK29 sample 82-84
4.4.1.1. SDS PAGE and silver stain analysis of ancient SK29 tooth extract 82-83
4.4.1.2. Western blotting analysis of ancient SK29 tooth extract 83-84
4.4.2. Analysis of tooth SK22 and SK35 samples 84-87
4.4.2.1. SDS PAGE and silver stain analysis of ancient tooth extracts 85-86
4.4.2.2. Western blotting analysis of ancient tooth extracts with collagenase treatment 86-87
4.4.3. LC-MS/MS-based sequencing of ancient proteins from tooth SK22 and SK29 samples 87-89
4.4.3.1. Preparation of the samples for LC-MS/MS 87-88
4.4.3.2. LC-MS/MS analysis of ancient SK22 and SK29 tooth 'pellet' fractions 89
4.5. Investigating the abnormal migration of ancient SQSTM1/p62 on western blot 90-91
4.6 Discussion 91-94

CHAPTER 5: Final summary 95

5.1. Final summary 95

References 96-105
Appendix 106-115

Abstract

The project included two interrelated elements relevant to disease mechanisms in modern and ancient Paget's disease of bone (PDB), a chronic bone disorder characterised by focal regions of increased osteoclast-mediated bone resorption accompanied by increased osteoblast-mediated formation of new, highly disorganised bone. Numerous different mutations (>30) affecting the *SQSTM1* gene have been identified in patients with PDB, to date several of which have been studied at the level of protein function. The UBA domain of SQSTM1/p62 is involved in the ubiquitin-binding ability of the protein, important for its roles in the regulation of osteoclast RANK-NF-κβ signalling and cargo recognition for autophagy. Regarding studies of 'modern' PDB, we found that a newly identified and uncharacterised PDB-associated UBA domain missense mutation of SQSTM1/p62, F406V, was associated with loss of ubiquitin-binding but normal LC3B-binding function *in vitro*. We went on to assess the effects of over-expression of different PDB-associated mutants of SQSTM1/p62 (including F406V) on autophagy markers (LC3B-I and LC3B-II) in HEK293T cells under different conditions. Results suggested that the crude transient transfection-based assays may be insensitive to determine any differences in autophagy that may be imparted by PDB-associated mutations of SQSTM1/p62. Regarding studies of 'ancient' PDB, we extended an ongoing project in the lab with the aim of unlocking the 'chemical memory' of ancient bones from the Norton Priory collection of medieval skeletons and specifically use a combination of molecular approaches to investigate if the individuals were affected by an ancient form of PDB. Our western blotting studies indicated that 1/2 petrous and 1/3 tooth samples tested from skeletons with PDB-like changes were positive for ancient SQSTM1/p62. Previous LC-MS/MS analyses combined with epitope mapping of the mouse antibody supported the notion that the positive samples may contain E396X mutant SQSTM1-p62 protein, known to be associated with familial PDB in modern cases. The results of this study provide, for the first time, a reliable diagnosis of PDB in ancient times, which gives new impetus to further studies in the field of the comparative evolution and the history of bone disease from ancient and to modern times.

CHAPTER 1. INTRODUCTION

1.1. Introduction

Paget's disease of bone (PDB) is a chronic bone disorder characterised by focal regions of increased osteoclast-mediated bone resorption accompanied by increased osteoblast-mediated formation of new, highly disorganised bone. After osteoporosis, it is the second most common bone disease in western populations currently affecting around 1-2% of adults over the age of 55, it is rare before the age of 40 and is more common in men than in women. If untreated, PDB can lead to bone deformity, pain, and other complications (Rea et al. 2013; Vallet and Ralston 2016).

Although its aetiology is still unclear, a combination of genetic and environmental factors seems to be the main cause of PDB. A significant decrease in the prevalence of PDB in the last two decades strongly supports the existence of an environmental component to the pathogenesis of PDB. Some studies implicate viral infections such as canine distemper and paramyxovirus as a possible cause of PDB, however these observations have not always been replicated, and viruses have not been isolated from affected tissue (Gkouva et al. 2011). Between 15 and 40% of patients have at least one affected first-degree relative indicating familial clustering, where the disease is inherited in an autosomal dominant fashion, although the penetrance is highly variable (Hiruma et al. 2008).

Mutations in four different genes have been associated with PDB or PDB-like disorders, but only mutations in the *SQSTM1* gene are associated with classical PDB. As many as 40% of familial PDB cases, and 10% of sporadic PDB cases, carry a *SQSTM1* mutation. The *SQSTM1* gene is ubiquitously expressed and encodes a protein which migrates on SDS PAGE at ~62 kDa (SQSTM1/p62). It functions in several signal transduction pathways that are activated by cytokines such as receptor activator of NF-κβ ligand (RANKL), tumour necrosis factor α (TNF-α) and interleukin-1 (IL-1), that promote osteoclast formation at least in part through NF-κβ activation. Most of the identified mutations in SQSTM1/p62 are localised in the ubiquitin-associated (UBA) domain within the carboxyl-terminal region of the protein, with P392L being the most common mutation, and appear to impact on osteoclast NF-κβ signalling. Moreover, a dysregulation of the process of autophagy (representing one focus of this thesis) where SQSTM1/p62 acts as a receptor for ubiquitin-mediated autophagy (see section 1.5.2.1.2.) might also be part of the pathogenesis of PDB, supported by the similar features between inclusion bodies found in PDB osteoclasts and the SQSTM1/p62-positive aggregates observed in other diseases involving defective autophagy (McManus et al. 2016).

The increased bone remodelling found in non-involved bone from patients with familial PDB might be explained by the increased osteoclastogenic microenvironment caused by expression of SQSTM1/p62 mutant proteins in stromal cells. However, what leads to the development of the highly-localised lesions found in PDB patients in the marrow microenvironment is still unclear. *SQSTM1* mutations are clearly a predisposing factor but sometimes these are not sufficient to induce PDB (i.e. there is incomplete penetrance); additional factors, genetic or environmental, might also be required. There are several other loci in addition to 5q35 (where the *SQSTM1* gene is located) that have been reported to be linked to familial PDB, such as the locus at 10p13 which appears to account for the majority of PDB in families of British descent who do not carry *SQSTM1* mutations. The differences in penetrance and disease severity could be explained by mutations or polymorphisms in more than one gene (Hiruma et al. 2008).

Osteoclasts are the cells principally affected in PDB; the pagetic phenotype is characterised by increased numbers of osteoclasts of increased size, being hyper-multinucleated and having an increased bone-resorbing capacity. Although osteoblasts and other cells in the bone microenvironment also participate in the disease, it is thought that the increased bone formation also shown in PDB is a secondary response of osteoblasts to the elevated bone resorption. Despite this, both abnormal resorption and formation of bone is responsible of the changes that result in PDB (Hiruma et al. 2008).

1.2. Bone

1.2.1. Bone structure and cell types (osteoclasts and osteoblasts)

Bone is a specialised tissue with several functions. Firstly, it serves as a mechanical support, secondly it protects other softer organs such as the brain, and finally it acts as a reservoir for mineral such as calcium. Bone marrow is responsible for generating red blood cells, certain white blood cells and blood platelets (Essentials of Rubin's Pathology 5th Edition).

The main component of bone is an extracellular matrix, which involves a non-mineral matrix of collagen (type I) protein and glycosaminoglycans (osteoid) that is the organic part of bone tissue, inorganic mineral salts deposited within the matrix, and a variety of cell types (Figure 1) among which are osteoprogenitor cells, resorbing cells (osteoclasts), bone-forming cells (osteoblasts) and support cells (osteocytes) (Essentials of Rubin's Pathology 5th Edition).

Osteoprogenitor cells are precursors of osteoblasts; these are essentially derived from the mesenchymal lineage and are responsible for synthesising and secreting osteoid collagen and other organic components to bone matrix which later mineralise through deposition of calcium and phosphate hydroxides (hydroxyapatite) by osteoblasts. When there is need for osteoid

deposition osteoblasts are active, whereas they are lying on the bone surface (bone lining cells) when they are inactive (Essentials of Rubin's Pathology 5th Edition). On the other hand, osteocytes are terminally differentiated, long-lived cells derived from synthesising osteoblasts which have been embedded in mineralised bone matrix. During this transition, a distinctive change in shape accompanied by an important reduction in cellular organelle content and size takes place in osteoblasts to become osteocytes (Hocking et al. 2012). Osteocytes have a primary role mechanotransduction. They convert mechanical forces on the bone into biological signals which lead to activation of the remodelling process (Shapiro et al. 2014).

In contrast, osteoclasts are bone cells which derive from hematopoietic (monocyte-macrophage lineage) stem cells under stimulation of macrophage colony stimulating factor (M-CSF; encoded by *CSF1*) as well as RANKL (*TNFSF11*) (Hocking et al. 2012). These cells have multiple nuclei (typically between three or five) and are highly mobile which allow them to remove the mineralised matrix of bone through a process known as bone resorption (Moscat et al. 2007). Osteoclasts undergo apoptosis at the end of the bone resorption process (Hughes et al. 1996). Moreover, osteoclasts are also characterised by the presence of extended Golgi complexes around each nucleus, as well as containing large number of mitochondria, transport vesicles, and lysosomes (Mundy 1999). Osteoclasts present a folded plasma membrane at a location facing the bone matrix called the ruffled border where the secretion of digestive enzymes and hydrogen ions occurs to dissolve bone matrix. The cavity where bone resorption takes place is known as lacunae. It consists of the area between the ruffled border of the osteoclasts and bone matrix. After resorption, the by-products of bone degradation are endocytosed transversely to the ruffled border and transcytosed to the apical membrane (Hocking et al. 2012).

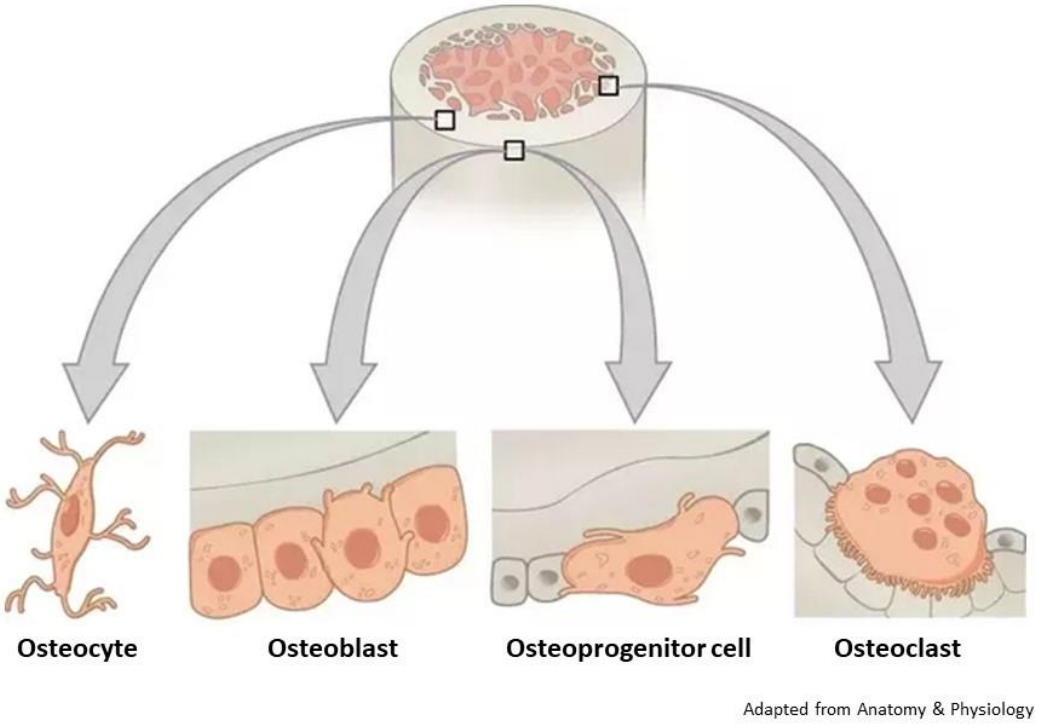


Figure 1. Localisation and morphology of the different bone cell types (Figure explained in the main text)**.**

1.2.2. Bone remodelling

The renovation and replacement of the bone under normal circumstances occurs through the process known as bone remodelling where firstly osteoclasts carry out the resorption of the bone, and then osteoblasts carry out bone formation. During this second step, some osteoblast become trapped in the bone matrix and differentiate into osteocytes which act as mechanosensors and seem to play an important role in regulating osteoblast and osteoclast activity, by producing RANKL and sclerostin (Vallet and Ralston 2016). Bone remodelling is maintained at a homeostatic state in healthy bone, however, when the balance between these two processes is disturbed, and there is a predominance of one of the processes, different bone disorders can occur such as in PDB, where the rate of osteoclastogenesis increases focally at one or more sites leading to a disorganised secondary increase in osteoblast formation (Shapiro et al. 2014) or in Osteopetrosis, where the impaired activity of osteoclast results in too much bone and the persistence of mineralized cartilage (Helfrich et al. 2008).

1.2.3. Bone in PDB

Macrostructurally, the secondary increase in osteoblast activity in PDB has as a consequence the formation of denser bones, which are weaker than normal bone, and more susceptible to fractures and mechanical deformities (Shapiro et al. 2014).

Further, the bone in PDB shows a highly abnormal microstructure where osteoclasts are increased in number, size, and nuclearity and the rate of osteoclast bone resorption is higher than in normal bone. Furthermore, a typical feature of pagetic osteoclasts is the presence of nuclear (and sometimes cytoplasmic) inclusions which were initially thought to be paramyxovirus-derived because of their similarity with paramyxovirus nucleocapsids. However, this idea has changed more recently, for example McManus et al. 2016 suggests that defects in the autophagy pathway (see 1.3.) may lead to formation of aggregates of undegraded proteins which could be related to these structures, as is the case in Huntington's disease (a neurological disorder) where proteinaceous nuclear inclusions can be observed (Taylor et al. 2002). Finally, pagetic osteoclasts are also characterised by a higher hypersensitivity to agents that further promote osteoclast differentiation and bone resorption such as $1,25(OH)_2D_3$, RANKL, and TNF-α (Vallet and Ralston 2016).

By contrast, pagetic osteoblasts show similar morphology to normal osteoblasts, supporting the idea that the condition is principally a disease that affects to osteoclasts. However, an increased expression of IL-1, interleukin-6 (IL-6), Dickkopf 1 (Dkk1) and alkaline phosphatase (ALP) was observed from osteoblasts cultured form pagetic bone lesion (Naot et al. 2007) indicating the possibility of an inherent defect in this cell type. The role of osteoblasts in PDB has not been investigated extensively and more research is needed to draw definitive conclusions about their contributions (Layfield et al. 2006).

1.2.4. Signalling pathways in bone

Bones are an ancient rather than a relatively new skeletal structure in the history of vertebrates. Bone mass, structure, and function is strongly regulated through the activated and joined processes of bone resorption and bone formation, so the maintenance of skeletal homeostasis depends on the coordinated action of osteoclasts, osteoblasts, and osteocytes. Several disorders including PDB are caused by an imbalance between bone formation and resorption. Hormones such as estrogen, PTH (parathyroid hormone) and PTHLH (parathyroid hormone-like hormone) or vitamin D metabolites are the first regulators of these processes (Hocking et al. 2012; Shapiro et al. 2014). The autophagy pathway has also been demonstrated to be crucial in bone homeostasis; osteoclast, osteoblast, as well as osteocyte function is

mediated by proteins which are involved in autophagic protein degradation (Hocking et al. 2012).

1.2.4.1. Signalling in osteoclasts

Osteoclastogenesis is a complicated process which is regulated negatively and positively by at least 24 genes in humans (Boyle et al. 2003). Each step of osteoclastogenesis is regulated by some of these genes with several signalling pathways and transcription factors involved in each step of osteoclastogenesis.

The most important regulator of osteoclastogenesis is the pathway known as the RANKL/RANK/osteoprotegerin (OPG) signalling axis (Figure 2). The amount of bone resorption depends on the balance between RANKL and OPG; as RANKL increases bone resorption increases and if OPG increases bone resorption decreases. RANKL is a cytokine expressed by preosteoblastic cells and interacts with the RANK receptor on the surface of osteoclasts. RANKL is the key cytokine required for differentiation, activation, and survival of osteoclastic cells (Khosla 2001). The role of RANKL on osteoclast differentiation is mediated *via* downstream effector molecules that lead to expression of osteoclast specific genes. Further, RANKL also enhances osteoclast survival and is involved in new cycles of bone degradation. RANKL promotes osteoclastogenesis by stimulation of MAPK pathways, the serine/threonine kinase Akt, and activation of transcription factors such as NF-κβ, activator protein 1 (AP-1), C-Fos/Fra-1 or c-Jun, and nuclear factor of activated T cells (NFAT). The activation of these transcription factors which depends on TNF receptor-associated factor (TRAF6), an adaptor protein in cytokine-induced signalling in osteoclasts, is crucial for osteoclast formation (Rea et al. 2013). The activity of TRAF6 is regulated by SQSTM1/p62 and specifically mediated by its ubiquitin-binding UBA domain (explained in detail in section 1.4.2.1.1.). OPG is a soluble decoy receptor also expressed by osteoblasts which prevents RANKL from interacting with RANK, thereby negatively regulating RANKL-NF-κβ signalling (Boyle et al. 2003).

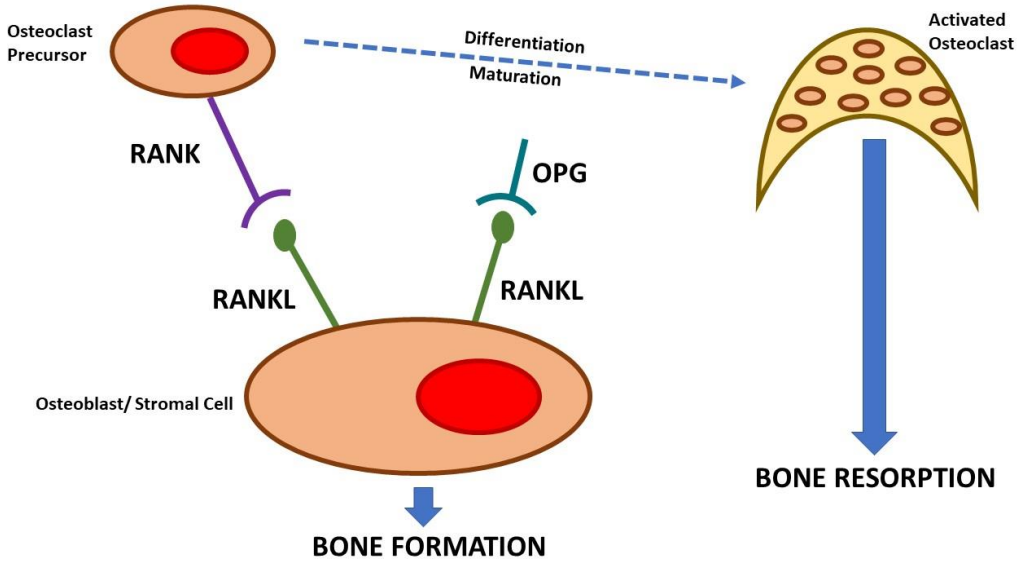


Figure 2. Schematic representation of the RANKL/RANK/OPG axis.

RANK is encoded by tumour necrosis factor receptor superfamily, member 11a (*TNFRSF11A*), its ligand RANKL is encoded by *TNFSF11*, and the decoy receptor OPG is encoded by *TNFRSF11B*. To generate activated osteoclasts, RANKL is secreted by osteoblasts and osteocytes in bone, and these bind to its natural receptor, RANK, on the surface of pre-fusion osteoclasts. To fine-balance this activation system, osteoblasts and osteocytes also secrete OPG, which is a natural decoy receptor for RANKL and prevents binding of RANKL to RANK.

In addition to the RANKL/RANK/OPG signalling axis, autophagy has also been demonstrated to play a crucial role in the regulation of osteoclasts precursor cell polarity as well as in consequent osteoclast formation and activation (Srinivas et al. 2009). Upregulation of autophagy under conditions of oxidative stress is also associated with osteoclast precursor cell differentiation. Autophagy also plays a crucial role in ruffled border formation and secretion of degradative enzymes during osteoclast activity where autophagy proteins have been demonstrated to regulate the secretory component of osteoclastic bone resorption (DeSelm et al. 2011). This leads to thinking that the modulation of autophagy in osteoclasts (and therefore osteoclast activity) could be a potential therapeutic target in PDB since several therapeutic agents have been known to influence the autophagic response and the activities of autophagy regulating pathways, so there is the real possibility that these agents could be used clinically to treat PDB (Hocking et al. 2012).

1.3. Autophagy

Autophagy represents an evolutionarily conserved and dynamic protein degradation pathway which acts in concert with the ubiquitin-proteasome system (UPS) with the aim of maintaining cellular homeostasis. The degradation system in autophagy is lysosome-dependent and has

the ability of targeting individual proteins, larger macromolecular complexes, and complete organelles for degradation (Kirkin et al. 2009; Hocking et al. 2012).

The generic term 'autophagy' includes various processes through which different cytosolic cargos are acquired by the lysosome:

- Macroautophagy: characterised by the formation of a crescent-shaped structure, called the phagophore, which expands to form the double-membrane autophagosome which can fusion with the lysosome.
- Microautophagy: here the cytosolic components are invaginated and sequestered directly by lysosomes.
- Chaperone-mediated autophagy: in this case involves the translocation of unfolded proteins across the lysosomal membrane.

Through genetic screening, 32 different autophagy-related genes (Atg) have been identified in yeast. Many of these genes are conserved in slime mould, plants, worm, flies, as well as mammals which demonstrates that autophagy has been an important process across phylogeny. Although the importance of autophagy is well recognised in mammalian systems, many of the mechanistic breakthroughs in delineating how autophagy is regulated and executed at the molecular level have been made in yeast (*Saccharomyces cerevisiae*) (Glick et al. 2010).

1.3.1. Functions of autophagy

Macroautophagy (henceforth referred as autophagy) acts mainly as a survival mechanism to enhance cell longevity under conditions of cell stress. In all cell types autophagy occurs at basal levels, however it can also be stimulated under different conditions of cell stress such as nutrient deprivation, hypoxia, or infection. The basal steady-state level of autophagy depends on the cell type and tissue. The main role of autophagy in bone, under basal conditions, is removal of damaged organelles and misfolded proteins. This role of autophagy is referred to as 'quality control autophagy' and it is fundamental for terminally-differentiated bone cells and especially for longer-lived bone cells such as osteocytes because the accumulation of damaged organelles and misfolded proteins can lead to several cellular malfunctions. Autophagy degradative activity increases under stressful conditions to prolong cell survival. In this case, it acts as a recycling mechanism which permits cells to re-use intracellular components, including amino acids. The fact that bone cells can survive under stressful conditions such as nutrient starvation or hypoxic environmental because of autophagy, is fundamental (Mizushima 2007).

Autophagy also provides, through autophagosomes, a spatial localisation of signalling complexes which is important for protein synthesis in cells where the secretory capacity is high to enhance rapid synthesis of secreted proteins. Thus, this spatial localisation can also mediate signal pathway activation by autophagic degradation of signalling pathway components. This spatial localisation is important to regulate the anabolic and catabolic function of osteoclasts and osteoclasts (Komatsu and Ichimura 2010; Hocking et al. 2012).

1.3.2. The process of autophagy

The process of autophagy (Figure 3) can be divided into five key stages: (1) phagophore formation or nucleation; (2) Atg5-Atg12 conjugation, interaction with Atg16L and multimerisation at the phagophore; (3) LC3 processing and insertion into the extending phagophore membrane; (4) capture of random or selective targets for degradation; (5) fusion of the autophagosome with the lysosome (or vacuole), followed by proteolytic degradation through lysosomal proteases of engulfed molecules.

Autophagy starts with the formation and subsequent elongation of the phagophore or isolation membrane which enwraps cytoplasmic components until its edges fuse with each other to form a double-membrane structure termed the autophagosome. An enzymatic cascade consisting of Atg7, Atg3 and Atg5-Atg12 enhances the covalent conjugation of the ubiquitin-like modifier, LC3, with phosphatidylethanolamine (PE). The PE-conjugated LC3, termed LC3-II, is localised to the inner and outer membranes of the isolation membrane (Glick et al. 2010). After autophagosome formation, the fusion between the outer membrane of the autophagosome and the lysosome takes place leading to the degradation by the lysosomal hydrolases of the sequestered cytoplasmic components together with the inner membrane of the autophagosomes where LC3-II plays a crucial role (Komatsu and Ichimura 2010; Nguyen et al. 2016; Tsuboyama et al. 2016). Finally, the LC3-II on the outer membrane is cleaved off by the cysteine protease Atg48 and recycled (Glick et al. 2010).

Autophagosomes have the ability of sequestering cytosolic material in a non-selective manner. However, in some circumstances, selective autophagic degradation takes place. In this case, various cargo such as protein aggregates, mitochondria, and microbes are degraded. Ubiquitin is involved in this process, ubiquitinated targets are delivered to the autophagosome through ubiquitin-binding autophagy receptors (Kirkin et al. 2009). The best characterised autophagy receptor is SQSTM1/p62, a polymeric, modular protein which plays crucial roles in autophagy interacting with LC3 through its conserved LC3-binding region (LIR) and with ubiquitinated-aggregated proteins and organelles through its also conserved UBA domain (explained in detail

in section 1.5.2.1.2.) (Hocking et al. 2012). As noted previously SQSTM1/p62 also functions in other cellular pathways such as RANK-NF-κβ signalling which may be both parallel and intersecting with autophagy (Ciuffa et al. 2015).

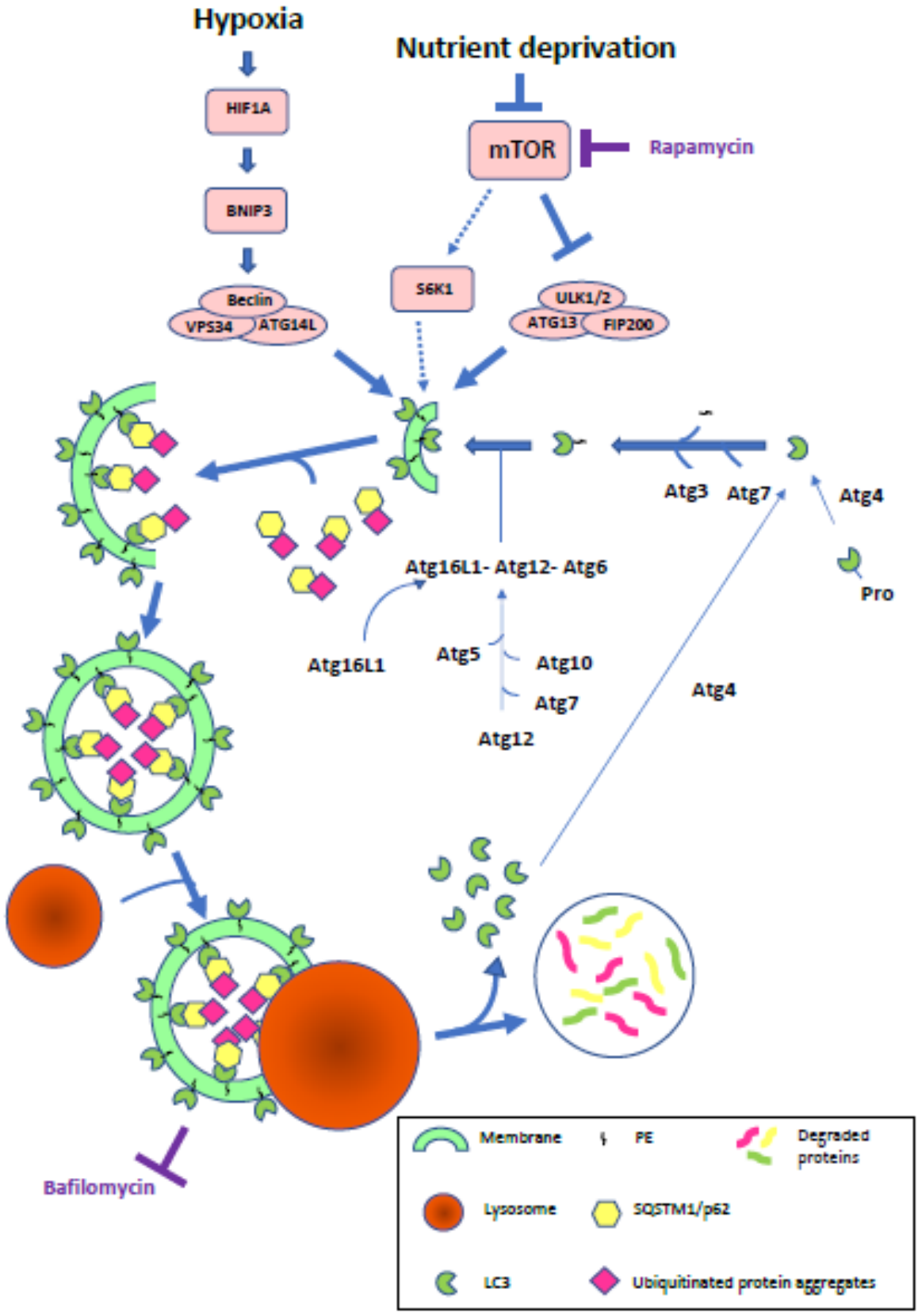


Figure 3. Autophagy

Macroautophagy, often referred to as autophagy, is a catabolic process that results in the autophagosomal-lysosomal degradation of bulk cytoplasmic contents, abnormal protein aggregates, and excess or damaged organelles. Autophagy is generally activated by conditions of nutrient deprivation but has also been associated with physiological as well as pathological processes such as development, differentiation, neurodegenerative diseases, stress, infection, and cancer. The kinase mTOR is a critical regulator of autophagy induction, with activated mTOR (Akt and MAPK signalling) suppressing autophagy, and negative regulation of mTOR (AMPK and p53 signalling) promoting it. Three related serine/threonine kinases, UNC-51-like kinase -1, -2, and -3 (ULK1, ULK2, UKL3), which play a similar role as the yeast Atg1, act downstream of the mTOR complex. ULK1 and ULK2 form a large complex with the mammalian homolog of an autophagy-related (Atg) gene product (mAtg13) and the scaffold protein FIP200 (an ortholog of yeast Atg17). Class III PI3K complex, containing hVps34, Beclin-1 (a mammalian homolog of yeast Atg6), p150 (a mammalian homolog of yeast Vps15), and Atg14-like protein (Atg14L or Barkor) or ultraviolet irradiation resistance-associated gene (UVRAG), is required for the induction of autophagy. The Atg genes control autophagosome formation through Atg12-Atg5 and LC3-II (Atg8-II) complexes. Atg12 is conjugated to Atg5 in a ubiquitin-like reaction that requires Atg7 and Atg10 (E1 and E2-like enzymes, respectively). The Atg12-Atg5 conjugate then interacts noncovalently with Atg16 to form a large complex. LC3/Atg8 is cleaved at its C-terminus by Atg4 protease to generate the cytosolic LC3-I. LC3-I is conjugated to phosphatidylethanolamine (PE) also in a ubiquitin-like reaction that requires Atg7 and Atg3 (E1 and E2-like enzymes, respectively). The lipidated form of LC3, known as LC3-II, is attached to the autophagosome membrane. The ubiquitinated targets are linked to the autophagosome through autophagic receptors. SQSTM1/p62 is an autophagy receptor, it binds to ubiquitinated targets through its UBA-domain and to the autophagosome through its LIR region which in turn interacts with LC3-II.

1.3.3. Regulation of autophagy

The target of rapamycin (mTOR) kinase is the main player in nutrient sensing and in regulating cell growth as well as autophagy. It is a signalling control point downstream of growth factor receptor signalling, hypoxia, ATP levels and insulin signalling. mTOR kinase is activated downstream of Akt kinase, PI3-kinase, and growth factor receptor signalling when nutrients are available. Thus, activated mTOR kinase promotes growth by induction of ribosomal protein expression and increased protein translation. mTOR inhibits autophagy through its inhibitory effects on Atg1 kinase activity (Glick et al. 2010). Apart from mTOR, there are other factors which have recently been reported to be involved in autophagy regulation such as insulin, amino acid signalling, Bcl-2, reactive oxygen species, and AMP-activated protein kinase (AMPK) amongst others (Mizushima 2007). However, these also act mostly via mTOR.

1.4. Paget's disease of bone

1.4.1. Definition

The first description of Paget's disease of bone was made in 1876, when Sir James Paget read a necropsy report *on a form of chronic inflammation of the bones (osteitis deformans)* before the Royal Medico-Chirurgical Society. He defined it as "*osteitis deformans: a focal disruption in the continuous remodelling of bone through the normal relationship between bone resorption and reformation, resulting in a disorganised mechanical structure and formation of thickened, but structurally weakened bone*" (Paget 1877). In 1889, 10 years before the death of Sir James, *osteitis deformans* became known as 'Paget's disease of bone' (PDB).

The current PDB clinical definition is 'a skeletal disorder whose main feature is an excessive bone resorption (increased bone turnover) and subsequent excessive bone formation (disturbed bone remodelling)'. It leads to extremely vascularised and structurally disorganised bone that results in deformity (abnormal bone structure), pain, and pathological fractures. PDB can be either monostotic involving one or more areas in a single bone or polyostotic involving multiple bones. The skull, pelvis, sacrum, lumbar spine, femur, and tibia are the typical sites affected by the disorder. It is of interest that the pagetic process does not tend to spread spontaneously to nearby bones. When the skull, jaw, clavicle, or a long bone of the leg is involved in the disorder, the skeletal expansion or distortion can be evident (Gkouva et al. 2011).

Although PDB is principally an osteoclast disorder, the disorder is actually divided in three main phases among which the difference is the 'prominence' of either osteoclastic or osteoblastic activity: the osteolytic phase where osteoclastic activity predominates and bone resorption (or absorption) occurs, a mixed phase where there is a combination of osteoblastic and osteoclastic activity, and an osteoblastic phase where new bone formation (apposition) occurs. Possibly, a fourth phase called the 'final stage' or 'inactive sclerotic phase' could exist, where new osteoclastic and osteoblastic formation ceases, but the bone retains a sclerotic architecture (Dell'Atti et al. 2007). All phases can otherwise be identified in the same patient and in different bones. During the three phases disturbances in both the osteoblastic and the osteoclastic activity take place leading to the formation of abnormal woven or mature bone displaying disorganised collagen, which results in raised susceptibility to deformities and fractures. Finally, the increased bone size can cause pain as a result of stretching of the periosteum and nerve endings (Gkouva et al. 2011).

1.4.2. Origin

It is thought that the origin of the disease was in Western Europe, and specifically in the United Kingdom more than 2000 years ago, due to the fact that all the historical cases of PDB which have been identified are from this region, and that ancient patterns of migration may be responsible for its current distribution. However, in the United Kingdom as well as in New Zealand, the incidence and severity of the disease have declined substantially over the last 20-30 years (Rea et al. 2013).

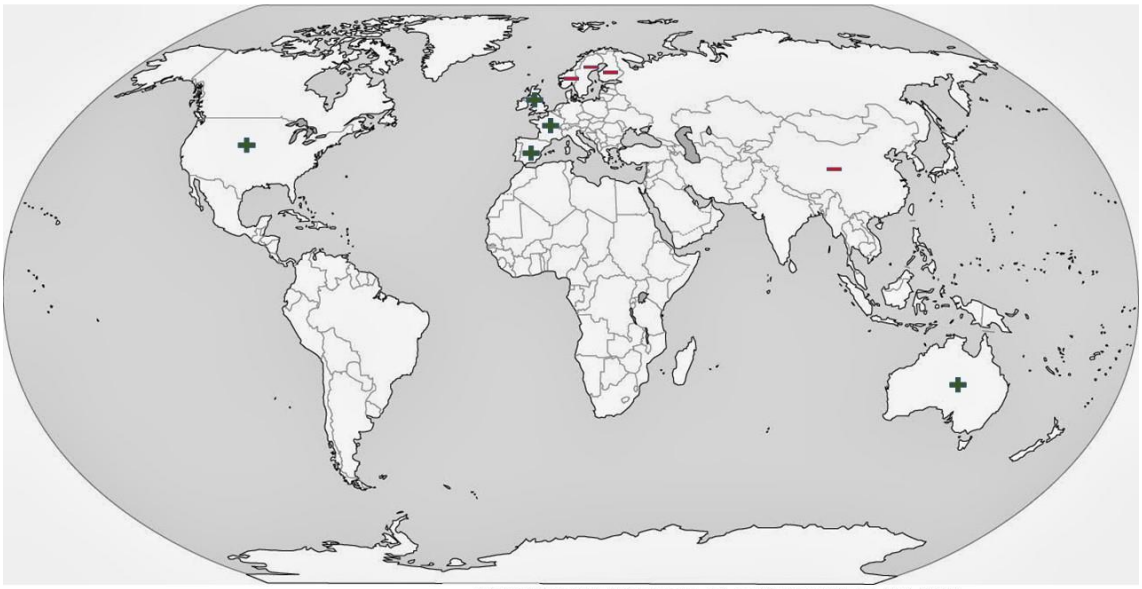
This hypothesis was supported by a study carried out by Mays where more than 100 archaeological cases of PDB were analysed. Between them, the earliest cases come from the Roman Empire (first to fourth centuries AD), there was no case from outside Western Europe, and approximately 94% of cases come from England (Mays 2010). However, the study had some limitations: it only included those cases in which the findings were double-checked by means of a radiological study, as well as a histological study, which is considered to be essential for the diagnosis of the disease (Menéndez-Bueyes and Soler-Fernández 2011); and a lack in the literature of credible archaeological cases from other regions of the world, such as the great civilizations of ancient Egypt, the Middle and Far East, and Andean South America, due to a lack of developed archaeological infrastructure in these countries, where moreover, buried human skeletal remains are often worst preserve (Mays 2010).

For these reason, the search was extended including all cases which had been only analysed by radiological studies in this way, the total cases increased, both in number and in geographic regions, including those outside the European continent. This led to several observations: an increase in the European distribution throughout the Mediterranean area and southwestern Europe, with evidence in Greece, Italy, France and Portugal; a growing importance of the disease in Spain, which was especially significant during or immediately before the Roman period; and a marked increase in the geographic distribution of the disorder in both South and North America. Therefore, the earliest cases points were found in the Mediterranean region: French Neolithic, Aegean Late Bronze and, very significantly, the Roman period, in which the cases multiplied, both numerically and geographically. During that period, populations were moving constantly. These observations suggest that the British origin of the disease was debatable and suggested a new hypothesis a multifocal origin of this disorder in the circum-Mediterranean region during the Roman period. Indeed, investigations of a PDB-like disorder in medieval skeletal remains from Norton Priory, Runcorn form part of the focus of this thesis (Chapter 4). Although this hypothesis disapproves the previous one, at the same time it

supports the thinking that migration of the local population and of residents from the Mediterranean to England during the Roman occupation may have brought with it an ancient form of PDB (Menéndez-Bueyes and Soler-Fernández 2011).

1.4.3. Geographic distribution

Modern PDB also has an irregular geographic distribution. There is a high prevalence in Northwest Europe, especially high in the United Kingdom (1-2% of the population over 55 years) and in recent emigration areas of this population, such as Australia, New Zealand, or the USA. Other countries with a high prevalence are France and Spain (0.7-1.3%) where there are areas with high concentrations of cases. Finally, the disorder is rare in Scandinavian countries, Asia and Africa (less than 1%) (Rea et al. 2013; Menéndez-Bueyes and Soler-Fernández 2017).



Adapted from Menéndez-Bueyes, L.R., and Soler Fernández, M.C., 2017.

Figure 4. Geographic distribution of modern Paget's disease of bone

Paget's disease of bone has an irregular geographic distribution. Areas where it is a high prevalence are highlighted in green whereas areas where the disorder is rare are highlighted in red.

1.4.4. Symptoms

PDB shows a highly variable severity as there are some patients with severe disease which has a negative impact on their quality of life but there also are patients who are completely asymptomatic. Indeed, PDB is asymptomatic in over 70% of affected individuals. Most of these cases are identified by routine laboratory tests such as an elevated serum ALP. When it is symptomatic, the more frequent symptoms are bone pain, bone deformity, pathologic fracture, secondary osteoarthritis, and deafness. Less common are spinal stenosis and nerve

compression syndromes, and finally, the least encountered are hypercalcemia, hydrocephalus, paraplegia, cardiac failure, and osteosarcoma (Ralston et al. 2008). An interesting feature is that the pain associated with PDB is different than mechanical or arthritic pain and furthermore, reflects different or multiple aetiologies. It usually is described as a deep, dull ache, unrelated to activity, and not relieved by rest, sleep, or nonsteroidal medications (Hadjipavlou et al. 1986). The factors which influence disease severity and extent of PDB are incompletely understood (Albagha et al. 2013).

1.4.5. Diagnosis

In most of the cases, the diagnosis is made incidentally by increased levels of bone metabolism markers, most usually serum ALP. Subsequently, specific skeletal changes are investigated through radiographs and radionuclide bone scan to confirm the diagnosis. In case that the diagnosis is still unclear after that analysis, malignancy must be excluded, so bone biopsy is also performed, but it is the last option (Gkouva et al. 2011). Nevertheless, the observation of a declining prevalence, rising age of presentation, and tendency for monostotic disease (single bone affected) may now limit the diagnostic usefulness of the ALP testing which was always considered a useful marker of disease activity and effectiveness of treatment (Cundy and Bolland 2008).

Bone-specific ALP is a more sensitive test and can detect smaller degrees of increased bone activity in patients who have been treated or those with mild disease activity. It reflects the extent and activity of PDB. However, it has the disadvantage that when only a small volume of bone is affected or PDB is monostotic, levels are normal which covers up the disease. For this reason, other markers are also used for the diagnosis of PDB such as osteocalcin and procollagen type 1, or N-terminal propeptide (P1NP) which are bone formation markers, or C-terminal telopeptide of type I collagen and N-telopeptide of type I collagen which are bone resorption markers. Other sensitive markers which are extremely important in the diagnosis are urinary deoxypyridinoline and pyridinoline levels. Despite this wide variation in markers to confirm PDB, to determine the burden of involvement as well as the differential diagnosis, bone imaging is essential (Theodorou et al. 2011). The typical radiographic appearance of PDB is characterised by excessive bone density, cortical thickening, and deformity of the affected bone and raised trabecular pattern. Radionuclide bone scanning is carried out during the diagnosis of PDB to know the extent of skeletal involvement (Gkouva et al 2011).

1.4.6. Causes

The aetiology of PDB is unknown although as noted earlier current evidence suggests the interplay of both environmental and genetic factors, because of an overall decrease in prevalence and severity of PDB over the last 20-30 years (Cooper et al. 2006; Ralston 2008; Bastin et al. 2009) and clear familial inheritance patterns.

1.4.6.1. Genetic factors

PDB has a strong genetic component. The single most important susceptibility gene which has been identified is *SQSTM1*. SQSTM1 encodes SQSTM1/p62 which is a scaffold protein. This protein plays an important role in the regulation of nuclear factor kappa β (NF-κβ) signalling, autophagy, and apoptosis. Mutations in this gene are present in up to 40% of the cases with a family history of PDB and in ~10% of the cases without family history (sporadic PDB; Layfield 2006; Rhodes et al. 2008; Goode and Layfield 2010; Albagha et al. 2013). The mechanism by which mutations in *SQSTM1* predispose to PDB is not completely defined. Most of the mutations which have been identified in the *SQSTM1* gene are localised within or close to the UBA domain, and the majority result in SQSTM1/p62 being unable to bind polyubiquitin chains (Cavey et al. 2006). This could underlie a unifying mechanism by which PDB occurs because of the involvement of the UBA domain in the different SQSTM1/p62 functions (Daroszewska et al. 2011).

Further, seven additional genetic loci have been associated with the disease in noncarriers of *SQSTM1* mutations by recent genome-wide association studies (GWAS). Within these loci there are genes which have a known role in bone metabolism such as *CSF1*, *TNFSF11*, *TM7SF4* (dendritic cell-specific transmembrane protein), and optineurin (*OPTN*) (Obaid et al. 2015). These functions support a plausible pathogenic role in PDB. The other genes identified with no current established role in bone metabolism were nucleoporin 205 KDa (*NUP205*), Ras and Rab interactor 3 (*RIN3*), and promyelocytic leukemia gene (*PML*). Although, they are not obviously involved in bone metabolism, the processes which are controlled by them may be relevant to the pathogenesis of PDB. The final identified gene was that encoding valosin-containing protein (*VCP*), a protein which plays a complex triple role in cell death (Rea et al. 2013; Goode et al. 2014; Vallet and Ralston 2016).

There is a significant association between the presence of mutation in risk alleles with the number of affected bones and disease severity in PDB, with evidence of an allele dose effect. However, there is no significant association between the presence of mutation in risk alleles and the sex, age, age at diagnosis of PDB, quality-of-life, the presence of deafness, fractures, or

bone deformity. The presence of mutations in *SQSTM1* increase severity and extent of PDB and the presence of mutations in risk alleles combined with *SQSTM1* mutations has an additive effect which further increases the severity of PDB (Albagha et al. 2013). So, the overlap between major susceptibility loci within families affected with PDB suggests the possibility that two independent genetic variants are necessary to cross-some 'threshold' rate. In that sense PDB may be a Mendelian disorder with a digenic mode of inheritance, where affected individuals carry mutations in two unlinked genes that together produce the disease phenotype (Helfrich and Hocking 2008).

1.4.6.2. Environmental factors

In some regions of countries where there has been a high prevalence of PDB, the disorder has become less common over recent years which suggest that environmental factors contribute to the pathogenesis of PDB. In current generations, carriers of *SQSTM1* mutations develop PDB at a later age than their parents. The potential environmental triggers are unclear, however some which have been proposed include:

- Diet: low calcium intake during childhood and vitamin D deficiency are associated with an increased risk of PDB; these conditions could cause osteoclast activation and increase bone turnover as consequence of a secondary hyperparathyroidism. In the case of primary hyperparathyroidism, it could cause increase severity and activity of PDB (Siris 1994; Roodman and Windle 2005; Vallet and Ralston 2016).
- Environmental toxins: Although, there is no experimental evidence to support or refute that environmental toxins may cause PDB, in the North West of England which is an area of high PDB prevalence it is thought that the cause could involve the pollution from cotton mills (Lever 2002; Vallet and Ralston 2016).
- Biomechanical factors: The thought of biomechanical factors influencing susceptibility to PDB is supported by the predilection for lesions in the axial skeleton and weight bearing limbs (Solomon 1979; Barry 1980; Vallet and Ralston 2016).

1.4.6.3. Viruses and PDB

The existence of a viral causative agent such as slow paramyxovirus infection of osteoclast precursors is supported by the presence of inclusion bodies in osteoclasts which resemble viral particles. Furthermore, the identification of canine distemper virus (CDV) in bone cells from PDB patients supports that the close contact with domestic animals during childhood or the consumption of brain or other viscera can also be a risk factor for PDB. It is further supported

by the finding that CDV infection of human precursor osteoclasts enhances osteoclastogenesis (Rea et al. 2013). All of this raises the possibility of one or more infectious agents acquired from animals having a pathogenic role in PDB. Measles virus has been also reported to play a role in PDB pathogenesis because measles virus nucleocapsid protein (MVNP) transcripts have been detected in PDB patients. However, there is conflicting evidence such as failed detection of viral transcripts from long-term culture of PDB patient-derived osteoclast cultures or no isolation of live virus from pagetic samples, which makes controversial the viral hypothesis in PDB (Helfrich and Hocking 2008; Rea et al. 2013; Vallet and Ralston 2016).

1.4.7. Treatment of PDB

PDB treatment has as main aim to provide a continued biochemical remission in disease and to ease pain caused by skeletal complication of the disease. The main treatment consists of the administration of bisphosphonates which decrease osteoclastic activity, restore normal bone turnover, and relieve bone pain. A crucial aim of the treatment at long-term, in addition to control the disease activity, is to try to decrease the risk of complications such as deformity, fracture, and degenerative joint disease (Gkouva et al. 2011).

1.5. The SQSTM1/p62 protein

The name sequestosome 1 (SQSTM1) originally derives from the ability of the protein to form cellular aggregates known as 'sequestosomes' which may be sites of intracellular protein degradation (Layfield and Hocking 2004). The SQSTM1 protein (also known as p62) is often referred to as a scaffold/adaptor protein. Scaffold/adaptors are non-catalytic proteins that are necessary for the efficient and selective transmission of information during cell signal transduction, for example controlling the nonspecific access of enzymes to undesirable substrates which could produce unwanted cellular effects. SQSTM1/p62 is especially important when promiscuous kinases such as the atypical protein kinase C enzymes (aPKCs) are the catalytic components of the signalling complexes. These kinases are called 'atypical' since they are insensitive to Ca^{2+} and lipid second messengers, in contrast to the other members of the family which are sensitive to Ca^{2+} and lipid second messengers. Although SQSTM1/p62 does not have the ability to directly regulate the enzymatic activity of aPKCs, it can modulate the function of these enzymes, playing an active role as a scaffold protein *via* interactions mediated by its N-terminal Phox and Bem1p (PB1) domain. In this context SQSTM1/p62 regulates cell signalling pathways relevant to cell differentiation in bone remodelling (Moscat et al. 2007).

In addition, SQSTM1/p62 has the ability to self-oligomerise through its PB1 domain, and can interact with ubiquitinated proteins through its C-terminal UBA domain. As noted earlier SQSTM1/p62 functions as a receptor for ubiquitin-mediated autophagy and is also degraded during this process. Thus, basal and constitutive autophagy regulates the intracellular levels of SQSTM1/p62 and/or the control of ubiquitin-aggregate formation (Komatsu and Ichimura 2010).

1.5.1. Structure of the SQSTM1/p62 protein

The higher order organisation of SQSTM1/p62 consists of a three-dimensional helical assembly, with a scaffold formed through the PB1 domain. The interaction between the cellular binding partners LC3 and ubiquitin and this assembly structure takes place through the LIR motif and UBA domain, respectively, which are accessible within this assembly (Ciuffa et al. 2015).

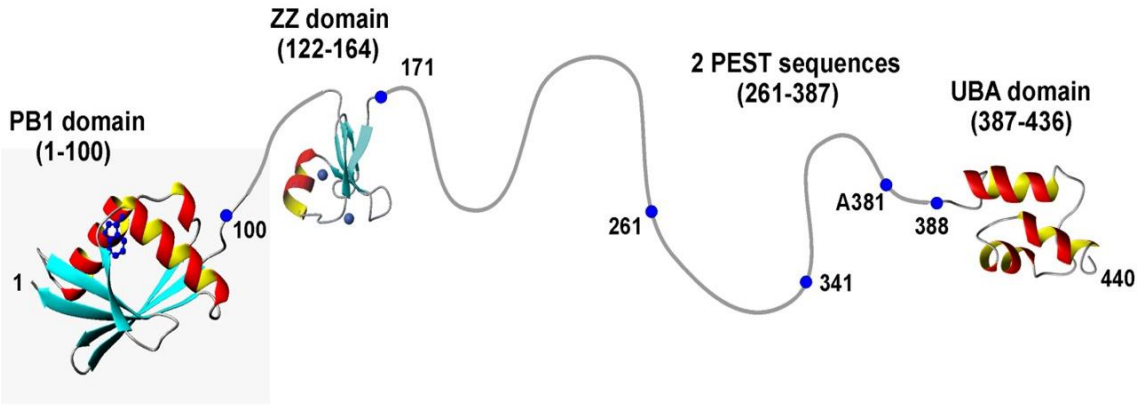


Figure 5. Proposed tertiary structure of the human SQSTM1/p62 monomer

The N-terminal PB1 (Phox and Bem1) domain which adopts an ubiquitin-like fold is shown (in this case the PB1 and ZZ domains of other proteins are presented). Numbering relates to the positions of specific residues in the 440 amino-acid sequence. From (Najat et al. 2009).

Comparison of the amino acid sequence of SQSTM1/p62 between several species reveals that it is highly conserved (Geetha and Wooten 2002). The SQSTM1/p62 structure consists of three structured regions as well as several binding motifs and internal regions. From its N-terminal extreme to its C-terminal extreme they are: a N-terminal PB1; a ZZ finger; a TF6-b motif; two PEST sequences; a LC3 Interacting region (LIR); a kelch-like ECH-associated protein 1 (Keap1) binding region (KIR); and finally a UBA domain which is localised on the C-terminal end of the protein (Vallet and Ralston 2016; Ciuffa et al. 2015).

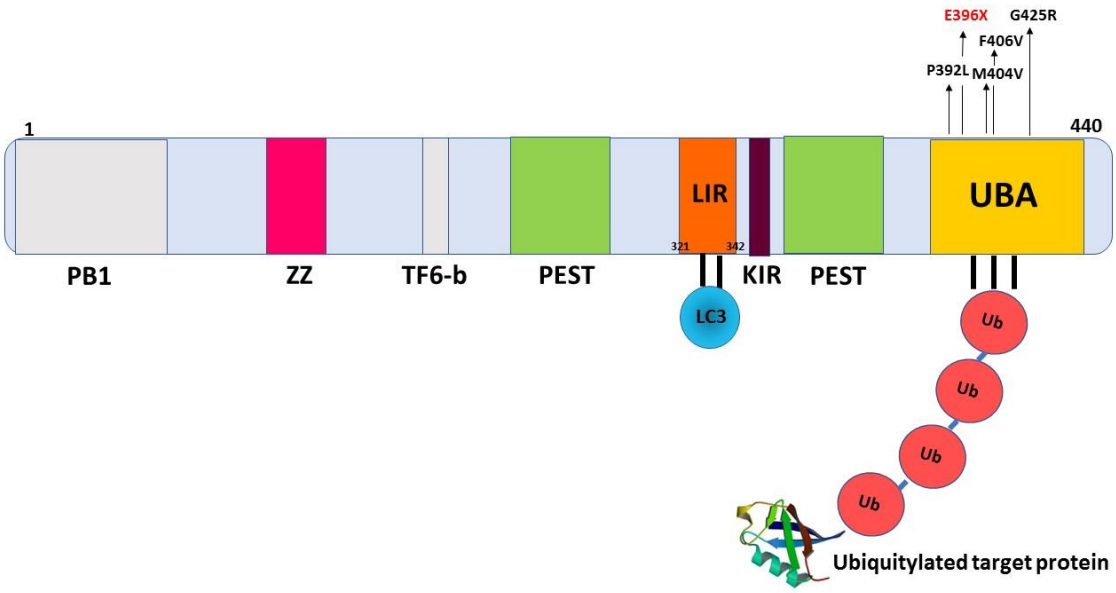


Figure 6. Schematic representation of the domain structure of SQSTM1/p62 indicating sites of PDB-associated mutations analysed in this study

The PB1 domain allows polymerisation of SQSTM1/p62 with itself and other proteins containing PB1 domains; ZZ (zinc finger motif) mediates binding with RIP (receptor-interacting protein), which is necessary for NF-κβ activation; TF6-b is the TRAF6-binding domain; PEST sequence is rich in Proline (P), Glutamic acid (E), Serine (S), and Threonine (T); LIR is the LC3-interacting region; KIR is the Keap1-interacting region; UBA is the ubiquitin-associated domain. All the PDB mutations analysed in this study are within the UBA domain (missense mutations are in black and truncating mutations are in red).

SQSTM1/p62 binds to ubiquitylated protein substrates through non-covalent interactions involving its UBA domain and to LC3 through its LIR region. Numbering relates to the position within the 440 amino-acid-sequence of the human protein.

1.5.1.1. PB1 Domain

The PB1 domain is a protein-protein interaction domain of around 100 residues which is present in 29 human proteins including SQSTM1/p62. This domain allows proteins with a PB1 domain to form specific heterodimers between family members or to mediate its own oligomerisation. The domain has critical residues which are involved in this protein-protein interaction: a 'basic cluster' of a conserved Lys residue and a conserved highly acidic motif of around 28 amino acids known as the OPCA motif (rich in Arg residues). The PB1 domain can be classified in three different groups depending on their domain architecture (Seibenhener et al. 2007):

- Type A: They have the canonical OPCA motif but lack the basic cluster.
- Type B: They have the basic cluster but lack the OPCA motif.
- Type C: These proteins have both the basic cluster and the OPCA motif.

The PB1 domain of SQSTM1/p62 is type C by virtue of containing oppositely charged areas through which oligomers can form. The PB1 domain also mediates other interactions of SQSTM1/p62 which could potentially compromise its polymerisation and limit further oligomerisation (Ciuffa et al. 2015).

The helical polymer of SQSTM1/p62 can be stabilised by an electrostatic PB1 bridge which is formed for the residues of the C-terminal region of the PB1 domain. The disturbance of this electrostatic bridge leads to the formation of ring oligomers which affects to the aggregation properties of SQSTM1/p62, but it can still be degraded by autophagy. There are several ubiquitination sites in SQSTM1/p62 in spatial proximity to the electrostatic bridge which may lead upon ubiquitin modification to the depolymerization of the helix (Ciuffa et al. 2015). Moreover, there are other post-translational modifications at residues located in the PB1 helix interface of SQSTM1/p62 such as the PKA-mediated phosphorylation of S24 and other modifications affecting the ubiquitin-binding affinity such as phosphorylation of S403 carried out by TANK binding kinase-1 (TBK1) (explained in detail in Chapter 3) by which the helical assembly of SQSTM1/p62 could also be regulated (Ciuffa et al. 2015).

1.5.1.2. ZZ finger

The ZZ domain consists in an atypical zinc finger domain localised between residues 128 and 163 of the human protein whose structure is not well characterised (Moscat et al. 2007). It binds to RIP leading to the activation of the NF-κβ signalling pathway (Numan et al. 2015). The presence of the ZZ domain in the SQSTM1/p62 structure includes it in the group of zinc finger proteins which is characterised by the presence of a putative finger structure which cluster around a tetrahedrically Zn^{+2} ion coordinated by cysteine and histidines residues, stabilising the folded structure of zinc finger peptide (Ponting et al. 1996).

1.5.1.3. TF6-Binding Motif

This consists in a short stretch of amino acids that includes a transformation booster sequence (TBS) sequence through which it binds to TRAF6 (TNF receptor-associated factor 6). TRAF6 is an important modulator of the inflammatory response and osteoclast differentiation (Moscat et al. 2007) through the activation of NF-κβ pathways (Numan et al. 2015).

1.5.1.4. PEST Sequences

PEST comes from the abbreviation of Proline (P), Glutamic acid (E), Serine (S), and Threonine (T). The human SQSTM1/p62 protein has in its structure two different regions rich in these amino acids. These are localised between residues 266-294 and 345-377. The presence of PEST

sequences in proteins often indicate their degradation through ubiquitin-dependent proteolysis (Rechsteiner et al. 1996).

1.5.1.5. LIR region

The LIR region is a fundamental motif which allows SQSTM1/p62 to bind to LC3 (human homolog of Atg8 in yeast). This is a highly-conserved region localised between amino acids 321 to 342 of human SQSTM1/p62, where the motif DDDWTHL, residues from 335 to 341, participates directly in the interaction with LC3. This region is essential for the role of the SQSTM1/p62 protein in autophagy, promoting delivery of autophagic cargo to autophagosomes through its interaction with LC3 (Numan et al. 2015). Accordingly, the ability of SQSTM1/p62 to be recruited into phagophores and thereafter acidic vesicles is strongly reduced by the deletion of this motif (Goode et al. 2016).

In humans, six different homologs of Atg8 exist with LC3 proteins the best defined, encoded by four genes. LC3, like ubiquitin, has a β sheet wrapped around a central α helix. However, two additional α helices located N-terminally to their UBL core distinguish it from ubiquitin. Thus, at the same time, there are important differences in the N-terminal subdomain between the different member of the Atg8 family. Despite that, all ATG8s pack onto the UBL core with the aim of forming a deep hydrophobic pocket. The hydrophobic residues of the central α helix and β strand 2 of the UBL core form also another hydrophobic pocket. LC3 is involved in interaction networks related to autophagy and membrane trafficking through its HP1, HP2, and β strand 2 regions. Furthermore, when LC3 is attached to PE, LC3-II, it binds through its N-terminal α helices to lipid bilayers and recruits other components of the autophagic machinery to the phagophore to regulate the closure of the phagophore, and to modulate the formation of selective autophagosomes by interaction with selective autophagy receptors (Rogov et al. 2014).

1.5.1.6. KIR region

The Keap1-interacting region (KIR) of SQSTM1/p62 regulates the activation of the oxidative stress response transcription factor Nrf2 through its interaction with Keap1 (cysteine-rich protein) (Ciuffa et al. 2015). It is immediately after the LIR region (residues 344-356 in the human protein). The Keap1-Nrf2 pathway has a cytoprotective action against oxidative stress and Keap1 can be downregulated by SQSTM1/p62 via degradation by autophagy (Numan et al. 2015).

1.5.1.7. UBA domain

The UBA domain of SQSTM1/p62 is localised between residues 387-436 at the C-terminus of the protein. The structure of the UBA domain was determined *via* protein NMR. It consists on a compact three-helix bundle, with a hydrophobic surface on one side which is the target interface for protein-protein interactions (Ciani et al. 2003).

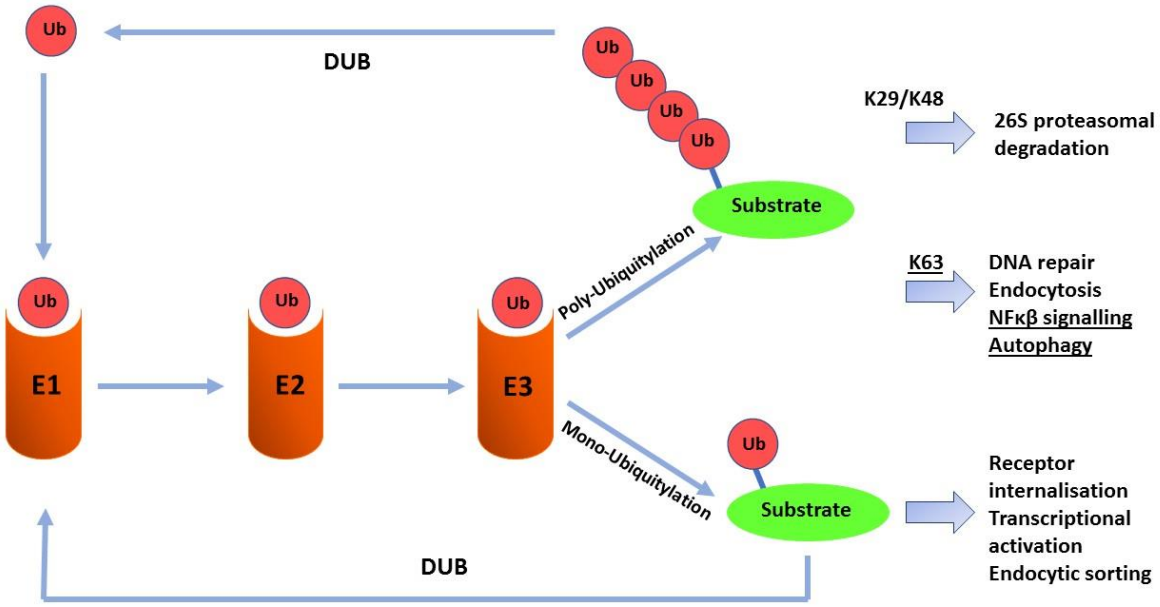
The UBA domain is required for the ubiquitin-binding capability of SQSTM1/p62. The "MGF" motif (Met404-Gly-405-Phe406) at the end of helix 1 of the UBA domain, and within helix 3 form the primary binding site for ubiquitin (Long et al. 2008). The property of SQSTM1/p62 to bind ubiquitin non-covalently was firstly described in 1996 (Vadlamudi et al. 1996). The UBA domain of SQSTM1/p62 was firstly described to act as a receptor deliver ubiquitinated proteins for degradation by 26S proteasome system (Mitch and Goldberg 1996) and later the same role was described in autophagy (Kirkin et al. 2009). The UBA has affinity for monoubiquitin as well as polyubiquitin chains, with preference for the latter (Geetha and Wooten 2002). The recognition of ubiquitin by the UBA domain involves a conformational switch to an 'activated' UBA form immediately prior to ubiquitin-binding and interaction (Helfrich and Hocking 2008).

1.5.1.7.1. Ubiquitin-mediated processes

Ubiquitin is a protein of 76 amino acids which is highly conserved from yeast to man. It has a tightly folded globular structure (β-grasp fold) whose main feature is the presence of five-stranded β sheet wrapped around a central α helix. Ubiquitin is synthesised as a precursor protein which is then proteolytically processed to expose its C-terminal Gly by which it can covalently link with the Lys (or N-terminal) of another ubiquitin or a target protein. Ubiquitin conjugates carrying either monoubiquitin or polyubiquitin chains are generated through a cascade of enzymatic enzymes, including E1, E2 and E3 (Figure 7). Ubiquitin controls different biological processes, including regulation of receptor internalisation, targeting proteins for degradation via the UPS or autophagy, or regulation of signal transduction pathways (e.g. RANK-NF-κβ signalling), depending on the nature of the ubiquitin modification. Proteins which contains ubiquitin-binding domains (UBDs, e.g. SQSTM1/p62) act as ubiquitin receptors by non-covalent binding of ubiquitin. The ubiquitin signal is reversed by a large class of deubiquitinating enzymes (DUBs) which are proteases that cleave the isopeptide bond between ubiquitin and its substrate (Rogov et al. 2014).

Ubiquitin has seven internal Lys residues which allow it to be attached to itself, leading it to the formation of chains with various topologies and functions. For example, when a protein is

modified with Lys48-linked polyubiquitin chains, it is targeted to the proteasomal pathway, whereas when the protein is modified with the attachment of a single ubiquitin (monoubiquitination) and/or Lys63-linked chains, can be targeted to degradation in lysosomes (autophagy). Thus, ubiquitin is a universal degradation signal which is recognised by two intracellular proteolytic systems, the proteasome, and the lysosome (Kirkin et al. 2009). As noted previously Lys63-linked polyubiquitin chains can also play non-degradative roles, such as in the RANK-NF-κβ signalling pathway *via* the modification of TRAF6.



Adapted from Layfield,R., and Hocking, L.J., 2004

Figure 7. Ubiquitin-mediated procesess

The ubiquitylation process is carried out by the sequential actions of three different enzymes. First, ubiquitin-activating enzyme (E1) binds to ubiquitin, activated ubiquitin is transferred to an ubiquitin-conjugating enzyme (E2) and to finish an ubiquitin-ligase enzyme (E3) transfers the substrate protein to the E2-ubiquitin complex. Deubiquitylating enzymes (DUBs) separate ubiquitin from the complex. Substrates can either be monoubiquitylated or polyubiquitylated. Depending on the particular ubiquitin modification, the fate of the substrate and/or process regulated varies. Autophagy and NF-κβ signalling are underlined because both processes have been demonstrated to be crucial in bone homeostasis and are regulated by the SQSTM1/p62 protein (Boyle et al. 2003; Hocking et al. 2012).

1.5.2. Biological functions of the SQSTM1/p62 protein

Through its N-terminal PB1 domain, SQSTM1/p62 interacts with the proteasome by binding to the S5a subunit. Moreover, SQSTM1/p62 can also participate in the formation of multimeric protein complexes by the interaction of its PB1 domain with other proteins which have also PB1 domain (Seibenhener et al. 2007).

Through its UBA domain, as described previously, one of the best described and extensively studied roles of SQSTM1/p62 is its involvement of as a scaffold protein in selective activation of the transcription factor NF-κβ. The interaction between SQTM1/p62 and TRAF6 enhances TRAF6 oligomerisation and subsequent activation, which at the same time leads to Lys63 polyubiquitination of TRAF6 that ultimately leads to the activation of NF-κβ signalling. On the other hand, the aggregation of CUL3-modified caspase-8 within SQSTM1/p62-dependent foci is also stimulated by SQSTM1/p62. This leads to committed cell death as result of the full activation and processing of caspase-8. So, cytosolic cellular protein aggregates which include SQSTM1/p62 and/or polyubiquitinated proteins may act as signal-organising centres where SQSTM1/p62 interacts with TRAF6 and caspase-8 and depending on the interaction, determine whether cells survive through activating the TRAF6-NF-κβ pathway, or die through facilitating the activation of caspase-8 and the downstream effector caspases (Komatsu and Ichimura 2010).

However, SQSTM1/p62 plays other roles which are also important in cellular homeostasis through this domain (Geetha and Wooten 2002). SQSTM1/p62 acts as a receptor for degradation of ubiquitinated proteins to via autophagy. In this context SQSTM1/p62 binds to its ubiquitin-modified targets and then both are transported into the autophagosome for their degradation. In addition to proteins, SQSTM1/p62 is also involved in the autophagic degradation of different cargos such as damaged midbody ring, peroxisomes, and intracellular microbes (Komatsu and Ichimura 2010). Although, the role of SQSTM1/p62 in damaged mitochondria degradation has now been disproven (Lazarou et al. 2015).

Finally, a further role for SQSTM1/p62 is its involvement in the regulation of the response to environmental stress. Nrf2 is a protein which regulates the gene expression of a battery of antioxidant proteins and detoxification enzymes. SQSTM1/p62 has the ability to interact with the Nrf2-binding site on Keap1 that is a component of Cullin3-type ubiquitin ligase for Nrf2 resulting in stabilisation of Nrf2 and transcriptional activation of Nrf2 target genes (Komatsu and Ichimura 2010; Rogov et al. 2014; Ciuffa et al. 2015; Vallet and Ralston 2016).

1.5.2.1. Functional Significance of the SQSTM1/p62 UBA Domain

1.5.2.1.1. SQSTM1/p62's role in RANKL-NF-κβ signalling in osteoclasts

The role of SQSTM1/p62 in the process of NF-κβ signalling (Figure 8) in osteoclast mediated via direct interaction with TRAF6 which is a key regulator of the signalling cascade induced by RANKL. Then, the formation of a TRAF6-SQSTM1/p62 ternary complex with an atypical protein

kinase C isoform (PKCζ/λ) occurs. This induces NF-κβ activation *via* the inhibitor of κβ (I-κβ) kinase (IKK) and as result the phosphorylation and degradation of I-κβ leading to NF-κβ release. It is though that here the role of SQSTM1/p62 is to regulate the covalent modification of TRAF6 with Lys63-linked polyubiquitin chains through directing chain formation on TRAF6, using its UBA domain. Specifically, SQSTM1/p62 controls osteoclast NF-κβ signalling through controlling Lys63-linked polyubiquitin chain extension of monoubiquitylated TRAF6 which results in the activation of TAK1 kinase (Cavey et al. 2005). As noted earlier RANK-NF-κβ signalling is important for osteoclast differentiation, function, and activity (Rea et al. 2014; McManus et al. 2016).

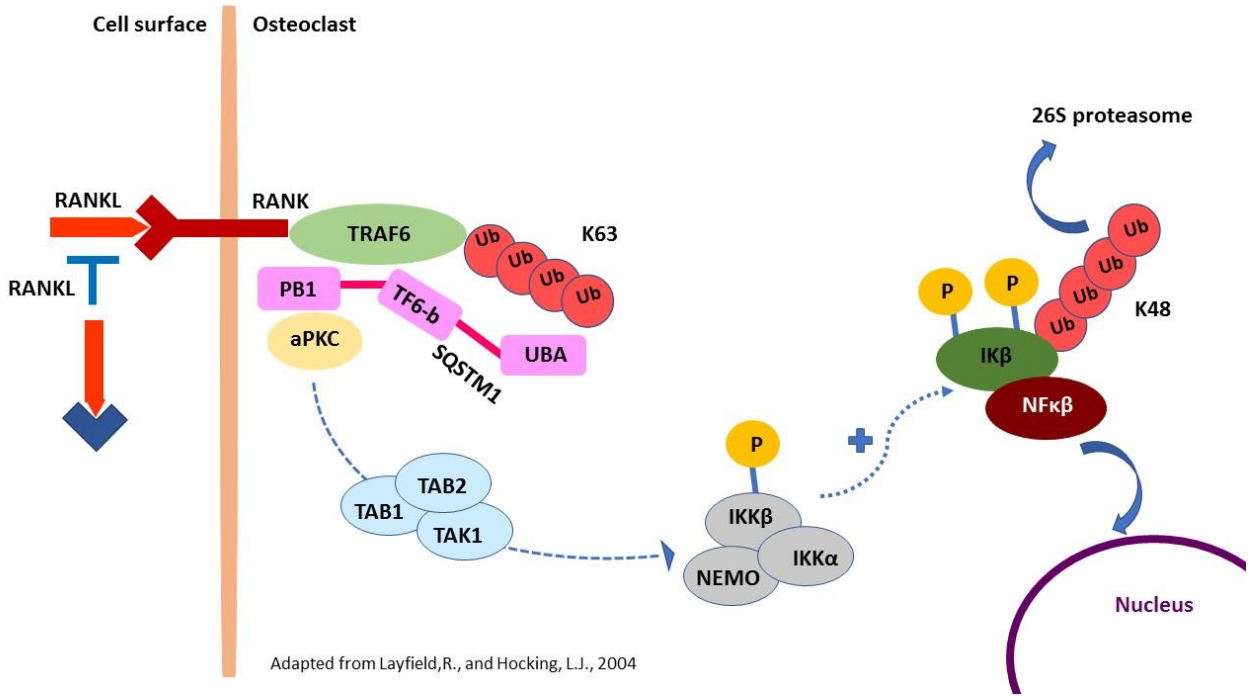


Figure 8. The RANKL-NF-κβ signalling pathway

Upon interaction of RANKL (cytokine) with RANK (receptor), the direct interaction between TRAF6 and RANK leads to autoubiquitination of TRAF6 through its intrinsic ubiquitin ligase activity. TRAF6 also binds to SQSTM1/p62 through its TF6-b region which is thought to facilitate the K63-linked polyubiquitination of TRAF6. aPKC is recruited to the signalling complex by SQSTM1/p62, and polyubiquitination of TRAF6 leads to TAK1 activation, which subsequently leads to phosphorylation and activation of the IKK complex (IKKα, IKKβ, IKKγ); finally, the activation of the IKK complex leads to phosphorylation of I-κβ and its degradation by the 26S proteasome, succeed by the release of NF-κβ to the nucleus.

The presence of SQSTM1/p62 is not necessary for basal bone remodelling in mice, but its deficiency affects osteoclastogenesis (Moscat et al. 2007). The over-expression of SQSTM1/p62 protein leads to a significant decreased of NF-κβ activity in cell models, so SQSTM1/p62 is thought to be a negative regulator of NF-κβ signalling. SQSTM1/p62 also inhibits NF-κβ signalling by linking the cylindromatosis (CYLD) DUB with one of its targets,

polyubiquitinated TRAF6, which enhances deubiquitination of TRAF6. This has as consequence decreased NF-κβ activity as well as inhibition of osteoclastogenesis. However, the over-expression of PDB-associated SQSTM1/p62 mutants in reporter assays increases NF-κβ activity (relative to wild-type) which suggests that mutant SQSTM1/p62 loses its ability to inhibit NF-κβ (Rea et al. 2013) which leads to an increased differentiation and bone resorption (Rea et al. 2014). This may be because SQSTM1/p62 carries out this regulation of TRAF6 through its UBA domain, so UBA-deficient SQSTM1/p62 protein cannot regulate correct modification of TRAF6 or form a complex with CYLD (Rea et al. 2013).

Defects in SQSTM1/p62-mediated NF-κβ signalling might ultimately manifest as changes in autophagic activity, in other words, both processes are interdependent, so changes in NF-κβ activity due to SQSTM1/p62 dysfunction can lead to changes in autophagy, and *vice versa*. For example, TRAF6 regulates both NF-κβ signalling and autophagy through interaction with SQSTM1/p62 and activation of mTOR (Rea et al. 2014), and autophagy can be induced by the IKK complex, an important mediator of the RANK-NF-κβ pathway. Further, levels of I-κβ, the inhibitor of NF-κβ, are regulated *via* autophagy (Shapiro et al. 2014).

1.5.2.1.2. SQSTM1/p62's role in autophagy in osteoclasts

In autophagy, SQSTM1/p62 acts as an autophagy receptor recognising ubiquitinated proteins through its UBA domain and interacting with the autophagosome *via* LC3 through its LIR sequence (Figure 9). When SQSTM1/p62 is associated with misfolded proteins and protein aggregates, it forms SQSTM1/p62 bodies which provide a scaffold for the formation of the nucleate autophagosome and their successive degradation. The interaction and sequestration of cargoes by SQSTM1/p62 as well as the delivery of SQSTM1/p62 to the autophagosome requires the oligomerisation of SQSTM1/p62 through its PB1 domain, as well as a functional LIR region and UBA domain (Rea et al. 2014; Rogov et al. 2014; Ciuffa et al. 2015; Goode et al. 2016).

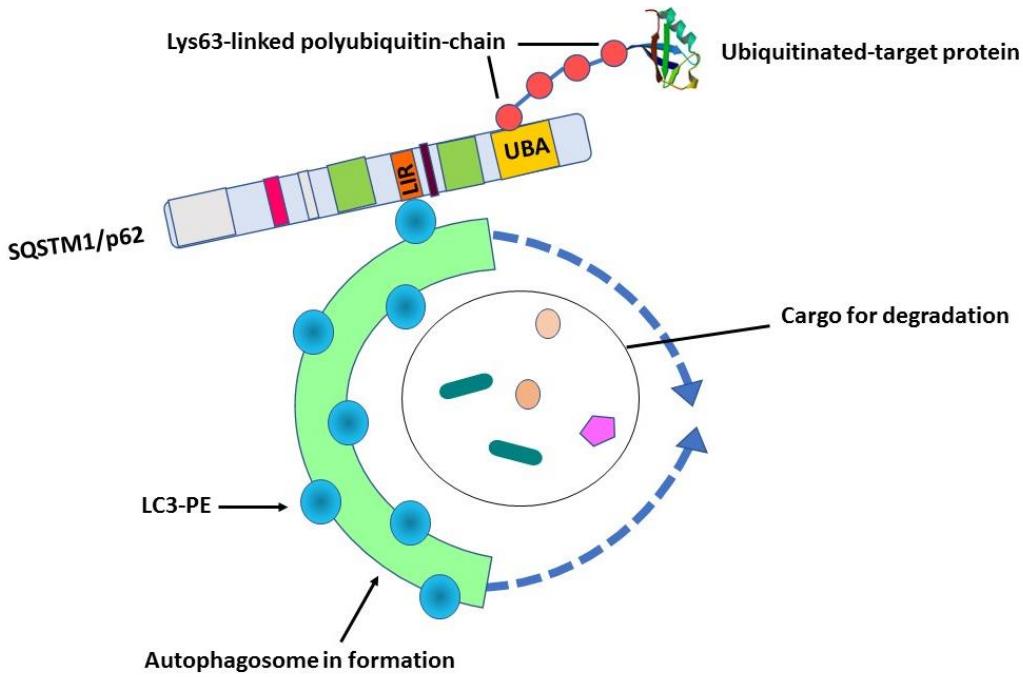


Figure 9. SQSTM1/p62-dependent autophagic degradation of ubiquitinated proteins

The isolation and formation of a double membrane structure (autophagosome) which engulfs the materials for degradation is the beginning of autophagy. SQSTM1/p62 can deliver ubiquitinated cargo to the autophagy machinery to be degraded at the later steps of autophagy *via* fusion of the autophagosomes with lysosomes. The interaction between SQSTM1/p62 and LC3-PE takes place through its LIR region (residues 321-342).

PE: Phosphatidylethanolamine (lipid modification of LC3 which anchors the protein to the autophagosome).

SQSTM1/p62 can also form a stable intermolecular homodimer through its C-terminal UBA domain which appears to block ubiquitin-binding for autophagic degradation. So, SQSTM1/p62 not only forms oligomeric scaffolds through its PB1 domain (Goode et al. 2016). This homodimer is stabilised by hydrogen bonds involving the side chain of Lys420 in the UBA domain of one SQSTM1/p62 molecule and Glu409 in another SQSTM1/p62 molecule. This intermolecular H-bond is the main force locking the UBA dimer and antagonising ubiquitin binding (Peng et al. 2017).

SQSTM1/p62 is constantly also degraded itself by autophagy, so any impairment of autophagy leads to the accumulation of SQSTM1/p62 and consequent formation of SQSTM1/p62 inclusions (Komatsu and Ichimura 2010). However, the role of SQSTM1/p62 in protein aggregation is subject to debate, some studies suggest that the cytotoxic body inclusions observed in some disease such as Alzheimer's are the result of the direct polymerisation of

SQSTM1/p62 itself, whereas others indicate that the inactivation of autophagy leads to increased SQSTM1/levels which enhances the formation of ubiquitinated protein aggregates, however protein aggregation *per se* can be exacerbated by genetic inactivation of SQSTM1/p62 (Ciuffa et al. 2015). Since ubiquitin is found in SQSTM1/p62 bodies, this implicates the necessity of a functional UBA domain during the formation of ubiquitin-positive SQSTM1/p62 structures, where the interaction between SQSTM1/p62 and ubiquitin is central to the biogenesis of such 'protein bodies' (Rogov et al. 2014).

1.5.3. SQSTM1/p62 and PDB: consequences of different disease-associated mutations

Approximately 30 different mutations have been identified in the *SQSTM1* gene in PDB patients with P392L being the most common. These result in either the truncation of the 440 residue SQSTM1/p62 protein or amino acid substitutions (missense mutations). The majority of these mutations are localised in the UBA domain (exon 8) causing the loss of ubiquitin-binding. PDB-associated mutations can impact on ubiquitin recognition by the UBA domain of SQSTM1/p62 through several mechanisms depending on the mutation (truncating or missense): either affect the structural integrity of the UBA domain and/or UBA dimer stability, or disturb key contacts at the UBA-ubiquitin interface. Indeed, the variation in PDB severity may depend on the particular SQSTM1/p62 mutation. In general, truncating mutations of SQSTM1/p62 are associated with a more severe PDB (earlier age at onset and increased number of affected sites) than common missense mutations (Najat et al. 2009; Rea et al. 2013; Goode et al. 2014). There are other non-UBA mutations such as the P387L mutation which is localised in a region very close to the N terminus of the UBA domain (exon 7), an unstructured region. The N-terminal region of the UBA domain is hydrophilic and glutamate and serine-rich and mutations here could affect UBA domain disturb binding kinetics; indeed, like UBA domain mutations, P387L also impacts on ubiquitin-binding function (Najat et al. 2009).

The loss of ubiquitin-binding function of SQSTM1/p62 seems to be an important mechanism by which the mutations cause osteoclast activation (ultimately due to an increased activation of the NF-κβ pathway) and differentiation (Vallet and Ralston 2016). Although, it is known that PDB-associated mutations of SQSTM1/p62 lead to an increase in osteoclast activity *via* changes in NF-κβ signalling, the precise impact of these mutations on autophagy is not fully known (Shapiro et al. 2014).

A dysregulation in the autophagic process is known to be implicated in the pathogenesis of a wide range of diseases such as some human neurodegenerative disorders (Alzheimer's disease and Parkinson's disease). In these disorders, defects in degradation of abnormal protein

aggregates by the proteasome and autophagy lead to the formation of intracellular inclusions. As noted earlier similar inclusions can be also seen in pagetic osteoclasts, and impaired autophagy in PDB could contribute to inclusion formation. SQSTM1/p62 mutations have also been associated with the neurodegenerative disorder Amyotrophic Lateral Sclerosis (ALS). Goode et al. 2016 shows that L341V mutant SQSTM1/p62, which affects the LIR region of SQSTM1/p62, is associated with defective autophagy in cell models. This raises the question as to whether PDB-associated mutations of SQSTM1/p62 might similarly impact on autophagy in PDB.

1.6. Aims and objectives:

The project included two interrelated elements relevant to disease mechanisms in 'modern' and 'ancient' PDB.

(1) Disease mechanisms in 'modern' PDB

The first part of the project investigated the impact of PDB-associated mutations of SQSTM1/p62 on autophagy, using *in vitro* models. Emphasis was placed on a previously uncharacterised F406V mutation, identified in a PDB patient screened during recruitment for the ZIPP study (an ongoing clinical trial whose main aim is to determine whether the drug zoledronic acid can prevent Paget's disease in people with *SQSTM1* mutations). This mutant was analysed alongside previously characterised PDB mutants P392L, M404V, G425R and E396X (truncating). Specific aims included determining the effects of:

1. The F406V mutation on the ubiquitin- and LC3-binding properties (autophagy-relevant interactions) of SQSTM1/p62 in pull-down assays
2. The F406V mutation on SQSTM1/p62 inclusion formation in HEK293T cells
3. Expression of different SQSTM1/p62 mutants on autophagy markers in HEK293T cells, under a range of conditions

(2) Disease mechanisms in 'ancient' Paget's disease

Norton Priory in Runcorn, Cheshire (Northwest England), is Europe largest monastic excavation with 130 articulated skeletons dating to the 12^{th}-15^{th} century. A recent analysis of the Norton collection revealed a remarkably high incidence of a bone disorder resembling PDB, with ~20% of the skeletons affected compared to 1-2% in other comparable excavations. Further, in affected individuals the disorder is much more extensive than in patients with 'modern' PDB and presents at a particularly young age, although bone deformities are mild. Given these profound phenotypic differences a key question arises, were the Norton individuals really affected by PDB or some other related bone disorder not seen in present times? Molecular analyses of the Norton remains in order to address this question represents an ongoing research project within the lab. Prior to the project commencing, a breakthrough involved the proteomic detection of ancient SQSTM1/p62 in a bone sample from the Norton collection. In this context, specific aims were to:

1. Determine if ancient SQSTM1/p62 could be detected different skeletal samples from the Norton collection

2. Use SQSTM1/p62 antibodies to provide information about the sequence of ancient SQSTM1/p62 protein
3. Refine methods for the extraction of ancient SQSTM1/p62 from skeletal samples
4. Provide further proteomic insights into the proteins preserved in skeletal samples from the Norton collection

CHAPTER 2. METHODS

Note: The recipes for all the reagents, which have been used in this study, are in the appendix.

2.1. DNA techniques

2.1.1. Plasmids

The provision of plasmids which were produced in the lab previously was a starting point for this study. The supplied plasmids were:

- pGEX-4T1-SQSTM1/p62-WT
- pGEX-4T1- SQSTM1/p62-E396X
- pGEX-4T1- SQSTM1/p62-M404V
- pcDNA3.1- EV (empty vector)
- pcDNA3.1- SQSTM1/p62-WT
- pcDNA3.1- SQSTM1/p62-E396X
- pcDNA3.1- SQSTM1/p62-P392L
- pcDNA3.1- SQSTM1/p62-M404V
- pcDNA3.1- SQSTM1/p62-G425R
- pcMV-HA-WT-TBK1
- pcMV-HA-K38A-TBK1

The pGEX-4T1- SQSTM1/p62 plasmids allow the expression of human SQSTM1/p62 in prokaryotic host cells and encodes a GST fusion protein, while the pcDNA3.1-SQSTM1/p62 and pcMV-HA-TBK1 plasmids allow the expression in eukaryotic host cells and encode a polyHis-FLAG- SQSTM1/p62 fusion protein or a HA-TBK1 fusion protein, respectively. All were provided as frozen bacterial stocks (30 % glycerol), stored at -80°C. For vector maps see appendix.

2.1.2. Plasmid DNA preparation

Plasmids were prepared by following the QIAGEN® kit minipred protocol. This method is based on alkaline lysis of bacteria, followed by adsorption of DNA on a silica gel membrane in the presence of high salt (www.biocompare.com).

Before starting, bacteria were grown in 10 ml culture of LB broth/ampicillin medium overnight and cell pellet was collected by centrifugation (5 minutes; 3000 rpm). After removing the supernatant, the pellet was re-suspended using 250 μl of buffer P1, then the suspension was transferred to a microcentrifuge tube. To lyse the suspension, 250 μl of P2 was added and the tube was inverted between 4-7 times, resulting in a viscous and slightly clear solution. After a

maximum of five minutes, 350 µl of neutralisation buffer (N3) was added, followed by mixing immediately by inverting the tube around 4-7 times again. With this step, the solution become cloudy to avoid localised precipitation. Following centrifugation for 10 minutes at 13000 rpm, 800 µl of the supernatant was transferred to a QIAprep spin column, which was centrifuged for 60 seconds at 13000 rpm. The flow through was discarded and the column was washed using 750 µl of buffer PE with centrifugation for 60 seconds. The flow through was discarded and the same process was repeated twice more to remove residual wash buffer. The last step to collect the DNA involved placing the QIAprep spin column in clean 1.5 ml microcentrifuge tube, followed by addition of 50 µl of nuclease-free deionised water. After 1 minute, the tube was centrifugated for 1 minute at 13000 rpm and the eluant which contains the purified plasmid DNA was collected, and stored at -20°C. For buffers and reagents see appendix.

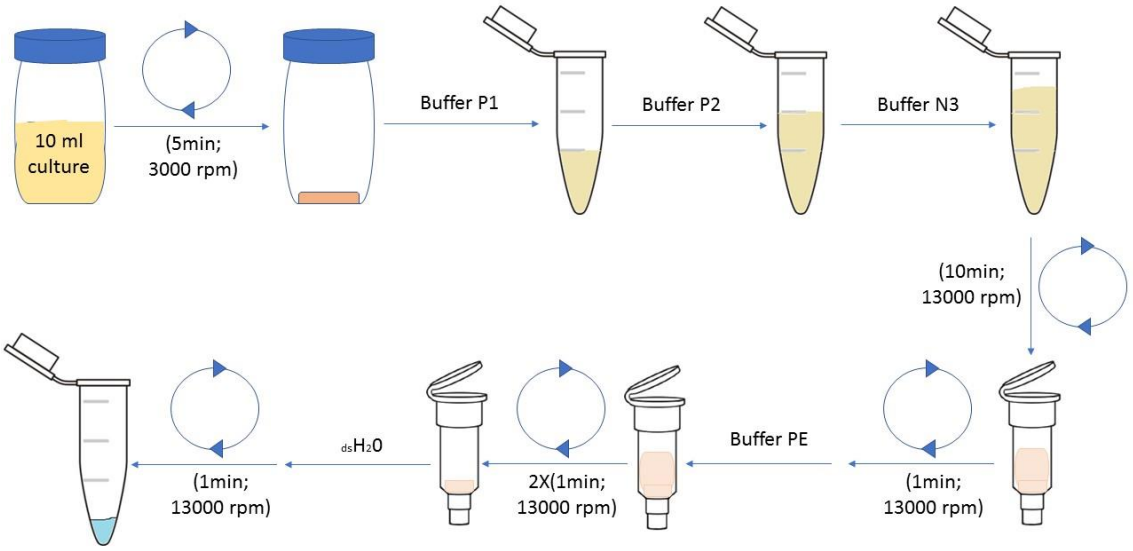


Figure 10. Schematic representation of plasmid DNA preparation procedure. All the procedures are explained in detail above (see section 2.1.2.)

2.1.3. Measurement of DNA concentration and purity

A NanoDrop (ND-1000) spectrophotometer (NanoDrop Technologies) was used to measure DNA concentration. 1 µl sterile deionised water was used to blank the spectrophotometer, then 1µl sample was introduced directly to the spectrophotometer. The numerical outcome of $A_{260/280}$ ratio on the spectrophotometer is used to determine the purity of the sample ($A_{260/280} \geq$ 1.8 indicates pure DNA, $A_{260/280} \leq 1.8$ indicates presence of impurities, such as proteins and aromatic compounds (for instance, phenol), while $A_{260/280} \geq 2$ indicates possible RNA impurities).

2.1.3. Storage of plasmid DNA

DNA samples which were prepared using the Qiagen purification kit (see 2.1.2), were kept at -20°C.

2.1.4. DNA Sequencing

All DNA sequencing was performed by the Biopolymer Synthesis and Analysis Unit (BSAU), School of Life Sciences, University of Nottingham. The sequencing was performed with the use of an ABI PRISM® 3130 Genetic Analyser, using dye terminator chemistry (Big Dye version 3.1). The sequences were analysed using the ebi.ac.uk 'Clustal Omega' alignment tool.

2.2. Mammalian cell culture methods

2.2.1. Cell handling

HEK293T cells which were obtained from ATCC were grown in DMEM growth medium (see appendix), which contains the necessary nutrients for cell culture. The cells were kept humidified in 75 cm^2 Corning cell culture flasks in a 5 % CO_2 incubator at 37 °C. The cells were split every 48 hours or when they were approximately 90 % confluent, with regular inspection for contamination.

2.2.2. Passaging cells

The cells were subcultured when they reached around 90% confluency. Firstly, the old DMEM media was discarded. Then, the cells were washed with 4 ml DPBS (see appendix), followed by introducing 2 ml of trypsin solution for 10-15 minutes to cells in the humidified 5 % CO_2 incubator at 37 °C. The detached cells were diluted at a ratio 1:12 with DMEM growth media, and kept humidified in the 5 % CO_2 incubator at 37 °C. Note that prior to splitting, EDTA-trypsin enzyme (see appendix) and the DMEM media were equilibrated to room temperature.

2.2.3. Thawing cells

Frozen cells stored in liquid nitrogen were thawed in a 37 °C water bath, and transferred to 10 ml of DMEM growth medium followed by centrifugation at 1000 rpm for 5 minutes. The pellets were re-suspended in a fresh 5 ml of DMEM growth medium and grown as usual in the humidified 5 % CO_2 incubator at 37 °C.

2.2.4. Counting cells with a haemocytometer

The cover slip and the counting chamber were cleaned carefully with ethanol and properly dried prior to performing this procedure. The cells were washed with DPBS, then were

detached from the flask using trypsin enzyme and diluted with DMEM to an appropriate dilution volume in order to avoid overloading the chambers (usually 1:2). Then the cover slip was placed on the haemocytometer followed by introducing 50 μl of the suspension carefully to both chambers of the haemocytometer. The suspension covered the whole chamber through capillary force. Average numbers of cells were counted using a light microscope as follows:

The haemocytometer is divided to several squares; since each square is equal to a volume of 0.1 mm^3 (10^{-4} cm^3), and 1 ml is equal to 1 cm^3, hence the total cell number per 1 ml solution was determined according to the following equation:

$$Cells/ml = (Average\ count) \times 10^4\ (chamber\ conversion\ factor)$$

$$Total\ cells = (Cells/ml) \times (original\ volume\ of\ solution)$$

2.2.5. Seeding cells

Around 70 % confluent cells (HEK293T) were split and seeded into 10 cm^3 dishes or 12 wells plate. An appropriate amount of the culture was added to the dishes in order to have 20x10^5 cells/dishes. Then, 10 ml of DMEM growth medium (see appendix) was added to each dish. Finally, the seeded dishes were grown as usual in the humidified 5 % CO_2 incubator at 37 °C.

2.2.6. Transient transfection/co-transfection based on non-lipid based transfection reagent

- **For 10 cm^3 seeded dishes:**

The cells were left to grow at least for 24 hours before performing transient co-transfection of the exogenous plasmids. This was achieved by introducing with gentle mixing 1.5 or 3 μg of each of the plasmids in separate Eppendorfs into a mixture of free medium (Opti-MEM; see appendix) and transfection reagent, LT1 GeneJuice (Novagen; composed of non-toxic cellular protein and a small amount of novel polyamine) which had been incubated at room temperature for 10 minutes in advance (100 μl free medium and 3 μl LT1 per 1 μg of plasmid) and incubating for 30 minutes at room temperature. Next, an appropriate amount of the mixture to transfect with 1.5 or 3 μg of DNA was added to each dish. Finally, the cells were incubated in the humidified 5 % CO_2 incubator at 37 °C for at least 24 hours before applying any treatment. Each transfection was performed in duplicate.

- **For 12 well seeded plates:**

The cells were left to grow at least for 24 hours before performing transient co-transfection of the exogenous plasmids. This was achieved by introducing with gentle mixing 125 ng or 250 ng of each of the plasmids in separate Eppendorfs into a mixture of free medium (Opti-MEM; see appendix) and transfection reagent, LT1 which had been incubated at room temperature for 10 minutes in advance (25 μl free medium and 0.375 μl LT1 per 125 ng of plasmid) and incubating for 30 minutes at room temperature. Then, an appropriate amount of the mixture to transfect with 125 or 250 ng of DNA was added to each dish. Finally, the cells were incubated in the humidified 5 % CO_2 incubator at 37 °C for at least 24 hours before applying any treatment. Each transfection was performed in duplicate.

2.2.7. Treatment of cells with H_2O_2

First, the medium was replaced for 10 ml of fresh DMEM growth medium. Then, an appropriate volume of H_2O_2 to have a concentration of 200 μM was added to each dish which were transfected 24 hours previously. Dishes were then incubated in the humidified 5 % CO_2 incubator at 37 °C for approximately 5 hours.

2.2.8. Scraping cells

The medium was removed from the dishes which were washed with 3 ml PBS. When the PBS was removed, 1 ml of RIPA with protease/phosphatase inhibitors (1:1000) (see appendix) was added and the dishes were scraped with a cell scraper on ice (during the scraping, the dishes were turned 90 °C to scrape the complete surface). Scraped cells were stored in an Eppendorf in the freezer at -20 °C.

2.3. Standard immunofluorescence method for DeltaVision microscopy

The principle of indirect immunofluorescence staining depends on laser excitation of a fluorescent dyes linked to specific secondary antibodies, followed by detecting the emitted light using a DeltaVision microscope. In this case, a wavelength of 488 nm (red) is used for the excitation of the fluorescent secondary antibody in complex with a primary antibody bound to antigens within the sample under study, resulting in the emission of green light. In addition, to facilitate efficient location and shape of the cells, the nucleus is stained with another fluorescent dye, in this case DAPI, which emits a blue light upon UV-excitation.

The procedure starts with the removal of DMEM from the cells. Once this was done, the cover slips were washed with 1 ml cold PBS for 5 minutes. Cells were fixed by incubating with 1 ml of

fresh cold 4 % formaldehyde for 15 minutes at room temperature and then the cells were quenched for 2X 5 minutes with 1 M glycine. next, the cells were washed with 1 ml of PBS for 5 minutes, followed by permeabilising with 0.2 % (v/v) Triton-X100 in PBS for 10 minutes at room temperature. Blocking of non-specific sites was carried out by incubating the cells with a PBS solution containing 0.2 % (w/v) BSA (99.9 % purity; Sigma-Aldrich) at room temperature for 30 minutes. Following the blocking step, primary and secondary antibodies were introduced to the cells as follows:

- The primary antibody mixture (250 μl mouse anti-SQSTM1/p62; see appendix) was introduced to the cells with a dilution ratio of 1:1000 in PBS and incubated for one hour at room temperature.
- The secondary antibody mixture (250 μl AlexaFluor488 anti-mouse; see appendix) was diluted in PBS (1:1000) and incubated for 1 hour at room temperature in the dark.

Between the primary and secondary antibodies and after the secondary antibody, the cells were washed three times with PBS. Finally, 20 μl mounting media with DAPI, which stains the nucleus, (VECTASHIELD mounting media; Vector Laboratories, Inc) was applied to the cover slips, followed by sealing the cover slips to the glass slides. Slides were kept at 4 °C in the dark until being visualised with a Delta-Vision microscope.

2.3.1. DeltaVision microscopy

Images were collected using a DeltaVision microscope, with a 40X objective lens, with around 20 averaged sequential scanning images collected. To deconvolute, analyse and process the images, we used Huygens software.

2.4. Protein extractions from bone

The procedure which was carried out was a modification of that described by *Schmidt-Schultz, T. et al. 2004.*

2.4.1. Extraction A

Bone samples were ground in a pestle and mortar at room temperature, being careful to collect all the resulting powder into a pre-weighed tube which was re-weighed to find the weight of the powdered bone samples. Then, an appropriate amount of Buffer A (see appendix) was added (1g bone/ 5 ml Buffer A). To finish, the samples were incubated by rotating overnight at 4 °C in the cold room.

2.4.2. Extraction B

The samples were re-pelleted by centrifugation at 13000 rpm for 1 minute at 4 °C. Next, the supernatant was removed and retained (extract A) at -20 °C. Then, the same volume of Buffer B (see appendix) was added to the pellet samples and these were incubated by rotating overnight at 4 °C in the cold room.

The following day, the samples were re-pellet by centrifugation at 13000 rpm for 1 minute at 4 °C again and the supernatant was removed and retained (extract B) at -20 °C. Pellets were then washed three times with 1 ml of autoclaved distilled water for 10 minutes. Between washes the samples were re-pelleted by centrifugation at 13000 rpm for 10 minutes at 4 °C, discarding the washes. After the last wash, as much of the final wash as possible was removed and the pellet was dried and stored at -20 °C.

2.4.3. TCA precipitation

The same volume of phosphate buffer as Buffer A and B was added (with inhibitors; 1:1000) (see appendix) to the pellet. This was resuspended and sonicated twice for 10 seconds each time and with 1 minute between each sonication. Next, the samples were re-pellet by centrifugation at 13000 rpm for 1 minute at 4 °C. An appropriate amount of TCA was added to a new Eppendorf (for 8 % TCA precipitation the amount of TCA was 8mg/ 100 μl phosphate buffer). Finally, the supernatant was added to the new Eppendorf with the TCA and stored at -20 °C, as was the final pellet. All processes were carried out on ice.

2.4.4. Collagenase digestion

The bone pellet samples were incubated by rotating overnight at 4 °C in 1.5 ml of bacterial collagenase digestion buffer (see appendix). Next, they were re-pellet by centrifugation at 13000 rpm for 1 minute at 4 °C and the supernatant was removed. An appropriate volume of bacterial collagenase digestion buffer containing 40 CDU bacterial collagenase was added and the samples were incubated rotating for 6 hours at 37 °C. Finally, the samples were re-pellet by centrifugation at 13000 rpm for 1 minute at 4 °C and the supernatant was removed and retained (collagenase extract). The collagenase-treated pellet was stored at -20 °C.

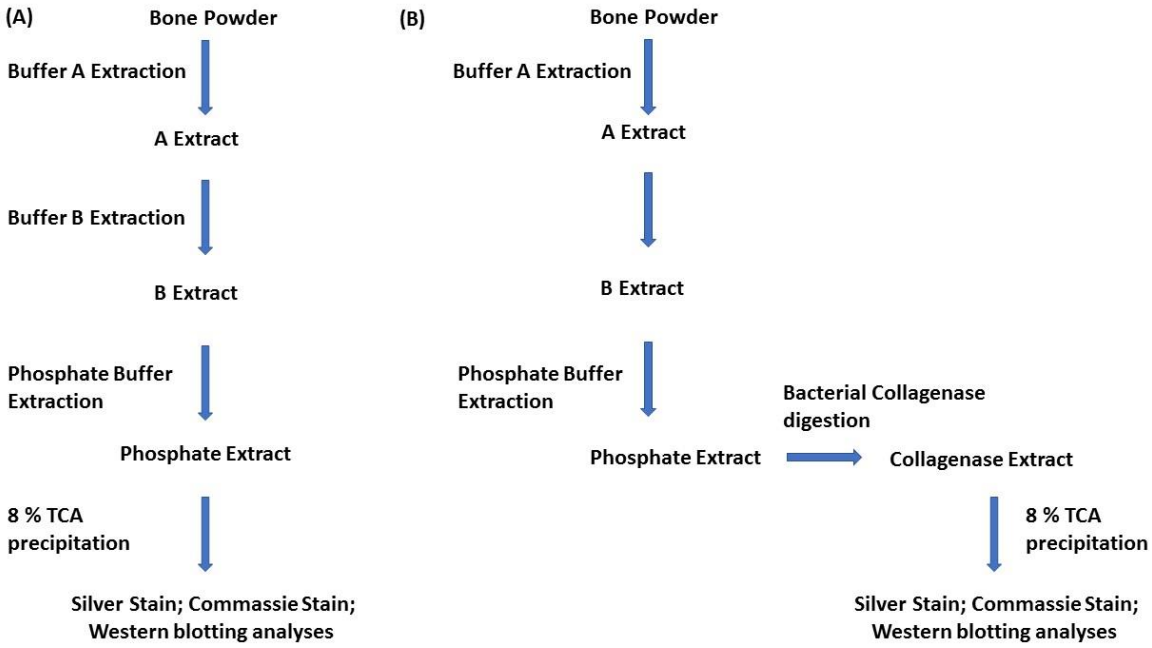


Figure 11. (A) Schematic summary of the general protein extraction procedure from bone. (B) Schematic summary of the bacterial collagenase digestion at the end of the extraction procedure. All the procedures are explained in detail above (see section 2.4.)

2.5. Western blotting and immunodetection techniques

2.5.1. Sodium dodecyl sulphate polyacrylamide-gel electrophoresis (SDS PAGE)

To generate a 5-20 % gradient gel a mixture of 5 % (10 ml) acrylamide resolving gel and 20 % (10 ml) acrylamide resolving gel, with the addition of 100 µl AMPS and 10 µl TEMED (added at the last step because catalysers of gel polymerisation) was poured using a gradient caster. Water-saturated butanol was immediately over-layed on to the gel, which was left for at least 45 minutes until polymerisation had taken place. Then, the butanol was removed using deionised water.

The stacking gel, which consisted in 5 ml stacking gel buffer, and 1 ml of 30 % acrylamide, with the addition of 100 µl AMPS and 10 µl TEMED, was poured, and a correct sized comb was inserted in order to form the loading wells. The gel was left for at least 10 minutes to polymerise, followed by the careful removal of the comb. After this, the gel was transferred to an ATTO electrophoresis unit (GRI), in which SDS PAGE running buffer (see appendix) is poured, and used to wash the lanes of the gel to remove any debris. Setting up the electrophoresis unit appropriately and loading the samples, gels were run at a constant current of 40 mA until the bromophenol blue dye reached the bottom of the gel.

To prepare the samples for their use in SDS PAGE, these were mixed with gel application buffer (GAB) (always the same volume of GAB and sample), heated at 95 °C for 5 minutes, and briefly spun-down.

2.5.2. Coomassie Blue staining of SDS PAGE gels

To perform the Coomassie staining procedure, the SDS PAGE gel was shaken carefully for at least 2 hours in Coomassie Blue staining solution (see appendix), then to remove background staining the gel was de-stained by incubation overnight with de-staining solution (see appendix)

2.5.3. Silver staining of SDS PAGE gels

To perform the staining procedure the PlusOne Silver Staining Kit from GE Healthcare was used. First, the gel was soaked in the fixing solution overnight at 4 °C. The next day, the fixing solution was removed and the sensitising solution was added. The gel was left for at least 1 hour. Next, the gel was washed 3 times for 5 minutes with distilled water. The silver solution was added and left shaking for 20 minutes. Then, the gel was washed again twice in distilled water but in this case for 1 minute each time. The next step was to add the developing solution and leave shaking for 2 to 5 minutes, this time dependent on the moment at which the bands reach desired intensity. When the bands reached this intensity, the developing solution was quickly removed and the stopping solution was added. The gel was kept in this for 10 minutes with shaking. Finally, the gel was washed 3 times with distilled water for 5 minutes each time. All the processes except the first step were carried out at room temperature.

2.5.4. Western blotting

When required, proteins resolved by SDS PAGE gel were transferred to nitrocellulose membrane (Hybond-C extra, GE Healthcare), by laying the gel on to the nitrocellulose membrane and layering between two western buffer-soaked filter papers. After elimination of the bubbles produced during the sandwiching of gel, the nitrocellulose membrane was directed to the positive anode of the western blotting unit (Fisher Scientific) then the sandwich was left over night to be transferred using a constant current of 40 mA. Ponceau staining was used to visualise reversibly the protein on the membrane (see 2.3.3). For the composition of transfer buffer see appendix.

2.5.5. Ponceau S staining of nitrocellulose membranes

The proteins on the nitrocellulose membrane were visualised by shaking the membrane slowly in Ponceau S (see appendix) solution for approximately 1 minute, followed by washing twice in deionised water, to eliminate background staining. For complete de-staining, the membrane washed several times with TBS-Tween 0.05 % (see appendix).

2.5.6. Immunodetection

The nitrocellulose membrane was blocked in blocking buffer (see appendix) for at least 3 hours at room temperature, in order to block non-specific binding sites. Next, the nitrocellulose membrane was incubated with the primary antibody overnight at 4 °C. Before the incubation with the second antibody, the nitrocellulose membrane was washed three times with TBS-Tween 0.05 % (see appendix), 5 minutes wash. The incubation with the second antibody was for 2 hours at room temperature. Then the nitrocellulose membrane was washed again with TBS-Tween for 5 minutes and three times for 5 minutes each time with TBS (see appendix).

Immunoreactive bands were visualised using high performance chemiluminescence film (HyperfilmTM, GE Healthcare), and the film developed by an automatic developing system (Curix 60 processor, Agfa Gevaaert Ltd.). Before exposure to the films, the nitrocellulose membrane was agitated gently for 1 minute in Enhanced Chemiluminescence Reagent (Western lightning TM, PerkinElmer Life Sciences) and sealed in cling-film. The emitted light from the membrane was left to react with the film for 1 minute or longer depending on the sensitivity of the antibodies.

2.5.7. Stripping membranes

To remove the antibodies from a membrane in order reuse it for a different western blot, the membrane was incubated with 10 ml of stripping buffer (Restore^{TM} PLUS Western Blot Stripping Buffer; ThermoFisher Scientific) for 30 minutes with shaking at 37 °C. Then the membrane was washed for 30 minutes with distilled water and the repeat immunodetection process (see 2.5.5.) was carried out.

2.6. General laboratory methods

2.6.1. Preparation of chemically competent bacterial cells

XL10-Gold ultracompetent *E. coli* bacterial cells were treated with $CaCl_2$ to make them competent for plasmid transformation. 300 ml of autoclaved LB broth (see appendix) was inoculated with 10 ml overnight cultures of XL10-Gold ultracompetent cells (obtained originally

from Strategene) and incubated at 37 °C in a shaking incubator until OD_{600} of the culture reached 0.4-0.5. This range is critical to obtain high quality competent cells. Then, the cells were cooled on ice for 20 minutes (it was necessary to keep all the solutions at 4 °C and on ice during mixing steps). The culture was centrifuged using a Beckman Avanti J-25 centrifuge, at 4000 rpm for 20 minutes at 4 °C and the supernatant was discarded, while the pellets were suspended with cold sterile $MgCl_2$ (0.1 M). The suspension was centrifuged again at 4000 rpm for 20 minutes at 4 °C, followed by discarding the filtrate and incubating the cells with cold sterile $CaCl_2$ (0.1 M) at 4°C for 20 minutes. The cells were harvested by centrifugation at 4000 rpm, 4 °C for 20 minutes. To finish, the cells were stored in 400 µl aliquots in a mixture of 86 % cold $CaCl_2$ and 14 % glycerol at -80 °C.

2.6.2. Oligonucleotide mutagenic primer preparation

The primers were designed following the instructions in the QuikChange® Site-Directed Mutagenesis Kit (Stratagene). Their features were:

- Both of the mutagenic primers (forward/reverse) contained the desired mutation and annealed to the same sequence on opposite strands of the plasmid.
- Primers were between 25 and 45 bases in length, with a melting temperature (T_m) of ≥ 78 °C. It was calculated following the next formula:

$$Tm = 81.5 + 0.41\ (\%\ GC) - (675/N) - \%\ mismatch$$

  Where:
  - N was the primer length in bases
  - Values for % GC and % mismatch were whole numbers
- The desired mutation was in the middle of the primer with around 10-15 bases of correct sequence on both sides.
- A minimum GC content of 40 %.
- They finished in one or more C or G bases.

Primers were synthesised by SIGMA, for sequences see Appendix.

2.6.3. Site-directed mutagenesis

The process followed the instructions in the QuikChange® Site-Directed Mutagenesis Kit (Stratagene). Note a control reaction was carried out for every mutation created in which the same protocol was performed, but without the addition of Pfu ultra II DNA polymerase to the reaction mixture.

A mixture of the following solutions was prepared in a thin-walled PCR tube, giving a final volume of 50 μl:

- 5 μl 10x Pfu ultra II reaction buffer
- A final concentration 40 ng/μl of the template (plasmid)
- A final concentration 125 ng/μl of oligonucleotide forward primer
- A final concentration 125 ng/μl of oligonucleotide reverse primer
- 1 μl (10 mM) of dNTP mixture
- Make up to a final volume of 50 μl $_dH_2O$.

The mixture was placed in a thermocycler, 1 μl Pfu ultra II was added and the following cycling programme was carried out:

Segment	Cycles	Temperature	Time
1	1	95 °C (initial denaturation step)	1 min
2	18	95 °C (denaturation step)	30 sec
3	18	55 °C (annealing step)	1 min
4	18	68 °C (extension step)	5 min
5	1	72 °C	10 min
6	Cooling reaction	4 °C	-

At the end of the last cycle, 1 μl of the restriction enzyme *Dpn1* was added to the mixture on ice to carry out digestion of the non-mutated template. To complete the following cycling programme was set up:

Segment	Cycles	Temperature	Time
1	1	37 °C (digestion step)	4 h
2	1	80 °C	20 min
3	Cooling reaction	4 °C	-

Finally, the mutated plasmid was transformed in XL10-Gold ultracompetent bacterial cells (see appendix).

2.6.4. Transformation of plasmid DNA to XL10-Gold® competent cells.

80 μl of XL10-Gold ultracompetent cells were mixed with 1/20 μl of the *Dpn1*-digested plasmid and left on ice for 30 minutes, followed by heat shocking the mixture at 42 °C, for 30 seconds and incubating on ice again for 5 minutes. The cells were inoculated into 800 μl sterile LB broth (without ampicillin), and incubated at 37 °C in a shaking incubator for around 45 minutes. The culture was spun down (7 seconds). The supernatant was removed and the pellet was re-suspended in 100 μl of LB broth (without ampicillin). Suspension was plated out on agar/LB broth plates with ampicillin (see appendix) and spread with a sterile spreader over the plate, followed by incubation overnight at 37 °C.

2.6.5. Protein expression

The pGEX-4T1 plasmid allows expression of the cloned protein (in this case SQSTM1/p62) fused at its N-terminal with GST in *E. coli* and confers ampicillin-resistance to the host cells which means that only the bacteria that contain the plasmid can replicate. Cells were grown overnight with shaking at 37 °C in 10 ml LB broth, with the addition of ampicillin (see appendix) (1:1000). The next day, 200 μl from the overnight culture were added to a new 10 ml ampicillin (1:1000)/LB broth and grown for 3 hours at 37 °C with shaking. Next, to induce recombinant gene expression IPTG (see appendix) was added to a final concentration of 200 μM, then the bacterial cells were grown for a further 3 hours at 37 °C. The pellet was collected by centrifugation and stored at -20 °C.

2.6.6. Bacterial storage

500 μl of 10 ml overnight cultures were made up to 500 μl with filter sterilised 30 % glycerol (see appendix) and stored in a cryovial tube at -80 °C.

2.6.7. Measurement of protein concentration using the BCA assay

This assay was first described by Smith et al. 1985. This assay is a detergent-compatible formulation based on bicinchoninic acid (BCA) for the colorimetric detection and quantitation of total protein. 9 standards (0, 25, 125, 250, 500, 750, 1000, 1500 and 2000), which were prepared from a stock solution (2 mg/ ml of BSA in the buffer used to prepare the protein under study) were used to generate a calibration curve. The unknown proteins were analysed with and without being diluted (1:10).

The assay was performed by mixing 200 μl of BCA reagent (see appendix) with 25 μl of each standard or unknown sample, followed by incubation for 30 minutes with shaking at 37 °C

(being covered). The standards and the unknown samples were measured in duplicate by introducing the samples to a microplate spectrophotometer (SpectraMax 340PC384) in 96 well plates (Falcon) and reading the absorbance at a wavelength of 562 nm.

2.6.8. Preparation of Control/Glutathione/Ubiquitin/LC3B-Sepharose

Cyanogen bromide-activated-Sepharose 4B (Sigma) was swollen for 30 minutes in 1 mM HCl solution, transferred to a polyprep colum (BioRad) and washed further in HCl. Then, the Sepharose was washed with 5 bed volumes of coupling buffer (see appendix). The Polyprep column was capped and the Sepharose incubated on a rotary mixer for 3 hours at 4 °C in a solution of ubiquitin or LC3B (5 mg of purified protein per 1 ml of Sepharose) in the case of ubiquitin/LC3 Sepharose and without any protein solution for the control Sepharose in coupling buffer. The Sepharose was washed extensively with coupling buffer and then incubated in 1 M ethanolamine solution on a rotary mixer overnight at 4 °C. The Sepharose was then washed alternatively with acetate and Tris buffer (10 bed volumes) (see appendix) at least 3 times with each was at least 30 minutes. Finally, the Sepharose was stored in column storage buffer (1:5) (see appendix) at 4 °C. Note commercial glutathione-Sepharose (GE Healthcare) was also included in the assay (see appendix).

2.6.9. Control/Glutathione/Ubiquitin/LC3-Sepharose binding assay

40 μl aliquots of control/glutathione/ubiquitin/LC3B-Sepharose beads (see 2.6.8.) were added to an individual Eppendorf, resuspended and equilibrated once in 1 ml TBS-Triton buffer (see appendix) for 5 min on ice. Then, the Eppendorfs with the Sepharoses were centrifuged for 1 minute at 2000 rpm. Bacterial supernatants (100 μl; derived by sonicating the pellet of a 10 ml culture prepared as in section 2.4.5. in 1 ml TBS-Triton buffer, and centrifugation at 13000 rpm in a microfuge) and 900 μl of equilibration buffer were added to each Eppendorf. Next, the Eppendorfs with the Sepharoses were incubated for 30 minutes at 37 °C with shaking to ensure complete binding. To eliminate unbound and nonspecific binding proteins the beads were washed three times in TBS-Triton buffer (1 ml) with centrifugation (1 min; 2000 rpm; 4 °C) between washes. The bound proteins were eluted using GAB, by heating at 95 °C for five minutes. The eluted proteins were analysed using SDS-PAGE (see 2.5.1.), and the bound GST-SQSTM1/p62 was detected by immunodetection (see 2.5.5.) with mouse anti-SQSTM1/p62 antibodies (see appendix).

CHAPTER 3: Disease mechanisms in 'modern' Paget's disease

3.1. Introduction

Numerous different mutations (>30) affecting the *SQSTM1* gene have been identified in patients with PDB, to date several of which have been studied at the level of protein function. Most of these mutations are localised within exon 8 of the *SQSTM1* gene and affect the UBA domain (residues 387-436) of the SQSTM1/p62 protein. As this region of SQSTM1/p62 is involved in the ubiquitin-binding ability of the protein, important for its roles in the regulation of RANK-NF-κβ signalling and cargo recognition for autophagy, the functional effects of many PDB mutations have been previously analysed using *in vitro* ubiquitin-binding (pull-down) assays. The mutations have been classified in two different groups depending on their effects in the ubiquitin-binding ability: those which led to a complete loss of ubiquitin-binding in these assays, and those which led to an impaired ubiquitin-binding ability (Cavey et al. 2006; Layfield et al. 2006). These findings led to the proposal of a unifying hypothesis that all PDB-associated mutations of SQSTM1/p62 cause loss or impairment of ubiquitin-binding, and this altered function is linked to disease aetiology (Cavey et al. 2006).

Limited current evidence points to a deregulation of autophagy in PDB aetiology. Firstly, SQSTM1/p62 is an autophagy receptor (Seibenhener et al. 2007) and certain ALS-linked mutations of *SQSTM1* are associated with autophagy defects in cell models (Goode et al. 2016). In addition, the *Sqstm1*-P394L mouse model of PDB (which mimics the human P392L mutant) shows skeletal defects alongside changes in LC3B lipidation in osteoclasts (Daroszewska et al. 2011). Together, this leads to the hypothesis that PDB mutations in the UBA domain of SQSTM1/p62 might lead to impaired autophagy with consequences for osteoclast formation and activity (Hocking et al. 2012). Our study was focussed on a novel PDB-associated UBA domain F406V mutation identified in *SQSTM1* carrier screening for the ZIPP clinical trial, which affects around 1% of *SQSTM1*-positive PDB patients. This amino acid is sited in a surface pocket which stabilises the hydrophobic core of the UBA domain, being part of and stabilising contacts in the 404-MGF-406 loop with ubiquitin. Impact of the mutation on autophagy-relevant protein function in various models was investigated.

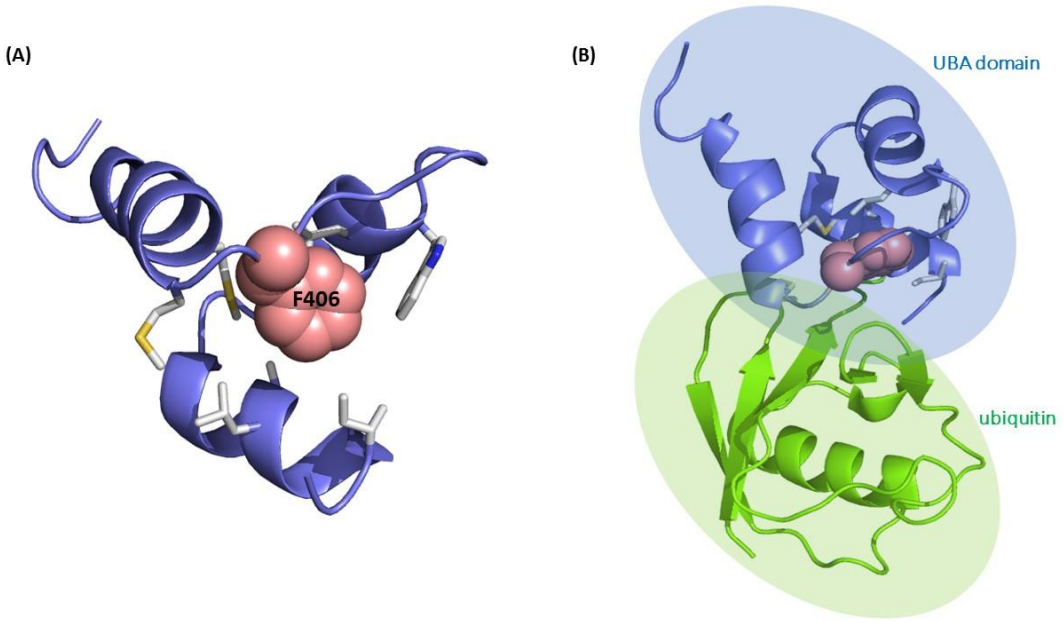


Figure 12. (A) Structure of the SQSTM1/p62 UBA domain. F406 sits in a surface pocket which stabilises the UBA hydrophobic core. **(B) Structure of the SQSTM1/p62 UBA domain (blue) in complex with ubiquitin (green).** F406 forms stabilising contacts in the MGF loop with ubiquitin so the F406V mutation is predicted to significantly destabilise the UBA domain. Figure courtesy of Prof. Mark Searle, School of Chemistry, University of Nottingham.

3.2. Results

3.2.1. Impact of F406V mutation on ubiquitin- and LC3B-binding properties of SQSTM1/p62

F406V mutant SQSTM1/p62 mutation was initially analysed in established *in vitro* ubiquitin-binding assays. In parallel, any indirect impact of the mutation on LC3B binding *in vitro* was also assessed, given that autophagy receptors require a functional UBA and LIR sequence in cells (Rea et al. 2014; Rogov et al. 2014; Ciuffa et al. 2015; Goode et al. 2016). Wild type SQSTM1/p62 and M404V mutant sequences were used as controls; the PDB-associated M404V mutation has previously been found to cause a loss of ubiquitin-binding of SQSTM1/p62 *in vitro* (Cavey et al. 2005).

3.2.1.1. Generation of prokaryotic expression constructs for F406V mutant SQSTM1/p62

A construct which allows wild type human SQSTM1/p62 to be expressed as a GST-fusion protein in *E.coli* was generated previously in the lab through introducing the *SQSTM1* cDNA into the multiple cloning site of the pGEX-4T-1 plasmid (Cavey et al. 2005). GST-SQSTM1/p62 M404V mutant was available in the lab, while the F406V mutation was introduced into the wild type sequence by site directed mutagenesis using the QuickChange® Site-Directed Mutagenesis kit (Stratagene). The mutant plasmid was analysed by DNA sequencing and resulting chromatograms were viewed using ChromasLite2 software. To confirm the presence

of the mutation, the sequence alignment with the wild type SQSTM1/p62 sequence was carried out using ClustalW2 [data not shown].

3.2.1.2. Effects of F406V mutation on ubiquitin- and LC3B-binding of SQSTM1/p62

To assess the effects of the F406V mutation on the interaction of SQSTM1/p62 with monoubiquitin and LC3B, *in vitro* pull-down assays were carried out (Cavey et al. 2005; Goode 2016). In this assay, the GST-tagged SQSTM1/p62 proteins are over-expressed in *E. coli* (see section 2.6.5.), followed by the precipitation of the bacterial supernatants containing the recombinant proteins with an excess of four types of beads: glutathione-Sepharose; control-Sepharose; monoubiquitin-Sepharose; or LC3B-Sepharose (Figure 13). The monoubiquitin-Sepharose beads have purified bovine ubiquitin covalently attached, the LC3B-Sepharose beads have also purified recombinant human LC3B covalently attached and the control-Sepharose beads are prepared in parallel without the addition of protein (see section 2.6.9.).

The total GST-SQSTM1/p62 protein available is indicated by binding to glutathione-Sepharose (through GST), the fraction of GST-SQSTM1/p62 protein able to bind ubiquitin through its UBA domain by binding to ubiquitin-Sepharose, the fraction of GST-SQSTM1/p62 protein able to bind LC3B through its LIR region by binding to LC3B-Sepharose, and non-specific binding is controlled for using the control-Sepharose beads. Bound proteins are eluted with gel loading buffer and detected by SDS PAGE followed by western blotting (anti-SQSTM1/p62). Loss of ubiquitin- or LC3B-binding function associated with any of the PDB mutants is indicated by a reduced immunoreactivity to GST-SQSTM1/p62 proteins precipitated by the ubiquitin- or LC3B-Sepharose respectively, relative to wild type.

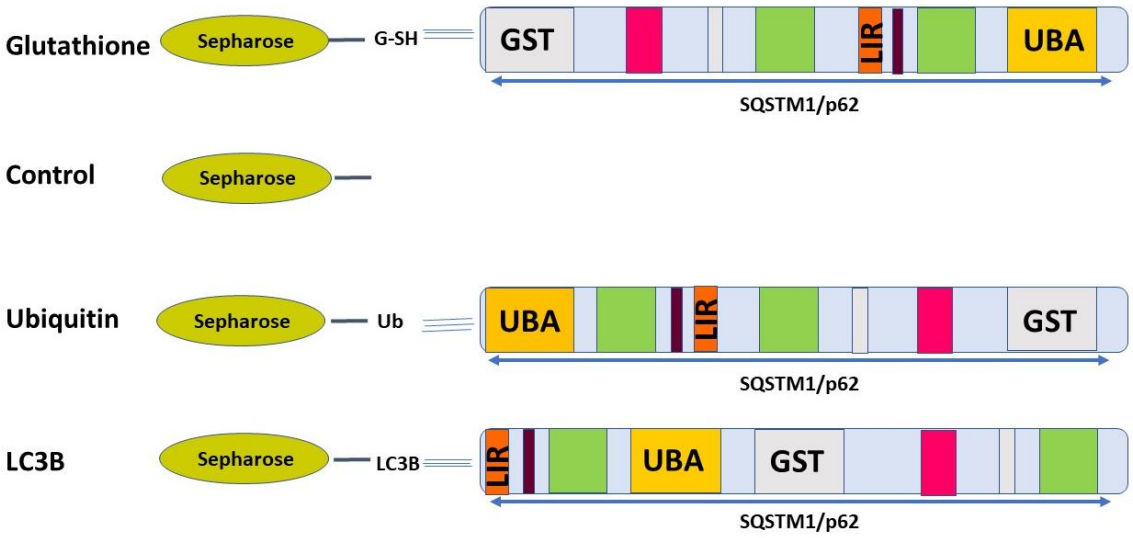


Figure 13. Schematic representation of ubiquitin and LC3B binding assay for GST-SQSTM1/p62 fusion proteins.

The SQSTM1/p62-ubiquitin and SQSTM1/p62-LC3B interactions depend on the non-covalent binding of the UBA domain and LIR region to covalently immobilised ubiquitin or LC3B proteins, respectively. When glutathione-Sepharose beads are used, the GST (Glutathione-S-Transferase)-tag binds non-covalently with immobilised glutathione. Control-Sepharose is used to control for non-specific binding to the beads. Bound GST-SQSTM1/p62 protein is detected by western blotting.

The assay was performed at 37°C (Cavey et al. 2005) on at least three independent occasions and representative blots are shown. The F406V mutant, like the previously characterised M404V mutant (Cavey et al. 2005), was not able to bind immobilised monoubiquitin. In contrast, neither mutation (M404V and F406V) affected the ability of SQSTM1/p62 to bind LC3B, consistent with their location outside of the LIR region (Figure 14).

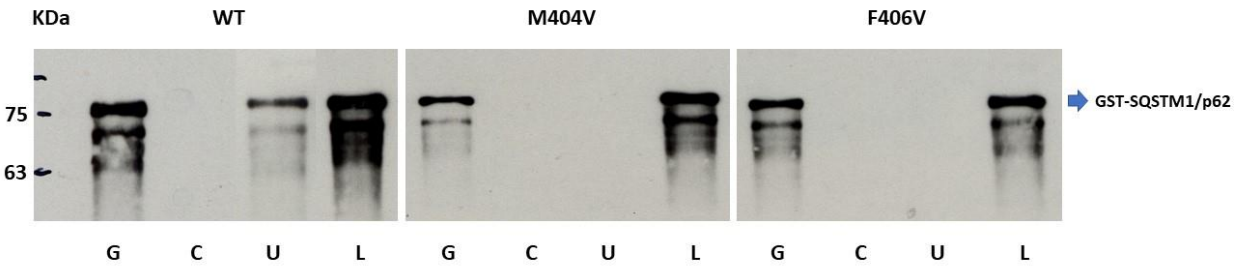


Figure 14. Effects of the PDB-associated F406V and M404V UBA domain mutations on ubiquitin- and LC3B-binding of GST-SQSTM1/p62 *in vitro.*

M404V, F406V or wild-type (WT) GST-SQSTM1/p62 as indicated was expressed using XL10-gold ultracompetent cells. The GST-tagged proteins were used in pull-down assays at 37 °C. Bacterial lysates containing the GST-SQSTM1/p62 fusion proteins were incubated with glutathione-Sepharose (G), control-Sepharose (C), ubiquitin-Sepharose (U), and LC3B-Sepharose (L) beads. Captured proteins were detected by western blotting (anti-SQSTM1/p62 antibody). Proteins in the (G) lanes were precipitated *via* the GST-glutathione interaction, and (U) as well as (L) lanes via the UBA-ubiquitin or LIR-LC3B interaction respectively. The wild type SQSTM1/p62 and the PDB-associated M404V mutants were used as controls. The M404V mutation has previously been shown to cause complete loss of ubiquitin-binding function in similar assays. Data are representative of at least three independent experiments.

3.2.2. Impact of PDB-associated SQSTM1/p62 mutations on cellular autophagy phenotypes

Following our initial analyses of the ubiquitin- and LC3B-binding ability of SQSTM1/p62 proteins using *in vitro* binding assays, we extended our study to examine the effects of SQSTM1/p62 and certain other PDB mutants in autophagy in a cellular context under different conditions. This extended work included three additional UBA domain-associated PDB mutations: E396X (truncating), P392L and G425R.

For these studies, we took advantage of earlier published work which showed that when transfected into mammalian cells, SQSTM1/p62 forms cytoplasmic bodies which are presumed to represent a combination of membrane-confined autophagosomes and membrane-free aggregates. Certainly, for the former a 'functional' UBA domain as well as an LIR region are necessary for the formation of these structures and their subsequent clearance by autophagy (Rea et al. 2014; Rogov et al. 2014; Ciuffa et al. 2015; Goode et al. 2016). In addition, studies have shown that transfected SQSTM1/p62 exhibits similar cellular phenotypes in a wide range of cell lines, including human HEK293T and U2OS cells (Bjorkoy et al. 2005). For our studies, we selected HEK293T cells which are human embryonic kidney cells, as a model system. Initially, effects of the F406V mutation on the gross SQSTM1/p62 cellular phenotype was determined. To examine the effects of over-expression of PDB mutant SQSTM1/p62 sequences on autophagy, cells were transiently transfected with SQSTM1/p62 sequences using

immunocytochemistry (ICC) assays and then western blotting for autophagy markers (LC3-I and LC3-II) was performed (Rogov et al. 2014; Ciuffa et al. 2015).

3.2.2.1. Generation of eukaryotic expression constructs for PDB mutant SQSTM1/p62 proteins.

A construct which allows wild type human SQSTM1/p62 to be expressed as a His-FLAG-SQSTM1/p62 fusion protein in HEK293T cells was generated previously in the lab through introducing the *SQSTM1* cDNA into the multiple cloning site of the pcDNA3.1 plasmid. His-FLAG-empty vector as well as certain SQSTM1/p62 mutants were already available in the lab, while the F406V mutation was introduced into the wild type sequence by site-directed mutagenesis using the QuickChange® Site-Directed Mutagenesis kit (Stratagene). The mutant plasmid was analysed by DNA sequencing and resulting chromatograms were viewed using ChromasLite2 software. To confirm the presence of the mutation, the alignment with the wild type SQSTM1/p62 sequence was carried out using ClustalW2 [data not shown].

3.2.2.2. Cellular phenotypes of transfected His-FLAG-SQSTM1/p62 and F406V mutant in HEK293T cells

The expression and subcellular localisation of the SQSTM1/p62 F406V mutant was first investigated to determine any effects on cellular phenotype, since a previous study using HEK293T cells transfected with GFP-tagged SQSTM1/p62 suggested that some PDB mutants, such as P392L, form larger inclusion bodies than those associated with the wild type protein (Leach et al. 2006). A later study failed to detect a significant difference in cellular phenotypes for a range of SQSTM1/p62 mutants (not including F406V) expressed as His-FLAG fusions in U20S cells (Najat et al. 2009), with the exception of the E396X truncating mutant which displayed very diffuse staining.

In this study, the localisation of endogenous SQSTM1/p62 was also performed to ensure that the subsequent expression of transfected proteins was associated with cellular phenotypes that were physiologically relevant. Transfected wild-type SQSTM1/p62 was analysed alongside the F406V mutant. HEK293T cells were transiently transfected with 500 ng of His-FLAG-SQSTM1/p62 or F406V mutant for 24 hours and fixed with formaldehyde. Mouse anti-SQSTM1/p62 was used as a primary antibody with anti-mouse Alexafluor 488 as secondary. In the case of HEK293T cells without ectopic expression of SQSTM1/p62 the procedure was the same but without transfection (see sections 2.2.6. and 2.3.).

The specificity of the secondary antibody was investigated after transfection of HEK293T cells with wildtype His-FLAG-SQSTM1/p62 as a control. Transfected cells were treated with an anti-mouse Alexafluor 488 secondary antibody, whilst primary antibody was omitted. Green channel of the collected images showed no evidence of non-specific binding of secondary antibody (Figure 15).

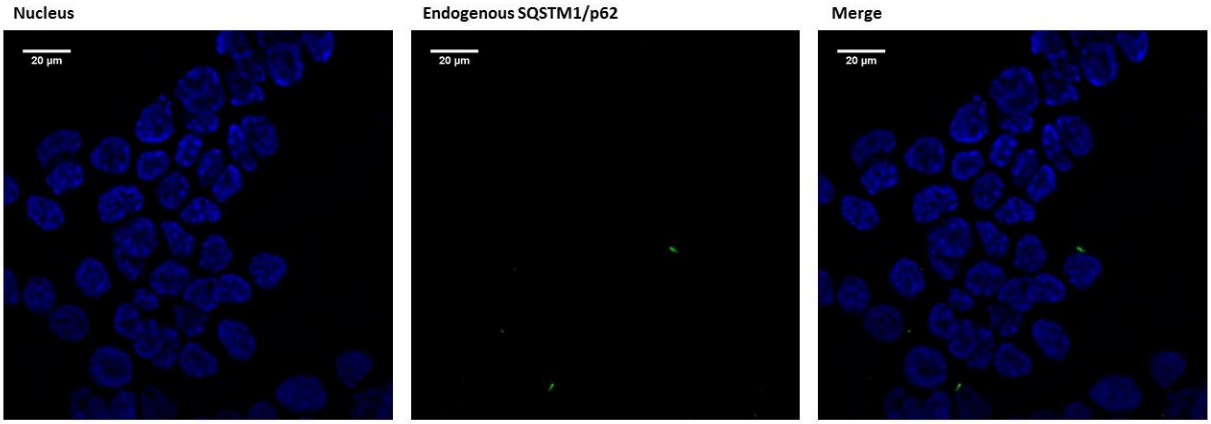


Figure 15. Specificity of secondary antibody

HEK293T cells transfected with wild type His-FLAG-tagged SQSTM1/p62 plasmid for 24 hours were fixed with formaldehyde. Cells were treated with an anti-mouse Alexafluor 488 secondary antibody, whilst primary antibody (anti-SQSTM1/p62) was omitted. A mounting medium containing DAPI was used for nuclear staining. All images were collected with a 40x Oil objective lens, with scale bar as indicated. Green channel of the collected images showed no evidence of non-specific binding of secondary antibody.

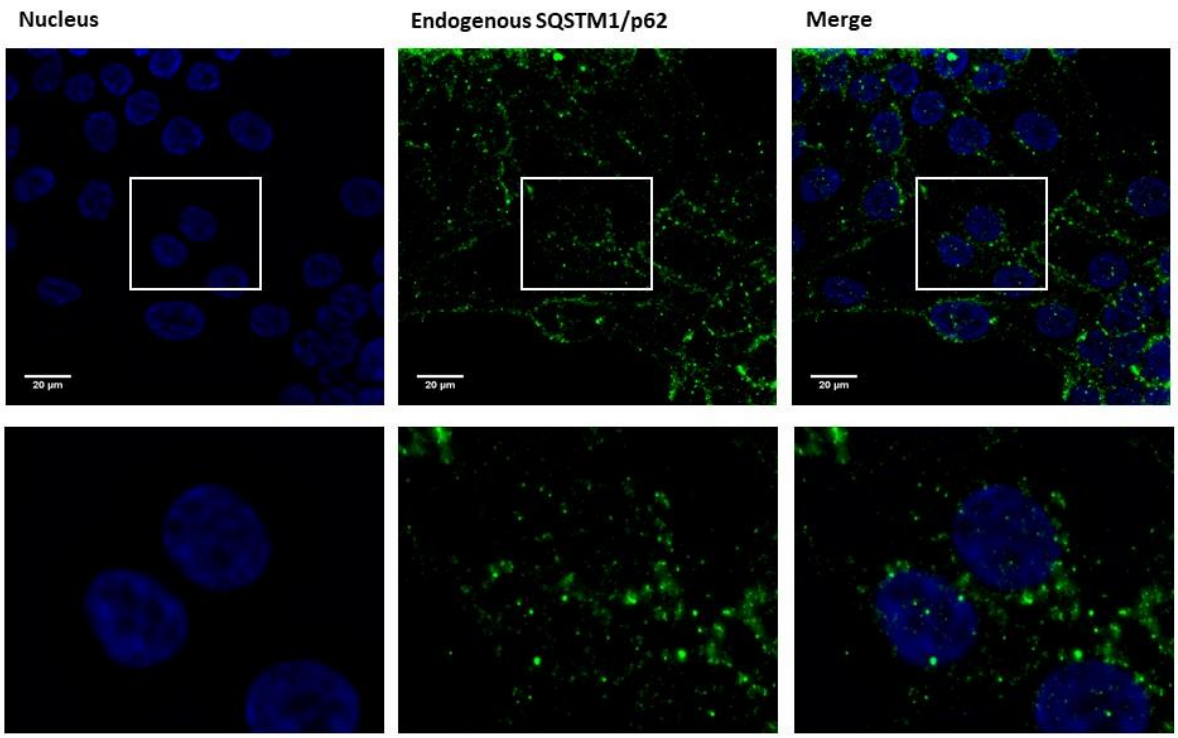


Figure 16. Representative examples of localisation of endogenous SQSTM1/p62 in HEK293T cells

HEK293T cells (not transfected with SQSTM1/p62 plasmid) fixed with formaldehyde were probed using an anti-SQSTM1/p62 primary antibody and stained green using an anti-mouse Alexafluor 488 antibody as secondary. A mounting medium containing DAPI was used for nuclear staining. All images were collected with a DeltaVision microscope using a 40x Oil objective lens, with scale bar as indicated.

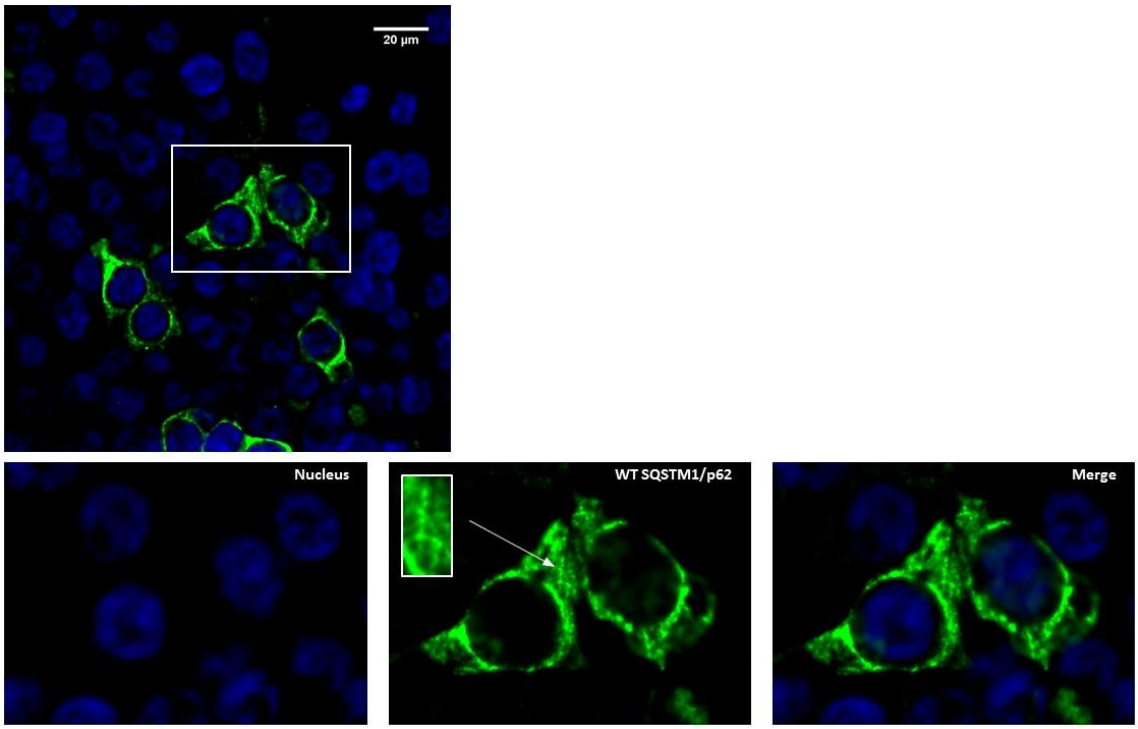


Figure 17. Representative examples of wild type His-FLAG-SQSTM1/p62 localisation in HEK293T cells

Wild type His-FLAG-SQSTM1/p62 was transfected into HEK293T cells which after 24 hours were fixed with formaldehyde. Detection of SQSTM1/p62 was performed using an anti-SQSTM1/p62 mouse antibody as primary and an anti-mouse Alexafluor 488 as secondary. A mounting medium containing DAPI was used for nuclear staining. DeltaVision microscopy images were collected using a 40X Oil objective lens, with scale bars as indicated. Rectangles represent electronic magnifications of a puncta area.

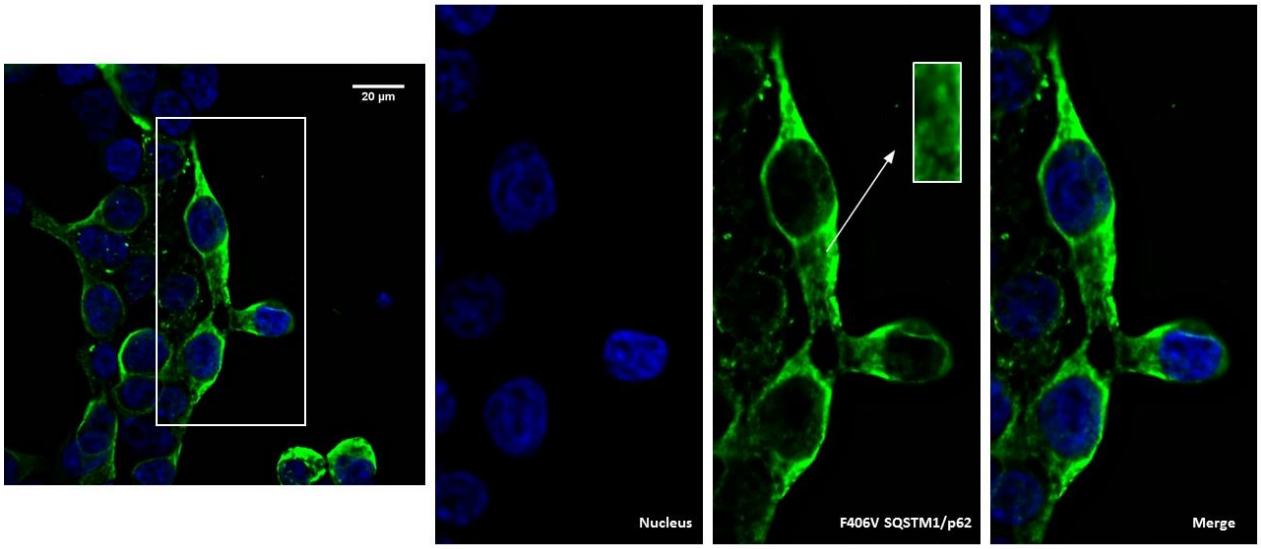


Figure 18. Representative examples of F406V mutant His-FLAG-SQSTM1/p62 localisation in HEK293T cells

F406V mutant His-FLAG-SQSTM/p62 was transfected into HEK293T cells, which after 24 hours were fixed with formaldehyde. Detection of SQSTM1/p62 was performed using an anti-SQSTM1/p62 mouse antibody as primary and an anti-mouse Alexafluor 488 as secondary. A mounting medium containing DAPI was used for nuclear staining. DeltaVision microscopy images were collected using a 40X Oil objective lens, with scale bars as indicated. Rectangles represent electronic magnifications of a puncta area.

Endogenous SQSTM1/p62 staining (Figure 16) was noted as small cytoplasmic bodies, presumably representing autophagosomes, as previously reported (Biorkoy et al. 2005). Transfected wild type SQSTM1/p62 (Figure 17) showed cytoplasmic bodies varying in their size and shape as in previous studies (Najat et al. 2009), but generally punctate in nature. In contrast F406V mutant SQSTM1/p62 (Figure 18) showed a much more diffuse staining throughout the cytoplasm, although still some cytoplasmic bodies could be differentiated. Increased staining towards the plasma membrane was also evident for the mutant. Although detailed quantitation was not performed, overall a subjective visual assessment indicated distinct differences in cellular phenotype between the wild type and F406V mutant SQSTM1/p62-transfected cells, which may indicate differences in autophagosome formation. Figures 16-18 also suggest the transfection efficiency was higher for the F406V mutant SQSTM1/p62 compared to the wild type protein; failure to visualise SQSTM1/p62 in all transfected cells supports the notion that transfected (rather than endogenous) protein was principally detected. In addition, Flag antibody could have been used to specifically recognise overexpressed protein.

3.2.2.3. Optimisation of His-FLAG-tagged SQSTM1/p62 transfections for LC3B lipidation assays in HEK293T cells

To determine the optimum concentration of plasmids to use in subsequent experiments examining the effects of mutant SQSTM1/p62 expression on autophagy markers (LC3B lipidation) four different concentration of His-FLAG-WT-tagged SQSTM1/p62 plasmid were selected and transfected into HEK293T cells. Approximately 24 hours after transfection, cells were lysed using RIPA buffer (see section 2.2.8.). A BCA assay was performed to allow equal amount of proteins from each lysate (40 μg) to be analysed by SDS PAGE and western blotting (see section 2.6.7.; 2.5.1.; and 2.5.4. respectively). Three different antibodies were used for the western blotting: anti-SQSTM1/p62 mouse; anti-actin (housekeeper) and anti-LC3B antibodies.

The representative western blot shown in Figure 19 indicates that 3 μg or 1.5 μg of DNA is sufficient to allow detection of transfected His-FLAG-SQSTM1/p62 in HEK293T cells (with concurrent detection of endogenous LC3-I/LC3-II proteins). Reduced levels of LC3-I and LC3-II associated with transfection of 6 μg of plasmid may represent an activation of autophagy imparted by transfected His-FLAG-SQSTM1/p62.

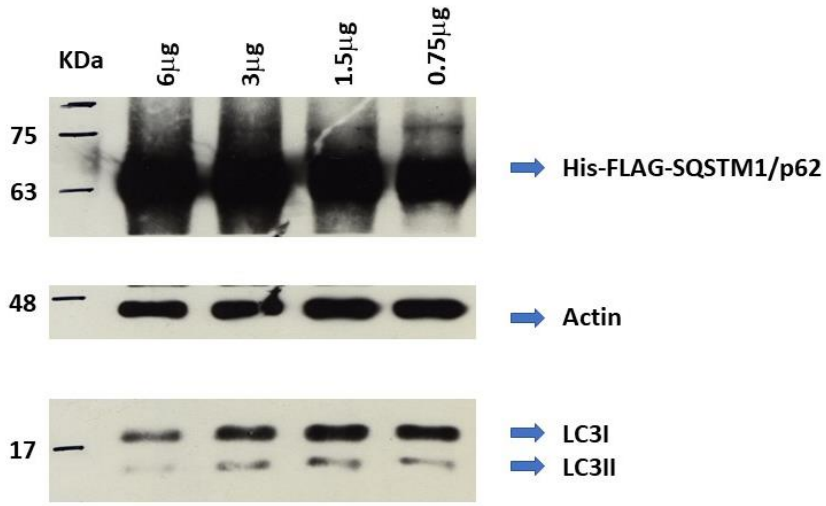


Figure 19. Expression levels of transfected His-FLAG-SQSTM1/p62 and endogenous LC3B proteins in HEK293T cell lysates

HEK293T cells were transfected with different amounts of His-FLAG-SQSTM1/p62 (wild type sequence in pcDNA3.1, amount of plasmid as indicated). After 24 hours, the medium was changed and, after 48 hours from transfection, the cells were lysed as detailed in section 2.2.8. and equal amount of proteins from each cell lysate were then analysed by western blotting (anti-SQSTM1/p62; anti-actin; anti-LC3B antibodies). Due to each antibody having a different reactivity, the dilution for each one was also different: anti-SQSTM1/p62 mouse (1:5000), anti-actin (1:30000) and anti-LC3B (1:500). Anti-actin antibody was used as control to confirm approximately equal loading of cell lysates. Data are representative of at least two independent experiments.

3.2.2.4. Effects of expression of PDB-associated mutant SQSTM1/p62 on autophagy markers under conditions of oxidative stress in HEK293T cells

Reactive oxidative species (ROS) are highly reactive and toxic and can lead to cell death by causing damage to proteins, lipids, carbohydrates, and DNA. Under oxidative stress (excess ROS), autophagy has been demonstrated to be induced as a defensive mechanism in several cell types (Scherz-Shouval et al. 2007; Xiong et al. 2007). We assessed the effects expression of PDB-associated SQSTM1/p62 mutants on basal and oxidative stress-induced autophagy (read-out LC3B lipidation) in HEK293T cells. In this case H_2O_2 was used as an as oxidative agent.

HEK293T cells were seeded and, after 24 hours, they were transfected with 3 µg of required His-FLAG-SQSTM1/p62 construct (pcDNA3.1, two dishes per plasmid). 24 hours later, the medium was changed and, after 48 hours from transfection, half of the dishes (one dish of each related plasmid) were treated for 5 hours with H_2O_2 in serum free media to induce oxidative stress, then lysed and analysed by immunoblot analysis for SQSTM1/p62, actin and, LC3B (Figure 20). The untreated cells were maintained in parallel for the same time period.

Proteins were harvested and before analysing the samples by SDS PAGE and western blotting, a BCA assay was performed allow loading of equal amounts of total protein from each lysate (40 μg) (see section 2.6.7.). The levels of transfected SQSTM1/p62, endogenous actin and LC3B were then quantified and actin and LC3B levels were normalised to the untreated pcDNA3.1 empty vector control because HEK293T cells as has been said before contain endogenous SQSTM1/p62.

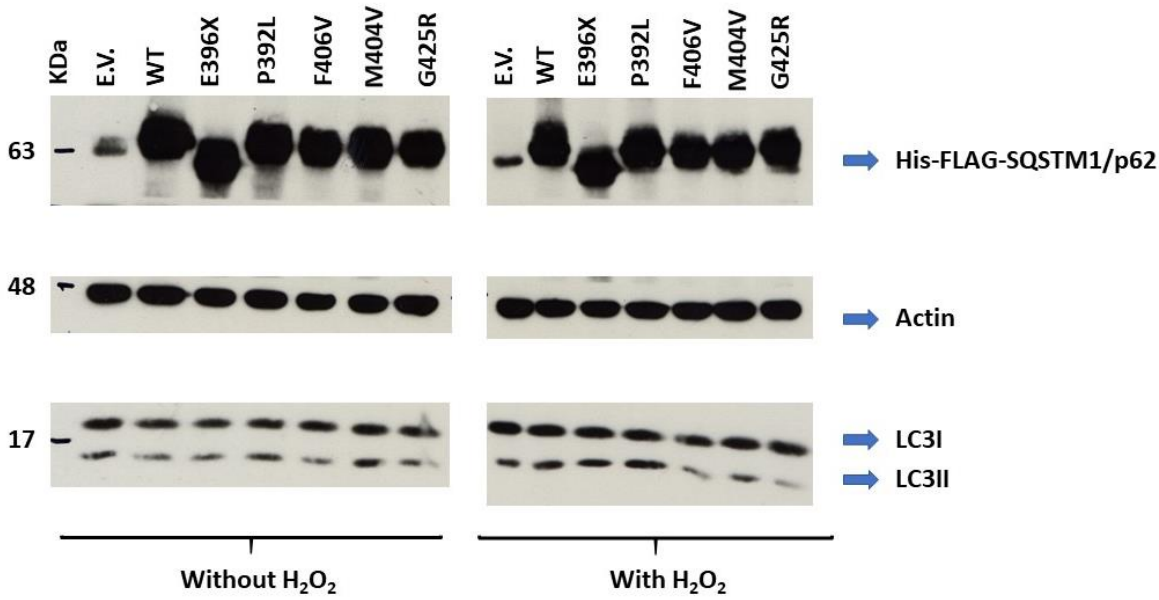


Figure 20. Expression levels of His-FLAG-SQSTM1/p62 and LC3B proteins in HEK293T cells transfected with 3 μg pcDNA3.1 plasmid as indicated, with cells treated with H_2O_2 or left untreated.

HEK293T cells were seeded in 10 cm^3 dishes ($20 \cdot 10^4$ cells/ml). After 24h, they were transfected with 3 μg of the indicated wild type or PDB-mutant SQSTM1/p62 plasmid. 24 hours later, the medium was changed and after 48 hours half of the samples were treated with H_2O_2 (200 μM) for 5 hours. Equal amount of proteins from each cell lysate were then analysed by western blotting (anti-SQSTM1/p62; anti-actin; anti-LC3B antibodies). Anti-actin antibody was used as loading control. The image represents results after 1 minute exposure (ECL). The band for SQSTM1/p62 in E.V. samples is the endogenous SQSTM1/p62 proteins in HEK293T cells. Data are representative of at least three independent experiments.

Densitometric analyses indicated that transfected SQSTM1/p62 levels were the same for the untreated samples and the H_2O_2-treated samples with no differences between the different transfected PDB-associated SQSTM1/p62 mutants and the wild type (data not shown). In the case of LC3-II, the levels (normalised to actin) were generally higher in the H_2O_2 treated samples compared to the untreated samples (data not shown). Notably, there were no significant differences in LC3-II/actin levels between the different PDB-associated SQSTM1/p62 mutant and the wild type extracts, in either untreated or H_2O_2 treated cells (Figure 21).

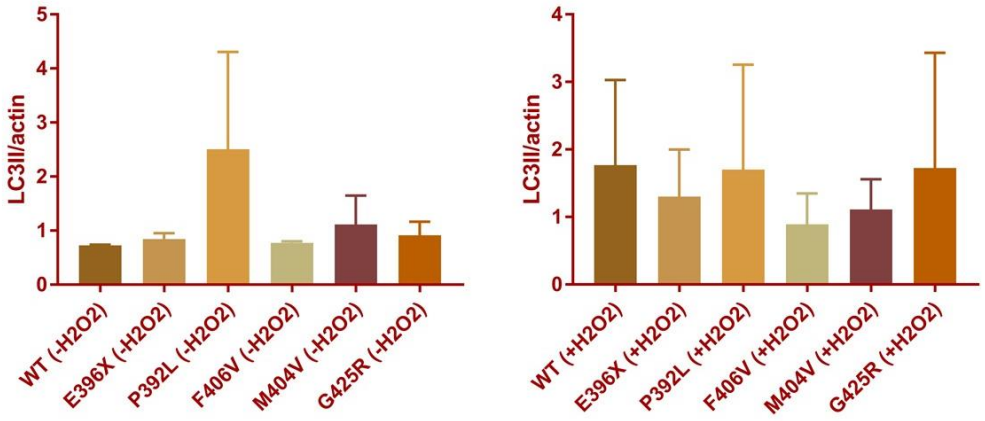


Figure 21. Effects of His-FLAG-SQSTM1/p62 expression on LC3B levels in HEK293T cells treated with H_2O_2 or left untreated.

Western blotting results were analysed using Fiji software and expressed as ratio of LC3-II/actin densitometric values relative to the empty vector control. Experiments were performed in duplicate, and assays were repeated on three independent occasions. A T-test (statistical analysis) was performed using GraphPad Prism software. Data are presented as mean values ± SE. No statistical significance was noted for mutants compared to wild type SQSTM1/p62 under either condition (n=3).

3.2.2.5. Effects of co-expression of PDB-associated mutant SQSTM1/p62 with TBK1 on autophagy markers in HEK293T cells

TBK1 belongs to the IKK family of kinases. IKKs can be divided into two different categories: canonical IKKs where are IKK-α and IKK-β, and IKK-related kinases where are IKK-ε and TBK1. While the canonical IKKs are involved in the induction of autophagy, the IKK-related kinase TBK1 mediates autophagy at later stages. Thus, members of the IKK family act sequentially in autophagy. One role of TBK1 in autophagy is the phosphorylation of the UBA domain of SQSTM1/p62. Pilli et al. 2002 demonstrated that the affinity of the UBA domain of SQSTM1/p62 for Lys48 and Lys63-linked polyubiquitin chains was strongly increased by the phosphorylation of Ser403 within the UBA domain, which also enhanced autophagic clearance of SQSTM1/p62 and polyubiquitinated protein aggregates (Figure 22).

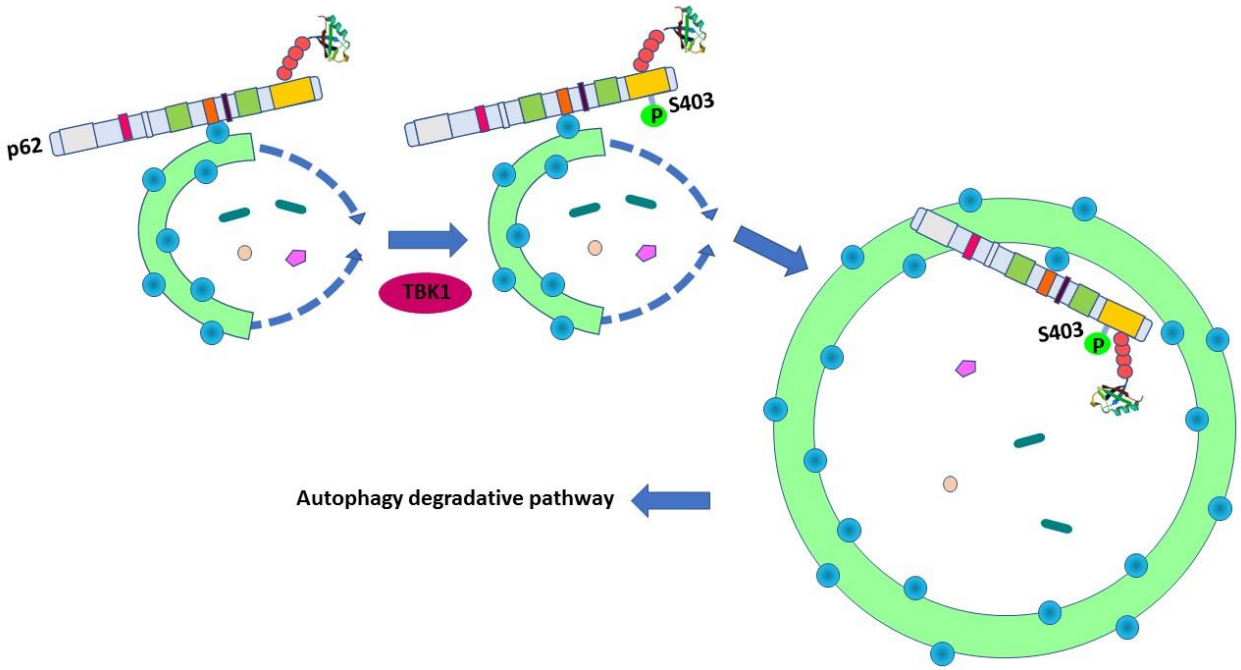


Figure 22. Schematic representation of the role of TBK1 with respect to SQSTM1/p62 and its connection with autophagy.

TBK1 phosphorylates SQSTM1/p62 at its Ser403 residue, which is crucial for the role of SQSTM1/p62 in autophagy. The affinity of the UBA domain of SQSTM1/p62 for Lys48 and Lys63-linked polyubiquitin chains is strongly increased by the phosphorylation of the Ser403 residue of SQSTM1/p62 which enhances autophagic clearance of SQSTM1/p62 and polyubiquitinated protein aggregates. When TBK1 is unavailable, SQSTM1/p62 is less efficiently removed by autophagy which leads to its accumulation in the cells.

We reasoned that co-expression of TBK1 with SQSTM1/p62 may help uncover autophagy defects associated with PDB mutant sequences. In this case, we also included a catalytically inactive TBK1 mutant (K38A) as a control. HEK293T cells were seeded and, after 24 hours, the dishes were co-transfected with 1.5 μg of required His-FLAG-SQSTM1/p62 plasmid (pcDNA3.1) plus 1.5 μg of TBK1 plasmid (pcDNA3.1, wild type or K38A mutant). 24 hours later, the medium was changed and, after 48 hours from the transfection procedure, cells were lysed (see section 2.2.8.) and a BCA assay was performed to allow loading of equal amount of total proteins from each lysate (40 μg) (see section 2.6.7.) for analysis by SDS PAGE and western blotting (Figure 23). The levels of transfected SQSTM1/p62 and endogenous actin and LC3B were then quantified by densitometry and actin and LC3B were normalised to the empty vector controls.

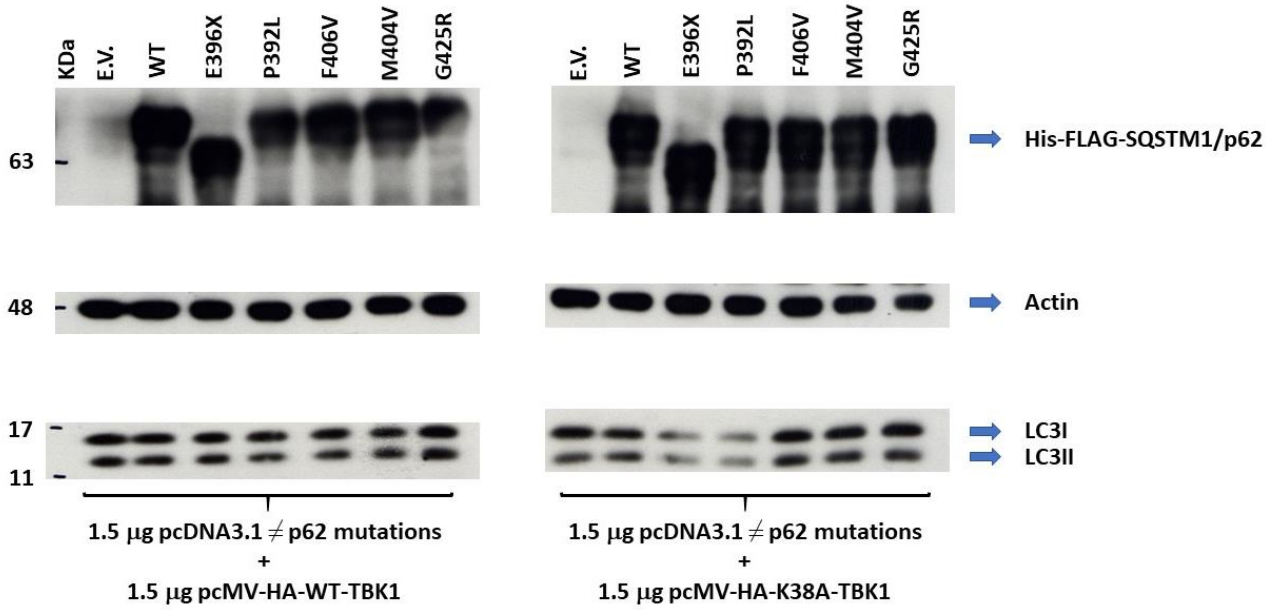


Figure 23. Expression levels of His-FLAG-SQSTM1/p62 and LC3B proteins in HEK293T cells co-transfected with wild type or catalytically inactive (K38A) TBK1

HEK293T cells were seeded in 10 cm^3 dishes ($20 \cdot 10^4$ cells/ml). After 24 hours, they were co-transfected with 1.5μg of the indicated wild type or PDB-mutant SQSTM1/p62 plasmid and 1.5μg of wild type or catalytically inactive TBK1 plasmid, as indicated. Equal amount of proteins from each cell lysate were then analysed by western blotting (anti-SQSTM1/p62; anti-actin; anti-LC3B antibodies). Anti-actin antibody was used as loading control. The image represents results after 1 minute exposure (ECL). Data are representative of at least three independent experiments.

Densitometric analyses indicated that transfected SQSTM1/p62 levels were the same for the wild type and mutant TBK1 co-transfections, with no differences between the different transfected PDB-associated SQSTM1/p62 mutants and the wild type (data not shown). Again, there were no significant differences in LC3-II/actin levels between the different PDB-associated SQSTM1/p62 mutant and the wild type extracts, in either wild type and mutant TBK1 co-transfections (Figure 24).

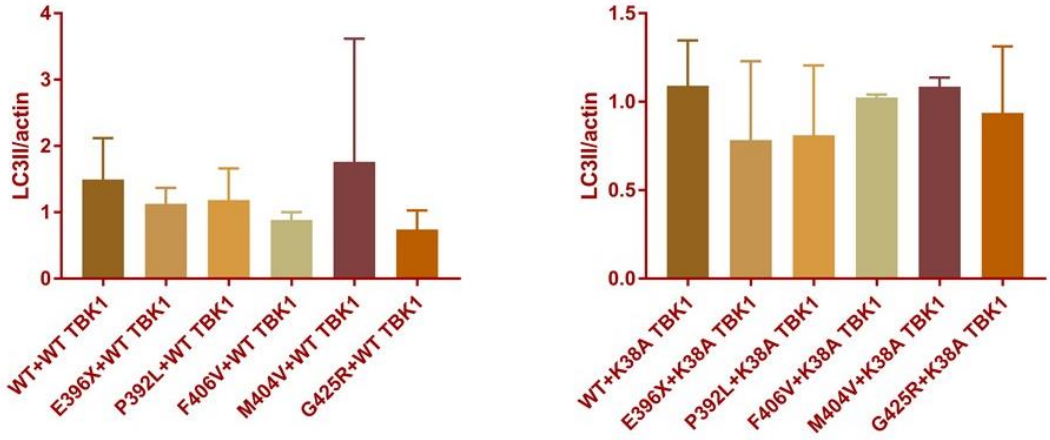


Figure 24. **Effects of His-FLAG-SQSTM1/p62 expression on LC3B levels in HEK293T cells co-transfected with wild type or catalytic inactive mutant of TBK1.**

Western blotting results were analysed using Fiji software and were expressed as percent LC3II/actin compared with the empty vector control. Experiments were performed in duplicate, and assays were repeated on three independent occasions. T-Test (Statistical analyse) was performed using GraphPad Prism software. Data are presented as mean values ± SE. No statistical significance was achieved (n=3).

3.3. Discussion

Autophagy has recently been shown to be crucial in bone homeostasis and disease with osteoclast, osteoblast, as well as osteocyte function mediated by proteins which are involved in autophagic protein degradation (Hocking et al. 2012). Different mutated genes have been identified in familial PDB patient and many of these are important regulators of osteoclastogenesis and also involved in autophagy e.g. *OPTN* (Liu et al. 2014) or *SQSTM1* (Layfield and Hocking 2014). SQSTM1/p62 is known to play a crucial role as an autophagy receptor selecting specific ubiquitinated substrate proteins for their incorporation into autophagolysosomes through a process that involves interaction of SQSTM1/p62 with the autophagy protein LC3. The interaction and sequestration of cargoes by SQSTM1/p62 as well as the delivery of SQSTM1/p62 to the autophagosome require the oligomerisation of SQSTM1/p62 through its PB1 domain, as well as, a functional LIR region and UBA domain (Rea et al. 2014; Rogov et al. 2014; Ciuffa et al. 2015; Goode et al. 2016). In this study, we investigated the effects of different *SQSTM1* mutations associated with PDB in the function of SQSTM1/p62 as autophagic receptor.

Firstly, we assessed the effects of a newly identified and uncharacterised PDB-associated UBA domain mutation of SQSTM1/p62, the missense mutation F406V, on the ubiquitin- and LC3B-binding function *in vitro*. This allowed a test of the proposal by Cavey et al. that all *SQSTM1*

mutations associated with PDB are associated with a loss or impairment of ubiquitin-binding function of the SQSTM1/p62 protein, indicating a possible unifying mechanism by which mutations of *SQSTM1* cause PDB (Cavey et al. 2006). Indeed, we found that the F406V mutation resulted in the loss of the ubiquitin-binding function of SQSTM1/p62 *in vitro*, however the LC3B-binding function was not affected by the mutation. The effects of the F406V mutation on ubiquitin-binding by SQSTM1/p62 can, at least in part, be explained from consideration of structural analyses of the UBA domain (Layfield et al. 2004). The F406V mutation involves a residue positioned in the hydrophobic patch of the UBA domain (Figure 10), which is the binding surface that contacts the corresponding hydrophobic surface in ubiquitin. Substitution of phenylalanine with the shorter side chain of valine presumably abolishes binding ability by disrupting interactions between the UBA domain and the ubiquitin surface.

During autophagy, the formation of autophagosomes which contain SQSTM1/p62 proteins linked to their ubiquitinated-cargoes occurs (Najat et al. 2009). An impaired autophagy leads to the accumulation of these structures which mature into inclusion bodies (Collet et al. 2007). Previous studies have shown that the inclusion bodies formed by PDB-associated mutated SQSTM1/p62 may be larger than those formed by the wild type protein (Leach et al. 2006). However, in accordance with Najat et al. 2009, we found no firm evidence that the F406V mutation leads to the formation of larger inclusion bodies in HEK293T cells, although generally the cellular phenotype of the F406V mutant SQSTM1/p62 in transfected cells was more diffuse and less punctate than in wild type expressing cells. The differences observed could be due to a combination of SQSTM1/p62 aggregates/inclusions as well as enlarged autophagosomes. Earlier investigations classified the SQSTM1/p62 cytoplasmic bodies in two populations depending on their size: large immobile cytoplasmic bodies (>0.5 μm) that were membrane-free structures and not related to endocytic vesicles; and small rounded highly mobile cytoplasmic bodies (<0.3 μm), which were suggested to be late endosomes or lysosomes (Biorkoy et al. 2005). Remarkably, all these SQSTM1/p62 bodies were ubiquitin-positive, consistent with the interaction of ubiquitin and SQSTM1/p62 *via* its UBA domain (Bjorkoy et al. 2005). Further, an important portion of the smaller rounded highly mobile SQSTM1/p62's cytoplasmic structures were shown to represent autophagosomes or autolysosomes (Bjorkoy et al. 2005). It would be interesting to perform co-localisation analyses of F406V mutant SQSTM1/p62 and ubiquitin as in previous studies (Najat et al. 2009) to confirm that a functional UBA domain (with respect to ubiquitin-binding) is required for the formation of ubiquitin-positive and SQSTM1/p62-positive cytoplasmic bodies.

We went on to assessed the effects of over-expression of different PDB associated mutants of SQSTM1/p62 (including F406V) on autophagy markers (LC3B) in HEK293T cells under different conditions. The first condition was oxidative stress. Once the generation of ROS exceeds the strategies by which cells regulate their intracellular ROS concentration, oxidative stress occurs and causes damage to cellular components such as proteins which has as consequence the induction of autophagy (Xiong et al. 2007). A local rise in H_2O_2 concentration has been demonstrated to lead to inactivation of Atg4 at the site of autophagosome formation, thereby promoting lipidation of LC3-I, an essential step in the process of autophagy, which has as last consequence an increased in the LC3-II levels (Scherz-Shouval et al. 2007). Our results support this general increase in the LC3-II levels under oxidative stress conditions, however, they did not show any difference in LC3 lipidation between the different mutations analysed indicating the mutations may not affect the function of SQSTM1/p62 as autophagic regulator.

The second condition examined was the co-expression of TBK1. TBK1 has been demonstrated to play a direct role in autophagy through the phosphorylation of autophagy receptors (Pilli et al. 2012). The role of TBK1 in autophagy has been more extensively studied with respect to the autophagy receptor OPTN (Li et al. 2016) where TBK1 was firstly demonstrated to phosphorylate directly OPTN to regulate its interactions with LC3-II as well as ubiquitinated cargoes promoting the autophagic clearance of dysfunctional proteins. For this function, the dimerisation of both TBK1 and OPTN in necessary and subsequent hetero-tetrameric complex formation (Morton et al. 2008) which is involved in the clearance of several intracellular microorganisms (Pilli et al. 2012; Sun et al. 2014). Later, Pilli et al. 2012 demonstrated how the phosphorylation of SQSTM1/p62 by TBK1 at Ser403 localised in the UBA domain increased the affinity for Lys48 and Lys63-linked polyubiquitin chains, promoting the autophagic clearance of SQSTM1/p62 and polyubiquitinated protein aggregates. However, we found no difference in LC3B lipidation in cells co-transfected with wild type or mutant SQSTM1/p62, and wild type or catalytically inactive TBK1.

These results suggest that the crude cell based assays may be insensitive to determine any differences in autophagy that may be imparted by PDB-associated mutations of SQSTM1/p62. Obviously more detailed investigation is needed to understand the potential role of PDB-associated *SQSTM1* mutations in the disruption of SQSTM1/p62 mediated autophagy. It would be interesting to try the same experiments using a better model system such as performing the experiments on a *SQSTM1*$^{-/-}$ background such that endogenous wild type protein does not interfere with or mask mutant phenotypes.

For now, we can only speculate that subtle effects on autophagy associated with *SQSTM1* (and other) variants predispose osteoclasts to a vulnerability, which over time may become exposed by, for example, an age-related decline in autophagy pathway activity, which may explain why most of those affected by PDB are over 50 years of age. Finally, the role of viruses and other environmental factors in PDB should not be disregarded to draw a combined theory for the disease aetiology because Taylor et al. 2009 have demonstrated how many viruses are able to escape mammalian autophagic systems and indeed impact on their function. Based on our results and current research on PDB pathogenesis, more detailed investigations are necessary to understand the molecular basis of PDB. Of interest autophagy proteins have been demonstrated to be involved in the regulation of secretory component of osteoclastic bone resorption (DeSelm et al. 2011); such non-canonical roles for autophagy complicate even more the understanding of PDB pathogenesis.

CHAPTER 4: Disease mechanisms in 'ancient' Paget's disease

4.1. Introduction

A curious feature of PDB is that the incidence and severity of the disorder have declined over the last 20-30 years (Rea et al. 2013) pointing to changes in unknown environmental factors relevant to disease aetiology during the same period. However, how the disorder has evolved over longer periods of time has not been directly addressed to date.

Norton Priory in Runcorn, Cheshire, is the largest monastic excavation in Europe and in recent years over 130 articulated skeletons have been uncovered at the site, dating back to the 12-15th century. Strikingly more than 20% of the adult remains in the Norton collection are affected by a bone disorder resembling PDB, compared to 1-2% in comparable excavations from the same period. Further, in affected individuals at Norton the disorder is much more extensive than in patients with 'modern' PDB, affecting numerous bones (in some cases the whole skeleton), and presents at a particularly young age, although bone deformities are mild. Given these profound differences a key question arises, were the Norton individuals really affected by PDB or some other related bone disorder not seen in present times?

An ongoing project in the lab aims to unlock the 'chemical memory' of ancient bones from the Priory, and specifically uses a combination of molecular approaches to investigate if the individuals were affected by an ancient form of PDB. A particular focus is on proteomic analyses of bone proteins with the goal of diagnosis of an ancient disease using protein sequence analyses alone.

4.2. Work leading up to the project

4.2.1. LC-MS/MS-based sequencing of ancient proteins from petrous bone

Previously in the lab, protocols were established (see section 2.4) to extract proteins preserved in bones from the Norton collection and to identify these by LC-MS/MS analyses. Initial analyses were performed (by Mr Barry Shaw) on a sample of petrous bone, part of the temporal bone in the skull, from a skeleton (Skeleton 101, SK101) with extensive PDB-like changes upon macroscopic and X-ray analyses. Petrous bone was selected as its high density gives maximum preservation of biomolecules over time (Dr. Turi King, personal communication). Remarkably, the 26 different proteins identified (tryptic digest, Orbitrap Velos, University of Leicester) within the complete final insoluble 'pellet' fraction from >2 unique peptide sequences included human SQSTM1/p62 (Table 1). To our knowledge, no other

paleoproteomic analyses have identified ancient SQSTM1/p62 protein sequences; this identification alone is strong evidence that the disorder within the Norton collection really was an ancient form of PDB. All other proteins identified were structural (collagens, intermediate filaments etc) and are common features of such analyses. Further, more targeted analyses of an SDS PAGE slice from a gel region of electrophoresed SK101 'pellet' within the molecular weight range of ancient SQSTM1/p62 protein (Table 1, 'Pellet (specific region)' and Figure 25A) also detected numerous human SQSTM1/p62 peptide sequences.

Table 1. Summary of the human proteins identified in different petrous SK101 extracts from at least two unique peptides (fragments) by LC-MS/MS.

'8% TCA' and 'Pellet' refer to different fractions from the extraction. 'Pellet (specific region)' refers to an SDS PAGE gel slice containing SQSTM1/p62. Trypsin sequences are derived from the enzyme used for sample digestion. Numbers relate to numbers of peptide sequences identified.

Proteins found by MS in petrous 1 (SK101) samples			
Protein	Number of fragments found (sequenced)		
	8% TCA	Pellet	Pellet (specific region)
Alpha-2-HS-glycoprotein OS	12	9	7
Collagen alpha-1(I) chain OS	27	18	14
Collagen alpha-1(II) chain OS	5	4	-
Collagen alpha-1 (V) chain OS	2	-	-
Collagen alpha-1(XXII) chain OS	3	-	-
Collagen alpha-2(I) chain OS	51	39	29
Collagen alpha-2(XI) chain OS	4	3	-
C-type lectin domain family 11 member A OS	3	4	-
Dentin matrix acidic phosphoprotein 1 OS	2	-	-
Insulin-like growth factor-binding protein 5 OS	2	-	-
Kininogen-1 OS	3	-	-
Keratin, type I cytoskeletal 10 OS	53	36	62
Keratin, type II cytoskeletal 1 OS	54	39	73
Keratin, type II cytoskeletal 72 OS	2	-	2
NudC domain-containing protein 2 OS	-	-	2
Osteomodulin OS	4	-	2
Osteopontin OS	3	-	-
Pigment epithelium-derived factor OS	2	-	-
Prothrombin OS	10	4	7
Sequestosome-1 OS	-	3	9
Serum albumin OS	5	2	6
SPARC OS	2	-	-
Thrombospondin-1 OS	4	4	2
Trypsin-1 OS	5	3	4
Ubiquitin carboxyl-terminal hydrolase 5 OS	-	-	2
Vitronectin OS	12	11	6

Additional targeted gel slice analyses of SK101 extracted protein using the more sensitive Orbitrap Luminos (elastase digest, University of Oxford) identified further peptides related to the human SQSTM1/p62 sequence (Figure 25B).



Figure 25. (A) Mass spectrometry confirms the ancient human SQSTM1/p62 protein sequence from petrous SK101 (Orbitrap Velos, University of Leicester). Sample was digested in gel with trypsin. Sequence in red detected by LC-MS/MS. **(B) Deeper mass spectrometry sequencing of ancient human SQSTM1/p62 protein from petrous SK101 (Orbitrap Luminos, University of Oxford)**. Sample was digested in gel with elastase. Sequence in red detected by LC-MS/MS. Highlighted are potential I/X elastase digestion sites within the sequence. [Note: human SQSTM1/p62 sequence from Gene ID: 8878].

Results derived from the Orbitrap Velos covered the 24% of human SQSTM1/p62 sequence; no mutations were detected although this error-intolerant approach only looked for the wild-type sequence. In contrast, results derived from the Orbitrap Luminos covered 48% of the human SQSTM1/p62 sequence. In this case an error tolerant search to look for missense mutations was employed, although none were detected. Notably however, no protein sequence after Ile395 (i.e. the majority of the UBA domain) was detected. SQSTM1/p62 contains four I/X sites (see Figure 25B), with three of these, I/R, I/Y, I/A all representing preferred elastase cleavage sites (R. Fischer, personal communication). In contrast, the Ile395-Glu396 site is least preferred by elastase. This led us to speculate that the extracted SQSTM1/p62 protein could be truncated at Ile396, making it equivalent to an E396X mutant previously identified in patients with familial PDB with a severe phenotype (Hocking et al. 2002). In other words, these data not only point to Norton individuals having been affected with PDB, but with *SQSTM1*-linked familial PDB.

4.2.2. Identification of ancient SQSTM1/p62 protein in petrous bone sample by western blotting

Further to the LC-MS/MS analyses of ancient petrous bone extracts (section 4.2.1), western blotting analyses were also undertaken with different SQSTM1/p62 antibodies. Consistent with the MS analyses, apparently intact SQSTM1/p62 was detected in SK101 petrous 'pellet' extracts with a mouse antibody (Figure 26) but not using a rabbit antibody (against the UBA domain, precise epitope unknown, data not shown). Ancient SQSTM1/p62 did not appear to be preserved (detected) in rib samples SK22, SK27, SK28, SK32 and SK37 (all from Norton skeletons affected by PDB-like changes, data not shown). Notably the ancient SK101 petrous SQSTM1/p62 gave two immunoreactive bands on western blot with the mouse antibody, both of which were higher molecular weight that cell culture-derived SQSTM1/p62 protein. Currently we interpret the higher molecular weight migration as representing some modification (post-translational or chemical) that may have occurred on the SQSTM1/p62 protein.

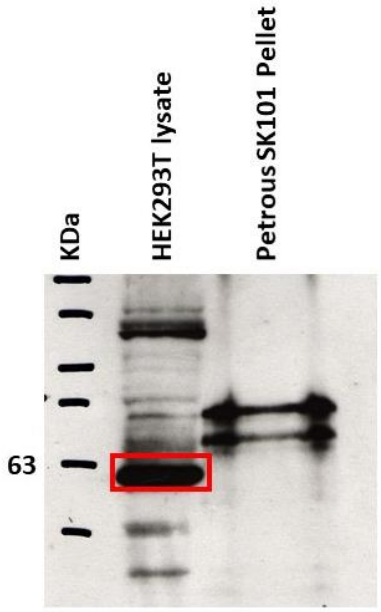


Figure 26. Ancient SQSTM1/p62 protein from SK101 petrous was detected by western blotting using an anti-SQSTM1/p62 mouse antibody.

Petrous SK101 sample was powdered and the general protein extraction procedure was carried out as explained in section 2.4. (without collagenase digestion). Gel loading buffer extract of the 'pellet' fraction (20µl) was analysed by SDS PAGE and western blotting (anti-SQSTM1/p62 mouse antibody). HEK293T lysate (50µg) was used as a positive control of anti-SQSTM1/p62 mouse antibody (western blotting image provided by Mr. Barry Shawn). The 62kDa protein is highlighted in red in HEK293T sample.

Finally, consistent with the LC-MS/MS and western blotting data, recombinant GST-SQSTM1/p62(E396X) protein was, like ancient SQSTM1/p62, detected by western blot using the mouse but not rabbit anti-SQSTM1/p62 (Mr Barry Shaw, data not shown but it can be seen in Figure 30). In summary, these combined results indicate that the ancient SQSTM1/p62 protein extracted from petrous SK101 may represent the PDB-mutant E396X sequence preserved within this particular bone.

4.3. Analyses of additional petrous bone samples from the Norton collection

To extend the analyses of ancient SQSTM1/p62 protein in the Norton collection, we first repeated the extraction procedure for SK101 petrous, and extended the analyses for an additional petrous bone taken from SK52. Further details of both skeletons are provided below (data courtesy of Dr. Carla Burrow, Liverpool John Moores University).

SK52: These remains date from the 14th Century. They belonged to a male estimated 50-59 years of age. The skeleton shows macroscopic evidence of PDB. Among the highly affected areas were the pelvis, sacrum, both hip joints (proximal femora), both shoulders (proximal humerus, entire clavicle and scapulae), as well as, numerous ribs, vertebrae and manubrium. Among the less affected areas were the cranium, right elbow (distal humerus, and proximal ulna and radius), proximal left radius, both knee joints (distal femur and proximal tibia), distal left fibula and some phalange (both hand and foot). Overall most of the skeleton was affected.

SK101: These remains date from the 15th Century. They belong to a male estimated 45-49 years of age. The skeleton shows macroscopic evidence of PDB. Among the highly affected areas were the cranium, the pelvis, sacrum, both hip joints (proximal femora), knee joints (distal femur, proximal tibia and fibula), both shoulders (proximal humerus, entire clavicle and scapulae), elbows (distal humerus and proximal ulna and radius), as well as numerous ribs, vertebrae and manubrium. Among the less affected areas were some phalanges. Again, overall most of the skeleton was affected.

Bone samples were weighed and physically ground (mortar and pestle) until bone was powdered. Powdered samples were placed in an individual Eppendorf and the chemical protein extraction was performed (see section 2.4 (without collagenase digestion)). Note in the case of petrous SK52, after the extraction with buffer B a TBS-Triton extraction was carried out rather than 8% TCA precipitation (a failed attempt to extract soluble SQSTM1/p62, data not shown). At the end of the extraction procedure, 50 μl of each fraction except the final 'pellet'

was mixed with 50 μl of gel loading buffer in individual Eppendorf. In the case of the final 'pellet' 100 μl of gel loading buffer was added. Samples were stored at -4°C until required.

4.3.1. SDS PAGE and silver stain analysis of ancient petrous bone extracts

To confirm that the protein extraction procedure was successful, 20 μl of each fraction of the processed petrous bones were analysed by SDS PAGE followed by silver stain (see sections 2.5.1. and 2.5.3).

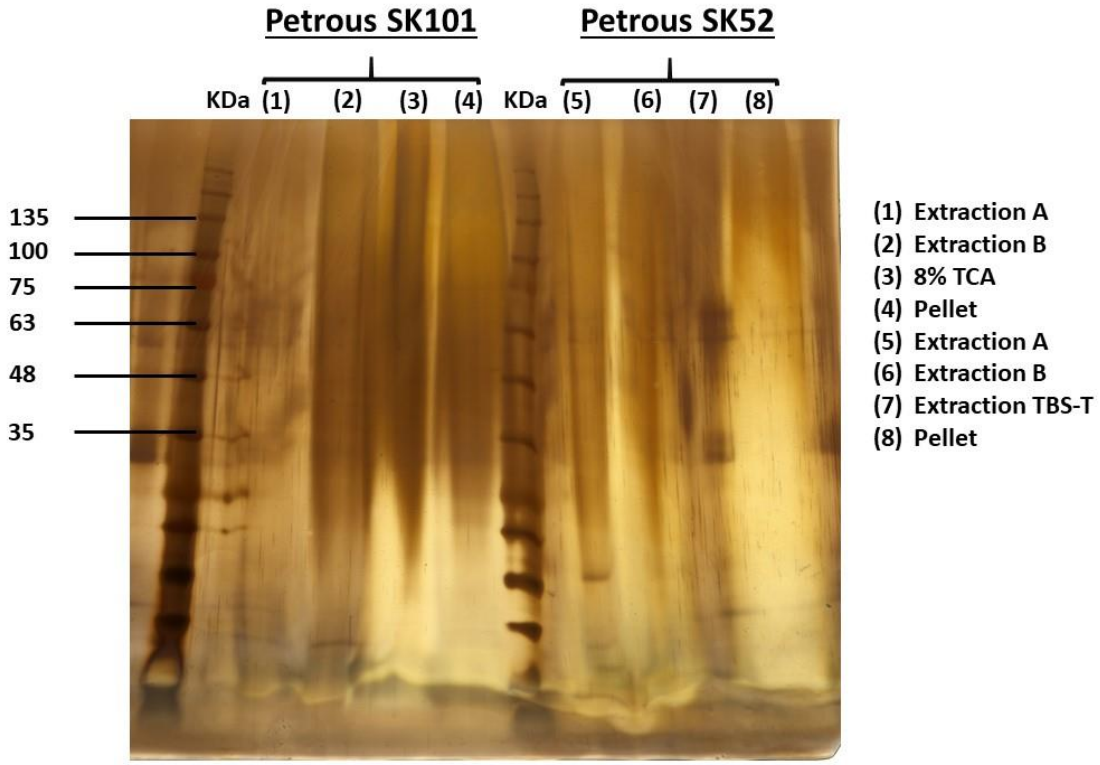


Figure 27. SDS PAGE and silver stain of different fractions of petrous SK101 and petrous SK52 bone samples.

Petrous SK101 and SK52 samples were powdered and the general extraction procedure was carried out as explained in section 2.4. (without collagenase digestion). Equal volumes of each fraction (excluding the 'pellets') were mixed with the same volume of gel loading buffer (1:1; 50μl:50μl). In the case of the 'pellet' 100 μl of gel loading buffer was added. Finally, fractions were analysed by SDS PAGE (5-20% gradient polyacrylamide) and visualised through silver stain.

Although the samples showed a degree of 'smearing' upon electrophoresis (characteristic of high collagen content), extracted proteins seemed to be remarkably well preserved (Figure 27). In particular both final insoluble 'pellet' fractions showed a high protein content, although distinct bands were not visible. A subjective visual inspection of the gel suggested that petrous SK52 sample was less well preserved than petrous SK101 sample.

4.3.2. Western blotting analysis of ancient petrous bone extracts

The next stage was to attempt detection of the ancient SQSTM1/p62 protein in the insoluble 'pellet' fractions of the petrous bone samples. Western blotting was performed using the two different SQSTM1/p62 antibodies (mouse and rabbit) carried out following the procedure described in section 2.5.4.

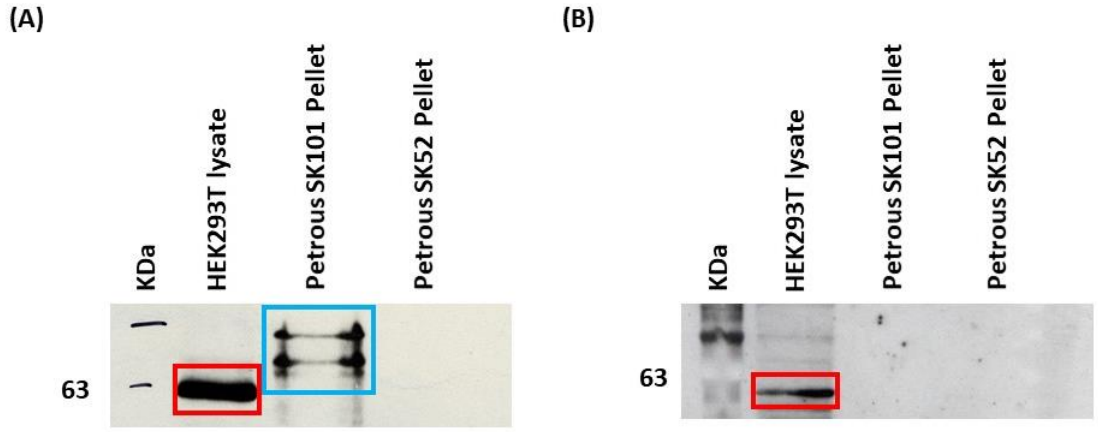


Figure 28. (A) Ancient SQSTM1/p62 protein was identified by western blotting using an anti-SQSTM1/p62 mouse antibody in petrous SK101 'pellet' sample but not in petrous SK52 'pellet' sample. (B) Ancient SQSTM1/p62 protein was not identified through western blotting using an anti-SQSTM1/p62 rabbit antibody in any of the two (SK101 and SK52) petrous 'pellet' samples.

Petrous SK101 and SK52 samples were powdered and the general extraction procedure was carried out as explained in section 2.4. (without collagenase digestion). 100 μl of gel loading buffer was added to each final insoluble 'pellet' sample. Pellets were analysed by SDS PAGE (5-20% gradient polyacrylamide) and western blotting (anti-SQSTM1/p62 mouse or rabbit antibodies respectively). Primary antibodies were diluted 1:500 while for the secondary antibodies were diluted 1:2000. HEK293T lysate (~50μg) was used as a positive control. The 62kDa protein is highlighted in red in HEK293T sample and ancient SQSTM1/p62 protein is highlighted in blue.

Consistent with the work leading up to the project, ancient SQSTM1/p62 was detected in the SK101 petrous 'pellet' fraction but only with the mouse antibody (Figure 28A). In contrast no SQSTM1/p62 was detected in the SK52 petrous 'pellet' with either of the antibodies (mouse and rabbit, Figure 28A, B), suggesting the sample was either genuinely negative or that any ancient SQSTM1/p62 had failed to be preserved in this particular sample.

4.3.3. Epitope mapping of the rabbit SQSTM1/p62 antibody

To provide further information about the nature of the epitope of the rabbit anti-SQSTM1/p62 antibody, and hence information on the sequence of the ancient SQSTM1/p62 extracted from petrous SK101, a series of C-terminal UBA domain truncating mutants of GST-SQSTM1/p62 were prepared: H436X, I431X, A426X, N421X, L416X and G411X (Figure 29). Mutations were introduced into the wild type GST-SQSTM1/p62 sequence by site directed mutagenesis following the instructions of the QuickChange® Site-Directed Mutagenesis kit (Stratagene). The mutant plasmids were analysed by DNA sequencing and resulting chromatograms were viewed using ChromasLite2 software. To confirm the presence of the mutations, the sequence alignment with the wild type SQSTM1/p62 sequence was carried out using ClustalW2. GST-tagged SQSTM1/p62 proteins were over-expressed in *E. coli* (see section 2.6.5.) and captured with glutathione-Sepharose beads. Bound proteins were eluted with gel loading buffer and detected by SDS PAGE followed by western blotting (anti-SQSTM1/p62 mouse and rabbit antibodies) (Figure 30).

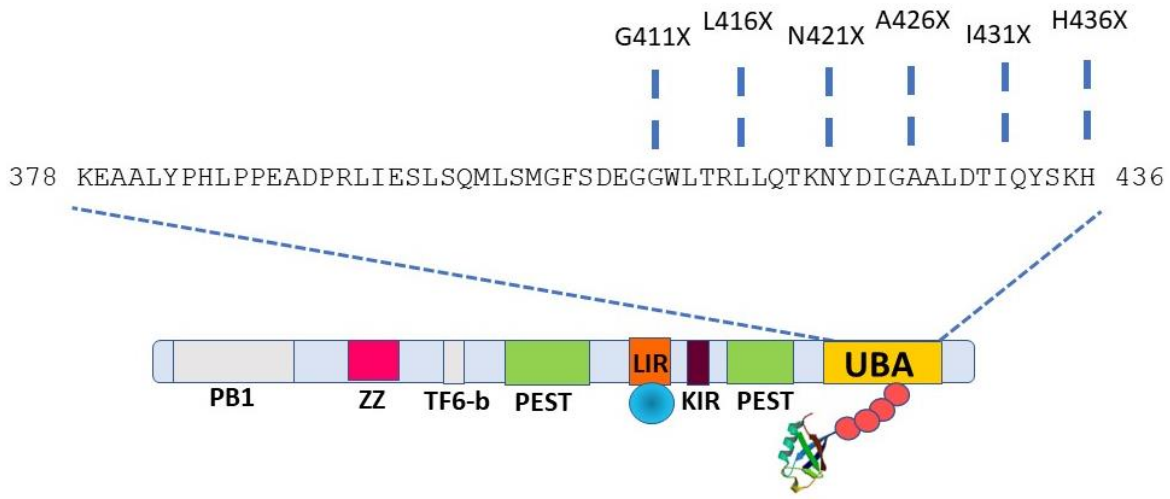


Figure 29. Scheme of the position of truncating mutants of SQSTM1/p62 used for the epitope mapping of the rabbit SQSTM1/p62 antibody

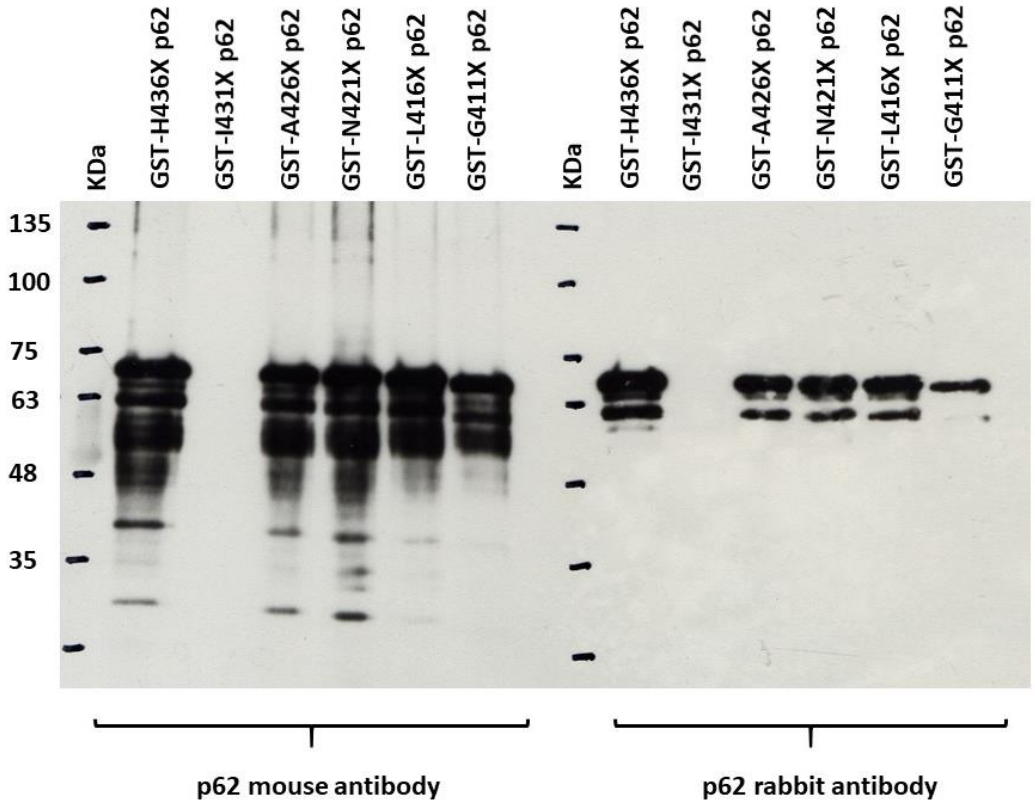


Figure 30. Western blotting of a series of C-terminal UBA domain truncating mutants of GST-SQSTM1/p62 with mouse and rabbit antibodies

The C-terminal domain mutants as indicated were introduced into the full-length GST-SQSTM1/p62 sequence and over-expressed in XL10-gold cells. The GST-tagged proteins were captured on glutathione-Sepharose. Captured proteins were detected by western blotting (anti-SQSTM/p62 mouse or rabbit antibodies). The concentration for the primary antibodies were 1:5000, and secondary antibodies 1:2000.

As is shown in the Figure 30, all of the C-terminal truncating mutants of SQSTM1/p62 were detected by both antibodies, including G411X (i.e. residues 1-410), with the exception of the I431X mutant which failed to express (confirmed with anti-GST, data not shown). A final western blot of wild type type, E396X (presumed Norton mutant) and G411X mutant proteins was performed for clarity (Figure 31), and confirmed failure of the rabbit antibody to detect the E396X mutant but detection of the G411X mutant. This maps the epitope of the rabbit antibody to between Glu396 and Gly410 of SQSTM1/p62. Failure to detect the ancient SK101 petrous SQSTM1/p62 with the rabbit antibody is consistent with the previous LC-MS/MS data and indicates this sequence is missing (or modified) in the ancient protein. The combined protein sequence data and rabbit antibody epitope mapping is presented in Figure 32.

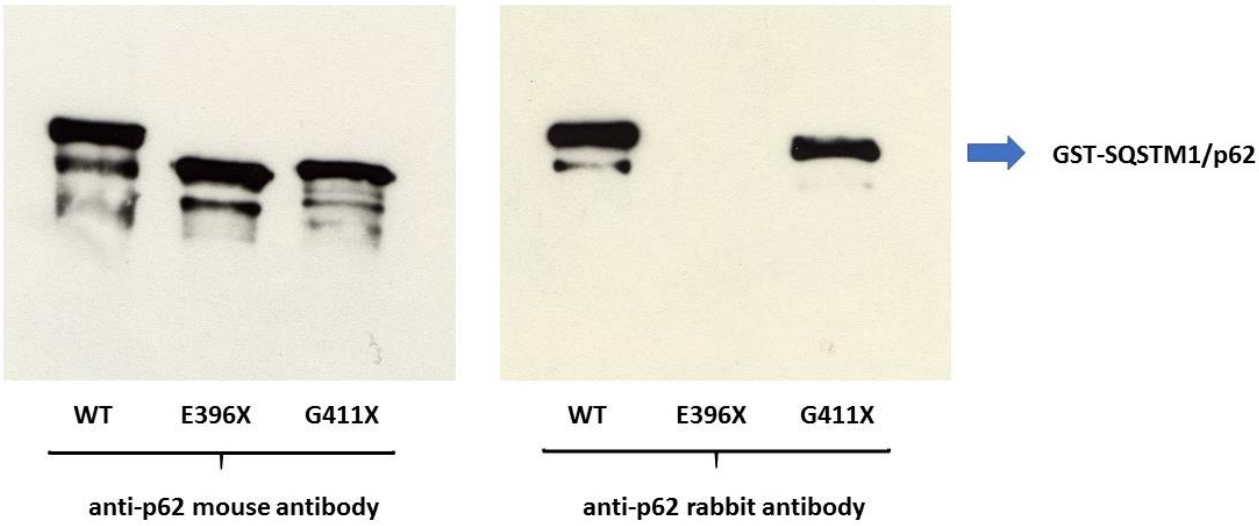


Figure 31. Western blotting of C-terminal UBA domain truncating mutants of GST-SQSTM1/p62 maps the epitope of the rabbit antibody

The C-terminal domain mutants as indicated (or wild type, WT) were introduced into the full-length GST-SQSTM1/p62 sequence and over-expressed in XL10-gold cells. The GST-tagged proteins were captured on glutathione-Sepharose. Captured proteins were detected by western blotting (anti-SQSTM/p62 mouse or rabbit antibodies). The concentration for the primary antibodies were 1:5000, and secondary antibodies 1:2000.

```
1   MASLTVKAYL LGKEDAAREI RRFSFCCSPE PEAEAEAAAG PGPCERLLSR 50
51  VAALFPALRP GGFQAHYRDE DGDLVAFSSD EELTMAMSYV KDDIFRIYIK 100
101 EKKECRRDHR PPCAQEAPRN MVHPNVICDG CNGPVVGTRY KCSVCPDYDL 150
151 CSVCEGKGLH RGHTKLAFPS PFGHLSEGFS HSRWLRKVKH GHFGWPGWEM 200
201 GPPGNWSPRP PRAGEARPGP TAESASGPSE DPSVNFLKNV GESVAAALSP 250
251 LGIEVDIDVE HGGKRSRLTP VSPESSSTEE KSSSQPSSCC SDPSKPGGNV 300
301 EGATQSLAEQ MRKIALESEG RPEEQMESDN CSGGDDDWTH LSSKEVDPST 350
351 GELQSLQMPE SEGPSSLDPS QEGPTGLKEA ALYPHLPPEA DPRLIESLSQ 400
401 MLSMGFSDEG GWLTRLLQTK NYDIGAALDT IQYSKHPPPL          440
```

Figure 32. Combined protein sequence data of ancient SQSTM1/p62 from petrous SK101

All MS/MS protein sequence data (Orbitrap Luminos and Velos data from Figure 23 combined) covered ~60% of the human SQSTM1/p62 sequence. Purple underline indicates the fine mapped epitope of the C-terminal SQSTM1/p62 antibody (not detected in Norton samples by western blotting). Together, the combined MS and western blotting data suggest that the ancient SQSTM1/p62 protein from petrous SK101 could represent an E396X mutant (previously associated with familial PDB).

4.4. Analyses of tooth samples from the Norton collection

No further petrous bone samples from pagetic remains were available from the Norton collection (which represents a museum collection still on current display). However, tooth samples from affected individuals were made available. Note that although teeth represent calcified tissues, there have been no reports to date of pagetic changes in such samples.
Three tooth samples (molars) were analysed from three different skeletons.

SK29: These remains date from the 14th Century. They belong to a male estimated 45-49 years of age. The skeleton shows macroscopic evidence of PDB. Among the highly affected areas were the pelvis, sacrum, both knee joints (distal femur and proximal tibia), as well as, left rib fragment (sternal end). Less affected areas were some phalanges. In this case the disease seemed to be more severe because there were both shoulders (specifically the proximal humerus and lateral portion of the clavicle), left elbow joint (distal humerus and proximal ulna and radius), some metacarpal bones (left and right sides) and cervical vertebrae.

SK22, SK35: No detailed information about these individuals was available, although macroscopic evidence of PDB-like changes was apparent (Dr. Carla Burrell, personal communication).

Tooth SK29 was processed initially followed by the remaining two samples.

4.4.1. Analysis of tooth SK29 sample

The tooth sample was weighed and physically ground (mortar and pestle) until powdered. Powdered sample was placed in an individual Eppendorf and the chemical protein extraction was performed (see section 2.4. (without collagenase digestion)). At the end of the extraction procedure, before adding loading buffer, the tooth 'pellet' sample was divided in two and half was stored at -4°C for future LC-MS/MS analyses. 50 μl of each fraction except the 'pellet' was mixed with 50 μl of gel loading buffer in individual Eppendorf tubes. In the case of the remaining 'pellet' 100 μl of gel loading buffer was added. Fractions were stored at -4°C until required.

4.4.1.1. SDS PAGE and silver stain analysis of ancient SK29 tooth extract

To confirm that the protein extraction procedure from tooth SK29 was successful, SDS PAGE and silver stain (20 μl of each extraction) was performed on different fractions.

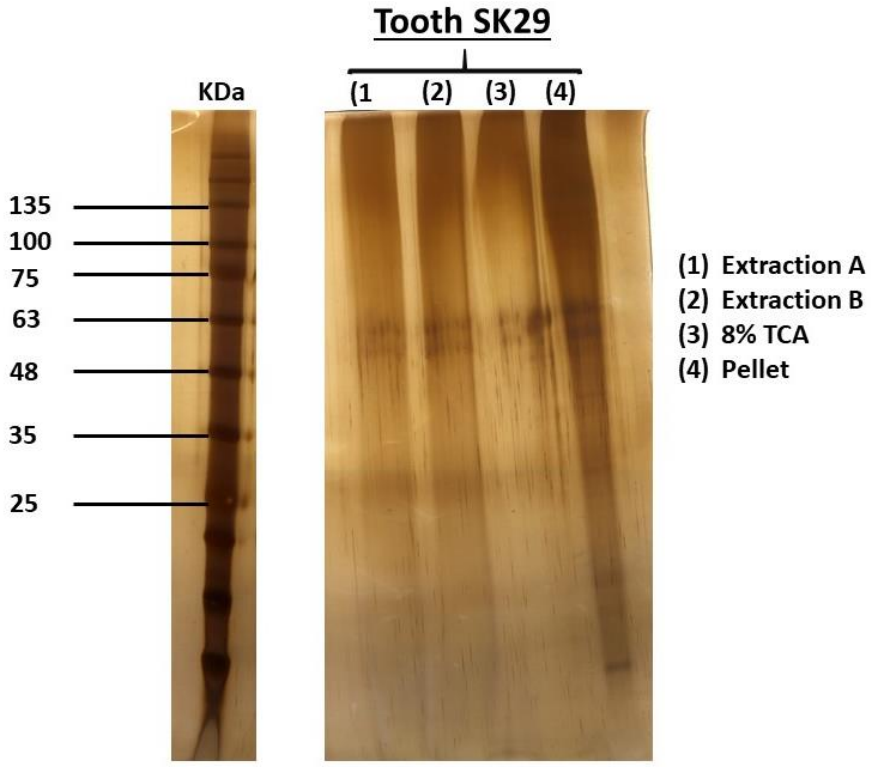


Figure 33. SDS PAGE and silver stain of different fractions of SK29 tooth sample.

Tooth SK29 sample was powdered and the general extraction procedure was carried out as explained in section 2.4. (without collagenase digestion). Equal volumes of each fraction (excluding the pellets) were mixed with the same volume of gel loading buffer (1:1; 50μl:50μl). In the case of the 'pellet' 100 μl of gel loading buffer was added. Finally, fractions were analysed by SDS PAGE (5-20% gradient polyacrylamide) and visualised through silver stain.

The results showed that extracted proteins from tooth SK29 seemed again well preserved (Figure 33), with the 'pellet' showing abundant protein. In this case some distinct bands could be discerned in the 'pellet' fraction, including in gel regions close to molecular weights where ancient SQSTM1/p62 was detected in petrous SK101.

4.4.1.2. Western blotting analysis of ancient SK29 tooth extract

The next step was to attempt detection of the ancient SQSTM1/p62 protein in the SK29 tooth extract. The procedure was the same as that for petrous samples, a western blot was performed using the two different SQSTM1/p62 antibodies (mouse and rabbit, in this instance only the 8% TCA extraction and final insoluble 'pellet' were analysed).

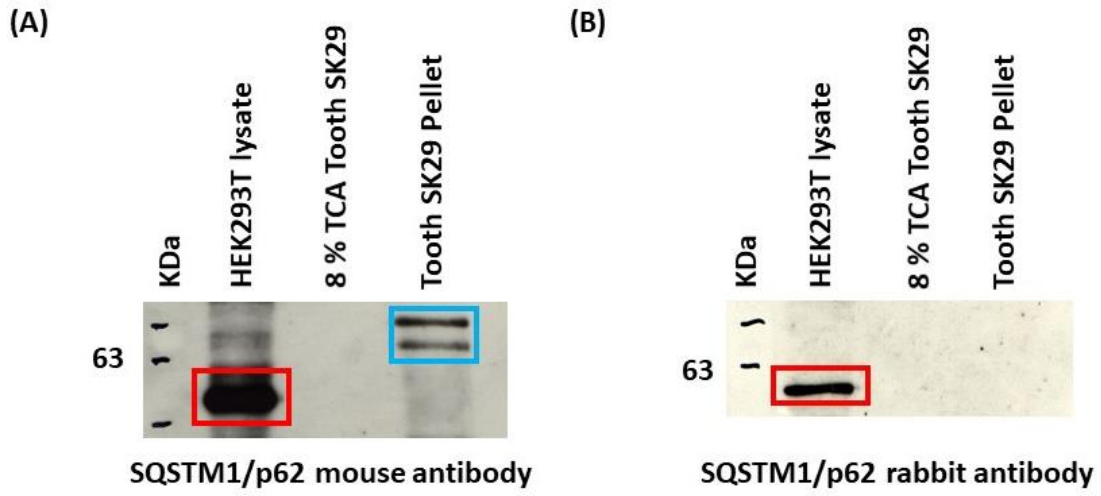


Figure 34. (A) Ancient SQSTM1/p62 protein was identified by western blotting using an anti-SQSTM1/p62 mouse antibody in tooth SK29 'pellet' sample (B) Ancient SQSTM1/p62 protein was not identified through western blotting using an anti-SQSTM1/p62 rabbit antibody in tooth SK29 'pellet' sample.

Tooth SK29 sample was powdered and the general extraction procedure was carried out as explained in section 2.4. (without collagenase digestion). Equal amount of each fraction except the 'pellet' was mixed with the same amount of gel loading buffer (1:1; 50µl:50µl). In the case of the pellet 100 µl of gel loading buffer was added. Finally, fractions were analysed by SDS PAGE (5-20% gradient polyacrylamide) and western blotting (anti-SQSTM1/p62 mouse or rabbit antibody respectively). HEK293T lysate was used as a positive control of anti-SQSTM1/p62 mouse and rabbit antibodies. The 62kDa protein is highlighted in red in HEK293T sample and ancient SQSTM1/p62 protein is highlighted in blue.

SQSTM1/p62 was detected in the insoluble 'pellet' fraction with the mouse antibody indicating that like SK101 petrous, the SK29 tooth was positive for ancient SQSTM1/p62 (Figure 34A). As for SK101 petrous the rabbit antibody did not cross-react with the tooth extracted proteins (Figure 34B). Consistent with the SK101 petrous, the ancient SQSTM1/p62 was detected as two bands with increased molecular weight compared to HEK293 cell-derived protein.

4.4.2. Analysis of tooth SK22 and SK35 samples

From previous LC-MS/MS analyses of petrous SK101 samples it was clear that much of the preserved protein in the ancient bone sample consisted of different types of collagen proteins (see Table 1.). For this reason, and encouraged by the distinct bands on SDS PAGE/silver stain in the SK29 tooth extract, we decided to process the other half of tooth sample (SK29) together with the additional tooth samples with an extraction procedure which included a collagenase digestion step at the end of the process (Grynpas et al. 1994). The rationale here was that exceptionally well-preserved collagen from the samples could be masking the

presence of potentially more informative but less abundant proteins (Wadsworth and Buckley 2014).

The additional two tooth samples (SK22 and SK35) were processed together with the stored SK29 pellet sample, following the general extraction procedure but incorporating a collagenase digestion step (see section 2.4.4.). In the case of the SK29 bone sample the collagenase step of the process was performed followed by a second 8% TCA precipitation. After this, 50 μl of each fraction except the final 'pellet' was mixed with 50 μl of gel loading buffer in an individual Eppendorf. In the case of the 'pellet', 100 μl of gel loading buffer was added. These were stored at -4°C until required.

4.4.2.1. SDS PAGE and silver stain analysis of ancient tooth extracts

SDS PAGE with silver staining of the different extractions of the three tooth samples (with collagenase) was carried out to confirm that the extraction procedure was successful. 20 μl of each extraction was analysed (see sections 2.5.1 and 2.5.3.)(Figure 35).

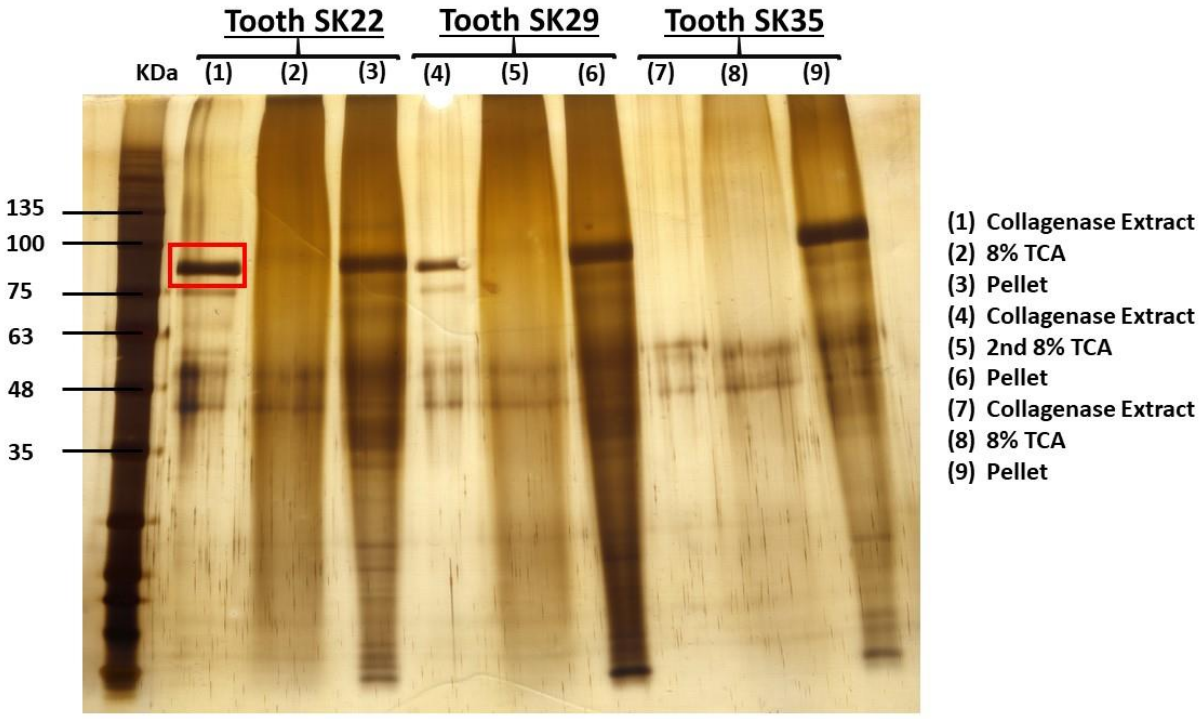


Figure 35. SDS PAGE and silver stain of different fractions of tooth SK22, SK29 and SK35 samples.

Tooth SK22, SK29 and SK35 samples were powdered and the extraction procedure was carried out as explained in section 2.4 with the collagenase digestion at the end of the procedure (see section 2.4.4.). Equal amount of each fraction except the pellet was mixed with the same volume of gel loading buffer (1:1; 50μl:50μl). In the case of the pellet 100 μl of gel loading buffer was added. Finally, fractions were analysed by SDS PAGE (5-20% gradient polyacrylamide) and visualised through silver stain. A collagenase band is highlighted in red.

Analyses of the resultant gels indicated an improvement in the overall gel profiles with the addition of collagenase (compared to the general extraction procedure without), with more distinct protein bands evident. This is highlighted by directly comparing gel images for corresponding samples derived from SK29 tooth with or without collagenase treatment (Figure 36).

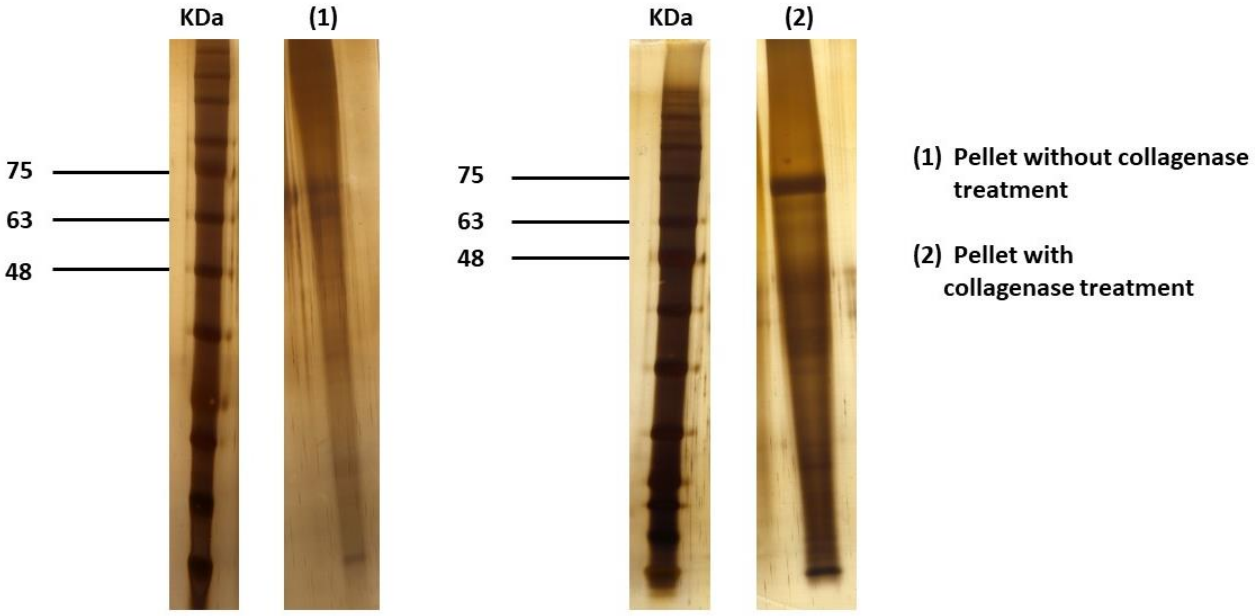


Figure 36. SDS PAGE and silver stain of tooth SK29 pellet fractions prepared with or without collagenase digestion

4.4.2.2. Western blotting analysis of ancient tooth extracts with collagenase treatment

As ancient SQSTM1/p62 was previously detected in only the final 'pellet' fraction of SK29 tooth by western blotting with the anti-SQSTM1/p62 mouse antibody, all three 'pellets' derived from the different samples (prepared with the addition of collagenase) were similarly analysed in parallel by western blotting (Figure 37).

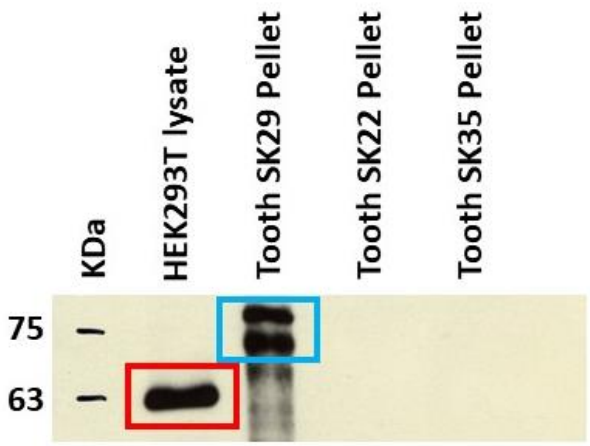


Figure 37. Ancient SQSTM1/p62 protein was identified by western blotting using an anti-SQSTM1/p62 mouse antibody in tooth SK29 'pellet' sample but not in SK22 and SK35 samples.

Tooth samples were powdered and the extraction procedure was carried out explained in section 2.4. 100 μl of gel loading buffer was added to each resulting final 'pellet' fraction and these were analysed by SDS PAGE (5-20% gradient polyacrylamide) and western blotting (mouse anti-SQSTM1/p62 mouse). The 62kDa protein is highlighted in red in HEK293T sample and ancient SQSTM1/p62 protein is highlighted in blue.

Ancient SQSTM1/p62 protein was still detected in tooth SK29 'pellet' following the collagenase treatment, and with the same immunoreactive profile (band size/pattern) as the untreated samples. However, SK22 and SK29 samples were found to be negative for SQSTM1/p62. Thus, ancient SQSTM1/p62 is detected in 1/2 petrous samples and 1/3 tooth samples tested.

4.3.3. LC-MS/MS-based sequencing of ancient proteins from tooth SK22 and SK29 samples

Since the final 'pellet' sample derived from SK29 tooth was (like SK101 petrous) positive for SQSTM1/p62 by western blotting, it was also submitted for LC-MS/MS analysis. Further, a SQSTM1/p62-negative sample – SK22 tooth final 'pellet' – was also included, in order to assess whether failure to detect SQSTM1/p62 could be due to general low protein preservation.

4.4.3.1. Preparation of the samples for LC-MS/MS

SDS-PAGE analysis with by Coomassie Blue staining (see sections 2.5.1. and 2.5.2.) was performed on 30 μl aliquots of each tooth 'pellet' sample (SK22 (SQSTM1/p62-negative) and SK29 (positive)). Since we sought to catalogue the range of proteins in each sample, electrophoresis was performed for only ~15 minutes to allow all proteins to migrate to within the top ~0.5 cm of the resolving gel. The acrylamide gel section corresponding to this complete

proteome within the ~0.5cm region was stained, destained, excised and stored in an Eppendorf at 4°C with 200 µl of distilled water.

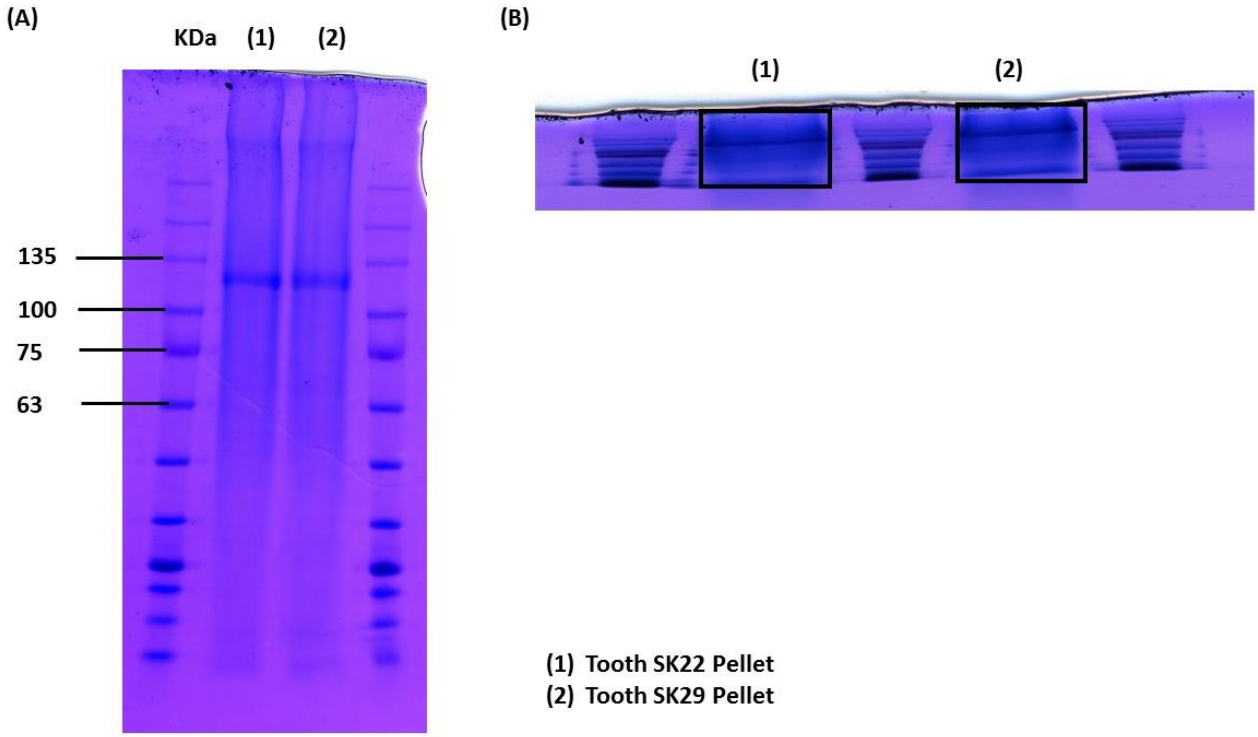


Figure 38. SDS PAGE and Coomassie stain analysis of ancient SK22 and SK29 tooth 'pellet' fractions prior to proteomic analysis

Tooth samples SK22 and SK29 were powdered and the extraction procedure was carried out as explained in section 2.4. with the collagenase digestion at the end of the procedure (see section 2.4.4.). 100 µl of gel loading buffer was added to each final 'pellet' fraction and these were analysed by SDS PAGE (5-20% acrylamide gradient gel) and visualised by Coomassie stain. (A) Conventional SDS PAGE analysis of samples (for comparison). (B) To prepare samples for LC-MS/MS analysis, a shorter electrophoresis ensured the majority of total protein was contained in an ~0.5cm gel region at the top of the resolving gel. Boxed gel regions were subjected to LC-MS/MS analysis (Orbitrap Velos, University of Leicester).

4.4.3.2. LC-MS/MS analysis of ancient SK22 and SK29 tooth 'pellet' fractions

Table 2. Summary of the human proteins identified in tooth SK22 and SK29 'pellet' samples from at least two unique peptides (fragments).

'Tooth SK22' and 'Tooth SK29' refer to pellet fraction from the extraction procedure of these tooth samples. Trypsin sequences are derived from the enzyme used for sample digestion. Numbers relate to numbers of peptide sequences identified.

Proteins found by MS in Tooth (SK22; SK29) samples		
Protein	Number of fragments found (sequenced)	
	Tooth SK22	Tooth SK29
Alpha-2-HS-glycoprotein OS	3	5
Byglycan OS	2	2
Collagen alpha-1(I) chain OS	68	57
Collagen alpha-1(II) chain OS	4	4
Collagen alpha-1 (III) chain OS	8	4
Collagen alpha-2(I) chain OS	64	57
Collagen alpha-2(V) chain OS	2	3
Collagen alpha-2(XI) chain OS	4	2
Extracellular superoxide dismutase [Cu-Zn] OS	2	-
Hornerin OS	3	2
Keratin, type I cytoskeletal 9 OS	17	26
Keratin, type I cytoskeletal 10 OS	23	22
Keratin, type I cytoskeletal 14 OS	4	13
Keratin, type II cytoskeletal 1 OS	51	57
Osteomodulin OS	-	3
Periostin OS	2	-
Prothrombin OS	3	7
Serum albumin OS	11	16
SPARC OS	-	2
Vitronectin OS	2	3

Twenty different human proteins were identified between the two samples. Several proteins not previously identified in petrous bone (e.g. byglycan and hornerin) were noted. Despite previous detection of ancient human SQSTM1/p62 by western blot in the SK29 'pellet' fraction, no peptide sequences were recovered by LC-MS/MS, indicating it may be below the limit of detection in this analysis. The level of total protein appeared be similar for both tooth samples based on approximately equal numbers of peptide samples identified, suggesting that poor protein preservation was unlikely to explain the failure to detect SQSTM1/p62 in tooth SK22. NOTE: A table comparing proteins identified from both petrous SK101 samples (including 8% TCA and pellet fractions) and tooth SK22 SK29 samples (including both pellets) is shown in the appendix (Table 4).

4.5. Investigating the abnormal migration of ancient SQSTM1/p62 on western blot

Our western blotting studies indicated that 1/2 petrous and 1/3 tooth samples were positive for ancient SQSTM1/p62, and previous LC-MS/MS analyses combined with epitope mapping of the mouse antibody supported the notion that the positive samples may contain E396X mutant SQSTM1-p62 protein, known to be associated with familial PDB. However, E396X represent a truncating mutation (removing residues 396-440) and would be expected to decrease the observed size of SQSTM1/p62 on western blot, rather than increase it as we noted for the ancient SQSTM1/p62. We therefore reasoned that the ancient SQSTM1/p62 may be 'modified' in some way that increases its apparent denatured molecular weight.

As well as functioning as a ubiquitin-binding protein recognising (poly)ubiquitin non-covalently, SQSTM1/p62 is also a target of covalent modification with ubiquitin (Vadlamudi et al. 1996; Geetha and Wooten 2002) with each single ubiquitin moiety increasing the protein molecular weight by ~8.6kDa. We therefore tested if abnormal ubiquitination could account for the unusual migration of the ancient SQSTM1/p62 protein. The procedure was the same as that for detecting ancient SQSTM1/p62. A sample of the final 'pellet' from tooth SK29 was analysed by SDS PAGE and western blotting with anti-ubiquitin antibodies, along with a polyubiquitin control (Figure 39).

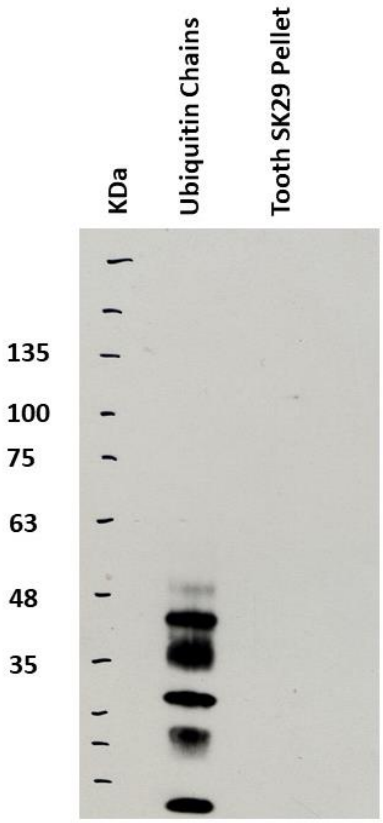


Figure 39. Ubiquitin reactivity was not associated with ancient SQSTM1/p62 protein as determined by western blotting.

A sample of the final 'pellet' from tooth SK29 (10 μl) was analysed by SDS PAGE (5-20% polyacrylamide gradient) and western blotting (anti-ubiquitin antibody). A commercial sample containing polyubiquitin chains of different length (ubiquitin ladder, 100ng) was used as a positive control.

The tooth SK29 'pellet' sample was found to be negative for ubiquitin (Figure 39), despite previously being found to be SQSTM1/p62 positive. Thus, aberrant ubiquitination is unlikely to account for the mass shift in ancient SQSTM1/p62 detected in tooth SK29 and petrous SK101 from the Norton Priory collections.

4.6. Discussion

The evolution of human life is always influenced by diseases, in the past, present, and in the future. In paleopathology, diseases are typically diagnosed macroscopically and microscopically, and increasingly by amplifying the degraded remains of DNA found in ancient samples (Schmidt-Schultz and Schultz 2007). However, in the past few years a new discipline has started to develop in the field of paleopathology, called 'paleoproteomics'. It consists in the investigation of intact largely extracellular matrix (ECM)-proteins of bone from individuals who lived hundreds or thousands of years ago using techniques which belong to the field of biochemistry (Schmidt-Schultz and Schultz 2015). Proteins are the functional entities of cells

and with paleoproteomics we potentially have a tool to establish a reliable diagnosis at the level of intact proteins from ancient bones, especially in in conditions where nucleic acid preservation is poor (Schultz et al. 2007).

Bone tissue has a better chance of being preserved than soft tissues over extended time periods due to its physical durability and resistance to decomposition and diagenesis. The conditions within the compact bone structure, which might also be characterised by the relatively low content of water and degradation enzyme, are favourable for the preservation of bone proteins. ECM of the living bone bind very tightly to hydroxyapatite. The apatite in which the proteins are embedded provides considerable protection against the destructive effects of temperature and chemical agents after death. For this reason, in ECM-proteins, unlike in DNA, there is almost no contamination risk. However, it is well recognised that archaeological skeletal remains are affected in the earth by biogenic and abiogenic processes following burial, which together constitute the phenomenon of diagenesis. Additionally, contamination occurring during and after archaeological excavation can alter the bone. These *post mortem* processes can falsify results of scientific examinations by affecting the identification of proteins among other molecules (Schmidt-Schultz and Schultz 2004) and so caution must be applied in interpreting proteomic data.

In well-preserved bones, many thousands of years after death, the proteins of the ECM are conserved, as well as in fresh bones. With reliable techniques, such those used in this study, it is possible to identify these proteins (Schmidt-Schultz and Schultz 2004). The mean aim of paleoproteomics is to try to identify ECM proteins of the normal bone metabolism as well as proteins which are typical for diseases (Schmidt-Schultz and Schultz 2015). In this project, we have extended these analyses to non ECM proteins, having realised that SQSTM1/p62 can be preserved in medieval bones over 700 years old excavated from Norton Priory. These skeletal remains show macroscopic characteristics of being affected by a bone disorder resembling, but distinct from, modern PDB. Using the extraction procedure followed in this study, we could solubilise SQSTM1/p62 protein from ancient bones and teeth in an intact state, a precondition to be able to establish reliable diagnoses of ancient disorders (Schmidt-Schultz and Schultz 2004).

We could detect ancient SQSTM1/p62 by western blotting in two of the five bone/teeth samples analysed (petrous SK101 and tooth SK29) but were unable to confirm the presence in the latter by protein mass spectrometry, probably due to insensitivities in detection. Fine epitope mapping of a rabbit SQSTM1/p62 antibody that failed to detect ancient SQSTM1/p62

provided further evidence that residues 396-411 of the protein, part of the UBA domain, are missing. Indeed, this observation is consistent with our earlier presumption (based on LC-MS/MS analysis of petrous SK101) that the ancient SQSTM1/p62 that we are detecting represents an E396X truncating mutant. This mutation was previously reported to be associated with a particularly severe form of modern familial PDB, with early age at onset (~47 years compared to ~68 years in sporadic PDB) and high number of bones affected (~6 compared to ~3 in sporadic PDB) (Hocking et al. 2002; Rendina et al. 2006). It would be necessary to confirm the mutation at the level of DNA sequencing (ongoing), and if found, would offer valuable insights into the natural history of PDB and its evolution since mediaeval times.

In addition to SQSTM1/p62, our MS results allowed us to identify a portion of the bone/tooth proteome which could be prerequisite for the understanding of the biochemistry and physiology of bone in ancient samples and consequently to recognising other indicators of disease (Cappellini et al. 2012). The ancient proteome of bone samples from Norton Priory included many extracellular and intracellular proteins that map to a broad range of molecular functions and which are involved in most aspects of bone tissue development and homeostasis. Structural proteins interacting with the bone mineral component and/or other ECM elements were found to be dominant, agreeing it with much of the previously published work on ancient proteins in that collagen, in particular the collagen alpha-2 (I) and alpha-1 (I) chains, was the longest surviving protein in ancient bone. However, our study has also highlighted the fact that there are several other NCPs which can be commonly identified in archaeological bone and tooth samples such as serum albumin, prothrombin as well as vitronectin (Cappellini et al. 2012; Wadsworth and Buckley 2014).

Future goals include to understand the apparent 'preferential' preservation of SQSTM1/p62 (over other NCP proteins) in ancient bone and tooth samples from Norton Priory. We speculate this may be due to its participation in the formation of the characteristic inclusion bodies previously observed in the nuclei of pagetic cells (Helfrich et al. 2007) which afford a degree of protection to the SQSTM1/p62 protein. The presence of inclusion bodies in the nucleus as well as in the cytoplasm in osteoclast within the affected areas of the bone is a pathognomic feature in all Pagetic diseases. However, not all osteoclasts contain these inclusions and in those that do, not all nuclei are affected. These inclusions are not found in any other cell type around affected bone. To be able to fully appreciate requires ultrastructural examination. Proteins mutated in PDB and related disorders including SQSTM1/p62 and VCP have been found in the inclusions by immunohistochemistry (Helfrich et al. 2007). Aggregates

of misfolded or ubiquitylated proteins combined with several key UPS proteins have also been detected (Helfrich and Hocking 2008). The additional presence of molecular chaperones indicate the inclusions are aggregates of proteins destined for degradation. The aggregation of proteins is considered as a mechanism of protection for the cells against the potentially toxic effects of accumulation of misfolded or otherwise dysfunctional proteins when the proteasomal or autophagy systems are overwhelmed or inhibited, supporting the 'preferential' preservation of SQSTM1/p62 in bone samples (Helfrich and Hocking 2008). On the other hand, these inclusions are undoubtedly similar to viral nucleocapsids and PDB was thought to have a viral origin, but there is no strong evidence which supports that measles virus being present in all patients presenting with such inclusions. Further, there is no definitive biochemical or histochemical proof for a viral component in the pagetic inclusions and no intact virus has ever been isolated from Pagetic bone. However, it could be that in ancient times, PDB had an unknown viral component which synergised with genetic factors (perhaps *SQSTM1* mutations within the Norton population) to make it more severe, but the improvement in the quality of life and health care since that time led to its disappearance. For this reason, more studies should be made in this field. As noted earlier, the role of viruses and other environmental factors in PDB should not be disregarded to draw a combined theory for the disease aetiology.

In summary, the results of this study provide, for the first time, key insights into a reliable diagnosis of PDB in ancient times, which gives new impetus to further studies in the field of the comparative evolution and the history of bone disease starting from ancient and leading up to modern times.

CHAPTER 5: Final summary

5.1. Final summary

In recent years there has been substantial research and conflicting theories related to the pathogenesis of PDB (Roodman and Windle 2005). One of the most recent advances in bone biology has been the identification of a role of autophagy in the regulation of osteoclasts precursor cell polarity and in consequent osteoclast formation and activation (Srinivas et al. 2009), as well as in ruffled border formation and secretion of degradative enzymes during osteoclast activity (DeSelm et al. 2011). This has led to thinking that the modulation of autophagy in osteoclasts (and therefore osteoclast activity) could be a potential therapeutic target in PDB (Hocking et al. 2012). For this reason, and that fact that *SQSTM1* mutations (encoding the autophagy receptor SQSTM1/p62) are common in patients with familial PDB, the role of autophagy in the disorder is currently being investigated. Autophagy has the advantage of being relatively easily pharmacologically manipulated *in vivo* (Goode and Layfield 2010).

Our study has provided limited indications that defective autophagy may be a relevant mechanism in 'modern' PDB with *SQSTM1* mutations. Although PDB-mutant SQSTM1/p62(F406V) was found to be defective in ubiquitin-binding (and presumably autophagic cargo recognition) and showed a different cellular phenotype to wild-type in HEK293T cells, no differences in autophagy markers (LC3B lipidation) were imparted by PDB-associated mutants when transiently transfected in these model cells. Presumably more physiologically relevant systems will be needed to uncover any subtle autophagy phenotypes associated with these mutants. However, added knowledge suggests that the 'ancient' PDB-like disorder at Norton Priory probably was a precursor of familial PDB with a *SQSTM1* truncating mutation (E396X) that persists to modern day. More detailed investigations are necessary to understand completely the molecular basis of PDB, and specifically why and how the disease phenotype of this disorder has evolved from ancient to modern times.

References

Albagha, O.M., Visconti, M.R., Alonso, N., Wani, S., Goodman, K., Fraser, W.D., Gennari, L., Merlotti, D., Gianfrancesco, F., Esposito, T., Rendina, D., di Stefano, M., Isaia, G., Brandi, M.L., Giusti, F., Del Pino-Montes, J., Corral-Gudino, L., Gonzalez-Sarmiento, R., Ward, L., Rea, S.L., Ratajczak, T., Walsh, J.P., Ralston, S.H., 2013. Common susceptibility alleles and SQSTM1 mutations predict disease extent and severity in a multinational study of patients with Paget's disease. *Journal of bone and mineral research,* vol 28, no. 11, 2338-2346. Doi: 10.1002/jbmr.1975

Anatomy & Physiology, 2013. *Openstax CNX™*

Barry, H.C., 1980. Orthopedic aspects of Paget's disease of bone. *Arthritis and Rheumatism*, vol. 23, no. 10, 1128-1130.

Bastin, S., Bird, H., Gamble, G., Cundy, T., 2009. Paget's disease of bone-becoming a rarity?. *Rheumatology*, vol. 48, no.10, 1232-1235. Doi: 10.1093/rheumatology/kep212

Bjorkoy, G., Lamark, T., Brench A., Outzen. H., Perander, M., Overvatn, A., Stenmark, H., Johansen, T., 2005. p62/SQSTM1 forms protein aggregates degraded by autophagy and has a protective effect on huntingtin-induced cell death. *The Journal of Cell Biology*, vol. 171, no. 4, 603-614. Doi: 10.1083/jcb.200507002

Boyle, W.J., Simonet, W.S., Lacey, D.L., 2003. Osteoclast differentiation and activation. *Nature*, vol. 423, no. 6937, 337-342. Doi: 10.1038/nature01658

Cappellini, E., Jensen, L.J., Szklarczyk, D., Ginolhac, A., da Fonseca, R.A., Stafford, T.W., Holen, S.R., Collins, M.J., Orlando, L., Willersley, E., Gilber, M.T., Olsen, J.V., 2012. Proteomic analysis of a Pleistocene mammoth femur reveals more than one hundred ancient bone proteins. *Journal of proteome research*, vol. 11, no. 2, 917-926. Doi: 10.1021/pr200721u

Cavey, J.R., Ralston S.H., Hocking, L.J., Sheppard, P.W., Ciani, B., Searle, M.S., Layfield, R., 2005. Loss of ubiquitin-binding associated with Paget's disease of bone p62 (SQSTM1) mutations. *Journal of Bone and Mineral Research*, vol. 20, no. 4, 619-624. Doi: 10.1359/jbmr.041205

Cavey, J.R., Ralston, S.H., Sheppard, P.W., Ciani, B., Gallagher, T.R., Long, J.E., Searle, M.S., Layfield, R., 2006. Loss of ubiquitin binding is a unifying mechanism by which mutations of SQSTM1 cause Paget's disease of bone. *Calcified Tissue International,* vol. 78, no. 5, 271-277. Doi: 10.1007/s00223-005-1299-6

Ciani, B., Layfield, R., Cavey, J.R., Sheppard, P.W., Searle, M.S., 2003. Structure of the ubiquitin-associated domain of p62 (SQSTM1) and implications for mutations that cause Paget's disease of bone. *The Journal of biological chemistry*, vol. 278, no. 39, 37409-37412. Doi: 10.1074/jbc.M307416200

Ciuffa, R., Lamark, T., Tarafder, A.K., Guesdon, A., Rybina, S., Hagen, W.J., Johansen, T., Sachse, C., 2015. The selective autophagy receptor p62 forms a flexible filamentous helical scaffold. *Cell Reports*, vol. 11, no. 5, 748-758. Doi: 10.1016/j.celrep.2015.03.062

Collet, C., Michou, L., Audran, M., Chasseigneaux, S., Hilliguin, P., Bardin, T., Lemaire, I., Cornélis, F., Launay, J.M., Orcel, P., Laplanche, J.L., 2007. Paget's disease of bone in the French population: novel SQSTM1 mutations, functional analysis, and genotype-phenotype correlations. *Journal of Bone and Mineral Research*, vol. 22, no. 2, 310-317. Doi: 10.1359/jbmr.061106

Cooper, C., Harvey, N.C., Dennison, E.M., Van Staa, T.P., 2006. Update on the epidemiology of Paget's disease of bone. *Journal of Bone and Mineral Research*, vol. 21, 3-8. Doi: 10.1359/jbmr.06s201

Cundy, T., Bolland, M., 2008. Paget disease of bone. *Trends in Endocrinology & Metabolism*, vol. 19, no. 7, 246-253. Doi: 10.1016/j.tem.2008.06.001

Daroszewska, A., van't Hof, R.J., Rojas, J.A., Layfield, R., Landao-Basonga, E., Rose, L., Rose, K., Ralston, S.H., 2011. A point mutation in the ubiquitin-associated domain of SQSTM1 is sufficient to cause a Paget's disease-like disorder in mice. *Human Molecular Genetics*, vol. 20, no. 14, 2734-2744. Doi: 10.1093/hmg/ddr172

Dell'Atti, C., Cassar-Pullicino, V.N., Lalam, R.K., Tins, B.J., Tyrrell, P.N.M., 2007. The spine in Paget's disease. *Skeletal Radiology*, vol. 36, no. 7, 609-626. Doi: 10.1007/s00256-006-0270-6

DeSelm, C.J., Miller, B.C., Zou, W., Beatty, W.L., van Meel, E., Takahata, Y., Klumperman, J., Tooze, S.A., Teitelbaum, S.L., Virgin, H.W., 2011. Autophagy proteins regulate the secretory component of osteoclastic bone resorption. *Developmental Cell*, vol. 21, no. 5, 966-974. Doi: 10.1016/j.devcel.2011.08.016

Essentials of Rubin's Pathology 5th Edition, 2009. *Lippincott Williams & Wilkins*

Geetha, T., Wooten, M.W., 2002. Structure and functional properties of the ubiquitin binding protein p62. *FEBS Letters*, vol. 512, no. 1-3, 19-24.

Gelman, A., Elazar, Z., 2011. Autophagic factors cut to the bone. *Developmental Cell*, vol. 21, no. 5, 808-810. Doi: 10.1016/j.devcel.2011.10.021

Gkouva, L., Andrikoula, M., Kontogeorgakos, V., Papachristou, D.J., Tsatsoulis, A., 2011. Active Paget's disease of bone with normal biomarkers of bone metabolism: a case report and review of the literature. *Clinical Rheumatology*, vol. 30, no. 1, 139-144. Doi: 10.1007/s10067-010-1579-z

Glick, D., Barth, S., Macleod, K.F., 2010. Autophagy: cellular and molecular mechanisms. *The Journal of Pathology*, vol. 221, no. 1, 3-12. Doi: 10.1002/path.2697

Goode, A., Butler, K., Long, J., Cavey, J., Shaw, B., Sollenberger, J., Gell, C., Johansen, T., Oldham, N.J., Searle, M.S., Layfield, R., 2016. Defective recognition of LC3B by mutant SQSTM1/ p62 implicates impairment of autophagy as a pathogenic mechanism in ALS-FTLD. *Autophagy*, vol. 12, no. 7, 1094-1104. Doi: 10.1080/15548627.2016.1170257

Goode, A., Layfield, R., 2010. Recent advances in understanding the molecular basis of Paget disease of bone. *Journal of Clinical Pathology*, vol. 63, no. 3, 199-203. Doi: 10.1136/jcp.2009.064428

Goode, A., Long, J.E., Shaw, B., Ralston, S.H., Visconti, M.R., Gianfrancesco, F., Esposito, T., Gennari, L., Merlotti, D., Rendina, D., Rea, S.L., Sultana, M., Searle, M.S., Layfield, R., 2014. Paget disease of bone-associated UBA domain mutations of SQSTM1 exert distinct effects on protein structure and function. *Biochimica et Biophysica Acta*, vol. 1842, no. 7, 992-1000. Doi: 10.1016/j.bbadis.2014.03.006

Gruener, G., Camacho, P., 2014. Paget's disease of bone. *Handbook of Clinical Neurology*, vol. 119, 529-540. Doi: 10.1016/B978-0-7020-4086-3.00034-5

Grynpas, M.D., Tupy, J.H., Sodek, J., 1994. The distribution of soluble, mirenal-bound, and matrix-bound proteins in osteoporotic and normal bones. *Bone*, vol. 15, no. 5, 505-513

Hadjipavlou, A., Lander, P., Srolovitz, H., 1986. Pagetic arthritis: pathophysiology and management. *Clinical Orthopaedics and Related Research*, vol. 208, 15-19

Helfrich, M.H., Crockett, J.C., Hocking, L.J., Coxon, F.P., 2007. The pathogenesis of osteoclast diseases: some knowns, but still many unknowns. *BoneKEy-Osteovision*, vol. 4, no. 2, 61-77. Doi: 10.1138/20060249

Helfrich, M.H., Hocking, L.J., 2008. Genetics and aetiology of Pagetic disorders of bone. *Archives of Biochemistry and Biophysics*, vol. 473, no. 2, 172-182. Doi: 10.1016/j.abb.2008.02.045

Hewitt, G., Korolchuk, V.I., 2017. Repair, Reuse, Recycle: The expanding role of autophagy in genome maintenance. *Trends in Cell Biology*, vol. 27, no. 5, 340-351. Doi: 10.1016/j.tcb.2016.11.011

Hiruma, Y., Kurihara, N., Subler, M.A., Zhou, H., Boykin, C.S., Zhang, H., Ishizuka, S., Dempster, D.W., Roodman, G.D., Windle, J.J., 2008. A SQSTM1/p62 mutation linked to Paget's disease increases the osteoclastogenic potential of the bone microenvironment. *Human Molecular Genetics*, vol. 17, no. 23, 3708-3719. Doi: 10.1093/hmg/ddn266

Hocking, L.J., Lucas, G.J., Daroszewska, A., Mangion J., Olavesen M., Cundy, T., Nicholson, G.C., Ward, L., Bennett, S.T., Wuyts, W., Van Hul, W., Ralston, S.H., 2002. Domain-specific mutations in sequestosome 1 (SQSTM1) cause familial and sporadic Paget's disease. *Human molecular genetics*, vol. 11, no. 22, 2735-2739.

Hocking, L.J., Whitehouse, C., Helfrich, M.H., 2012. Autophagy: a new player in skeletal maintenance?. *Journal of Bone and Mineral Research*, vol. 27, no. 7, 1439-1447. Doi: 10.1002/jbmr.1668

Khosla, S., 2001. Minireview: the OPG/RANKL/RANK system. *Endocrinology,* vol. 142, no. 12, 5050-5055. Doi: 10.1210/endo.142.12.8536

Kirkin, V., McEwan, D.G., Novak, I., Dikic, I., 2009. A role for ubiquitin in selective autophagy. *Molecular cell*, vol. 34, no. 3, 259-269. Doi: 10.1016/j.molcel.2009.04.026

Komatsu, M., Ichimura, Y., 2010. Physiological significance of selective degradation of p62 by autophagy. *FEBS Letters*, vol. 584, no. 7, 1374-1378. Doi: 10.1016/j.febslet.2010.02.017

Layfield, R., Cavey, J.R., Najat, D., Long, J., Sheppard, P.W., Ralston, S.H., Searle, M.S., 2006. p62 mutations, ubiquitin recognition and Paget's disease of bone. *Biochemical Society Transactions*, vol. 34, pt. 5, 735-737. Doi: 10.1042/BST0340735

Layfield, R., Ciani, B., Ralston, S.H., Hocking, L.J., Sheppard, P.W., Searle, M.S., Cavey, J.R., 2004. Structural and functional studies of mutations affecting the UBA domain of SQSTM1 (p62) which cause Paget's disease of bone. *Biochemical Society Transactions*, vol. 32, pt. 5, 728-730. Doi: 10.1042/BST0320728

Layfield, R., Hocking, L.J., 2004. SQSTM1 and Paget's disease of bone. *Calcified Tissue International,* vol. 75, 347-357. Doi: 10.1007/s00223-004-0041-0

Lazarou, M., Sliter, D.A., Kane, L.A., Sarraf, S.A., Wang, C., Burman, J.L., Sideris, D.P., Fogel, A.I., Youle, R.J., 2015. The ubiquitin kinase PINK1 recruits autophagy receptors to induce mitophagy. Nature, vol. 524, no. 7565, 309-314. Doi: 10.1038/nature14893

Leach, R.J., Singer, F.R., Ench, Y., Wisdom, J.H., Pina, D.S., Johnson-Pais, T.L., 2006. Clinical and cellular phenotypes associated with sequestosome 1 (SQSTM1) mutations. *Journal of Bone and Mineral Research*, vol. 21, 45-50. Doi: 10.1359/jbmr.06s208

Lever, J.H., 2002. Paget's disease of bone in Lancashire and arsenic pesticide in cotton mill wastewater: a speculative hypothesis. *Bone*, vol. 31, no. 3, 434-436

Li, f., Xie, X., Wang, Y., Liu, J., Cheng, X., Guo, Y., Gong, Y., Hu, S., 2016. Structural insights into the interaction and disease mechanism of neurodegenerative disease-associated optineurin and TBK1 proteins. *Nature communications*, vol., 13, no. 7, 12708. Doi: 10.1038/ncomms12708

Liu, Z., Chen, P., Gao, H., Gu, Y., Yang, J., Peng, H., Xu, X., Wang, H., Yang, M., Liu, X., Fan, L., Chen, S., Zhou, J., Sun, Y., Ruan, K., Cheng, S., Komatsu, M., White, E., Li, L., Ji., H., Finley, D., Hu, R.,2014. Ubiquitylation of autophagy receptor optineurin by HACE1 activates selective autophagy for tumour suppression. *Cancer cell*, vol. 26, no. 1, 106-120. Doi: 10.1016/j.ccr.2014.05.015

Long, J., Gallagher, T.R., Cavey, J.R., Sheppard, P.W., Ralston, S.H., Layfield, R., Searle, M.S., 2008. Ubiquitin recognition by the ubiquitin-associated domain of p62 involves a novel conformational switch. *The Journal of Biological Chemistry*, vol. 283, no. 9, 5427-5440. Doi: 10.1074/jbc.M704973200

Mays, S., 2010. Archaeological skeletons support a northwest European origin for Paget's disease of bone. *Journal of bone and mineral research,* vol. 25, no. 8, 1839-1841. Doi: 10.1002/jbmr.64

McManus, S., Bisson, M., Chamberland, R., Roy, M., Nazari, S., Roux, S., 2016. Autophagy and 3-phosphoinositide-dependent kinase 1 (PDK1)-related kinome in pagetic osteoclasts. *Journal of Bone and Mineral Research*, vol. 31, no. 7, 1334-1343. Doi: 10.1002/jbmr.2806

Menéndez-Bueyes, L.R., Soler-Fernández, M.D., 2017. Enfermedad ósea de Paget: aproximación a sus orígenes históricos. *Reumatología Clínica*, vol. 13, no. 2, 66-72. Doi: 10.1016/j.reumae.2016.02.009

Mitch, W.E., Goldberg, A.L., 1996. Mechanisms of muscle wasting. The role of the ubiquitin-proteasome pathway. *The New England Journal of medicine*, vol. 335, no. 25, 1897-1905. Doi: 10.1056/NEJM199612193352507

Mizushima, N., 2007. Autophagy: process and function. *Genes & Development*, vol. 21, 2861-2873. Doi: 10.1101/gad.1599207

Morton, S., Hesson, L., Peggie, M., Cohen, P., 2008. Enhanced binding of TBK1 by an optineurin mutant that causes a familial form of primary open angle glaucoma. *FEBS letters*, vol. 582, no. 6, 997-1002. Doi: 10.1016/j.febslet.2008.02.047.

Moscat, J., Diaz-Meco, M.T., Wooten M.W., 2007. Signal integration and diversification through the p62 scaffold protein. *TRENDS in Biochemical Sciences*, vol. 32, no. 2, 95-100. Doi: 10.1016/j.tibs.2006.12.002

Mundy, G.R., 1999. Cellular and molecular regulation of bone turnover. *Bone*, vol. 24, 35S-38S

Najat, D., Garner, T., Hagen, T., Shaw, B., Sheppard, P.W., Falchetti, A., Marini, F., Brandi, M.L., Long, J.E., Cavey, J.R., Searle, M.S., Layfield, R., 2009. Characterization of a non-UBA domain missense mutation of sequestosome 1 (SQSTM1) in Paget's disease of bone. *Journal of Bone and Mineral Research*, vol. 24, no. 4, 632-642. Doi: 10.1359/jbmr.081204

Naot, D., Bava, U., Matthews, B., Callon K.E., Gamble, G.D., Black, M., Song, S., Pitoo, R.P., Cundy, T., Cornish, J., Reid, I.R., 2007. Differential gene expression in cultured osteoblasts and bone marrow stromal cells from patients with Paget's disease of bone. *Journal of Bone and Mineral Research*, vol. 22, no. 2, 298-309. Doi: 10.1359/jbmr.061108

Nguyen, T.N., Padman, B.S., Usher, J., Oorschot, V., Ramm, G., Lazarou, M., 2016. Atge8 family LC3/GABARAP proteins are crucial for autophagosome-lysosome fusion but not autophagosome formation during PINK1/Parkin mitophagy and starvation. *The Journal of Cell Biology*. Doi: 10.1083/jcb.201607039

Numan, M.S., Amiable, N., Brown, J.P., Michou, L., 2015. Paget's disease of bone: an osteoimmunological disorder?. *Drug Des Devel Ther*, vol. 14, no. 9, 4695-4707. Doi: 10.2147/DDDT.S88845

Obaid, R., Wani, S.E., Azfer, A., Hurd, T., Jones, R., Cohen, P., Ralston, S.H., Albagha, O.M., 2015. Optineurin negatively regulates osteoclast differentiation by modulating NF-κβ and interferon signalling: implications for Paget's disease. *Cell Reports*, vol. 13, no. 6, 1096-1102. Doi: 10.1016/j.celrep.2015.09.071

Paget, J., 1877. On a form of chronic inflammation of bones (Osteitis Deformans). *Medico-Chirurgical transactions*, vol. 60, 37-64.9

Peng, H., Yang, L., Li, G., You, Q., Han, W., Li, T., Gao, D., Xie, X., Lee, B.H., Du, J., Hou, J., Zhang, T., Rao, H., Huang, Y., Li, Q., Zeng, R., Hui, L., Wang, H., Xia, Q., Zhang, X., He, Y., Komatsu, M., Dikic, I., Finley, D., Hu, R., 2017. Ubiquitylation of p62/ sequestosome1 activates its autophagy receptor function and controls selective autophagy upon ubiquitin stress. *Cell Research*, vol. 27, no. 5, 657-674. Doi: 10.1038/cr.2017.40

Pilli, M., Arko-Mensah, J., Ponpuak, M., Roberts, E., Master, S., Mandell, M.A., Dupont, N., Ornatowski, W., Jiang, S., Bradfute, S.B., Bruun, J.A., Hansen, T.E., Johansen, T., Deretic, V., 2012. TBK-1 promotes autophagy-mediated antimicrobial defense by controlling autophagosome maturation. *Immunity*, vol. 37, no. 2, 223-234. Doi: 10.1016/j.immuni.2012.04.015

Ponting, C.P., Blake, D.J., Dvies, K.E., KendrickJones, J., Winder, S.J., 1996. ZZ and TAZ: New putative zinc fingers in dystrophin and other proteins. *Trends in Biochemical Sciences*, vol. 21, no. 1, 11-13.

Ralston, S.H., Langston, A.L., Reid, I.R., 2008. Pathogenesis and management of Paget's disease of bone. *Lancet*, vol. 372, no. 9633, 155-163. Doi: 10.1016/S0140-6736(08)61035-1

Ralston, S.H., 2008. Pathogenesis of Paget's disease of bone. *Bone*, vol. 43, no. 5, 819-825. Doi: 10.1016/j.bone.2008.06.015

Rea, S.L., Majcher, V., Searle, M.S., Layfield, R., 2014. SQSTM1 mutations – bridging Paget disease of bone and ALS/FTLD. *Experimental Cell Research*, vol. 325, no. 1, 27-37. Doi: 10.1016/j.yexcr.2014.01.020

Rea, S.L., Walsh, J.P., Layfield, R., Ratajczak, T., Xu, J., 2013. New insights into the role of sequestosome 1/p62 mutant proteins in the pathogenesis of Paget's disease of bone. *Endocrine Reviews*, vol. 34, no. 4, 501-524. Doi: 10.1210/er.2012-1034

Rechsteiner, M., Rogers, S.W., 1996. PEST sequences and regulation by proteolysis. *Trends in Biochemical Sciences*, vol. 21, no. 7, 267-271.

Rendina, D., Gennari, L., De Filippo, G., Merlotti, D., de Campora, E., Fazioli, F., Scarano, G., Nuti, R., Strazzullo, P., Mossetti, G., 2006. Evidence for increased clinical severity of familial and sporadic Paget's disease of bone in Campania, southern Italy. *Journal of bone and mineral research*, vol. 21, no. 12, 1828-1835. Doi: 10.1359/jbmr.060822

Rhodes, E.C., Johnson-Pais, T.L., Singer, F.R., Ankerst, D.P., Bruder, J.M., Wisdom, J., Hoon, D.S., Lin, E., Bone, H.G., Simcic, K.J., Leach, R.J., 2008. Sequestosome 1 (SQSTM1) mutations in Paget's disease of bone from the United States. *Calcified Tissue International*, vol. 82, no. 4, 271-277. Doi: 10.1007/s00223-008-9114-9

Rogov, V., Dötsch, V., Johansen, T., Kirkin, V., 2014. Interactions between autophagy receptors and ubiquitin-like proteins form the molecular basis for selective autophagy. *Molecular Cell,* vol. 53, no. 2, 167-178. Doi: 10.1016/j.molcel.2013.12.2014

Roodman, G.D., Windle, J.J., 2005. Paget disease of bone. *The Journal of clinical investigation*, vol. 115, no. 2, 200-208. Doi: 10.1172/JCI24281

Scherz-Shouval, R., Shvets, E., Fass, E., Shorer, H., Gil, L., Elazar, Z., 2007. Reactive oxygen species are essential for autophagy and specifically regulate the activity of Atg4. *The EMBO Journal*, vol. 26, no. 7, 1749-1760. Doi: 10.1038/sj.emboj.7601623

Schmidt-Schultz, T.H., Schultz, M., 2004. Bone protects proteins over thousands of years: extraction, analysis, and interpretation of extracellular matrix proteins in archeological skeletal remains. *American Journal of Physical Anthropology*, vol. 123, no. 1., 30-39. Doi: 10.1002/aipa.10308

Schmidt-Schultz, T.H., Schultz, M., 2007. Well preserved non-collagenous extracellular matrix proteins in ancient human bone and teeth. *International Journal of Osteorchaeology*, vol. 17, no. 1, 91-99. Doi: 10.1002/oa.858

Schmidt-Schultz, T.H., Schultz, M., 2015. AG-85, a major secretion protein of *Mycobacterium tuberculosis*, can be identified in ancient bone. *Tuberculosis*, vol. 95, suppl. 1, 87-92. Doi: 10.1016/j.tube.2015.02.034

Schultz, M., Parzinger, H., Posdnjakow, D.V., Chikisheva, T.A., Schimidt-Schultz, T.H., 2007. Oldest known case of metastasizing prostate carcinoma diagnosed in the skeleton of a 2.700-year-old Scythian king from Arzhan (Siberia, Russia). *International Jorunal of Cancer*, vol. 121, no. 12, 2591-2595. Doi: 10.1002/ijc.23073

Seibenhener, M.L., Geetha, T., Wooten, M.W., 2007. Sequestosome 1/ p62 – More than just a scaffold. *FEBS Letters*, vol. 581, no. 2, 175-179. Doi: 10.1016/j.febslet.2006.12.027

Shapiro, I.M., Layfield, R., Lotz, M., Settembre, C., Whitehouse, C., 2014. Boning up on autophagy: the role of autophagy in skeletal biology. *Autophagy*, vol. 10, no. 1, 7-19. Doi: 10.4161/auto.26679

Siris, E.S., 1994. Epidemiological aspects of Paget's disease: family history and relationship to other medical conditions. *Seminars in arthritis and rheumatism*, vol. 23, no. 4, 222-225.

Smith, P.K., Krohn, R.I., Hermanson, G.T., Mallia, A.K., Gartner, F.H., Provenzano, M.D., Fujimoto, E.K., Goeke, N.M., Olson, B.J., Klenk, D.C., 1985. Measurement of protein using bicinchoninic acid. *Analytical biochemistry*, vol. 150, no. 1, 76-85

Solomon, L.R., 1979. Billiard-player's fingers: an unusual case of Paget's disease of bone. *Short Reports*, *British Medical Journal*, vol. 1, no. 6168, 931

Srinivas, V., Bohensky, J., Zahm, A.M., Shapiro, I.M., 2009. Autophagy in mineralizing tissues: microenvironmental perspectives. *Cell Cycle*, vol. 8, no. 3, 391-393. Doi: 10.4161/cc.8.3.7545

Sun, Q., Sammut, B., Wang, F.M., Kurihara, N., Windle, J.J., Roodman, G.D., Galson, D.L., 2014. TBK1 mediates critical effects of measles virus nucleocapsid protein (MVNP) on pagetic osteoclast formation. *Journal of Bone and Mineral Research*, vol. 29, no. 1, 90-102. Doi: 10.1002/jbmr.2026

Taylor, J.P., Hardy, J., Fischbeck, K.H., 2002. Toxic proteins in neurodegenerative disease. *Science*, vol. 296, no. 5575, 1991-1995. Doi: 10.1126/science.1067122

Taylor, J.P., Jackson, W.T., 2009. Viruses and arrested autophagosome development. *Autophagy*, vol. 5, no. 6, 870-871

Theodorou, D.J., Theodorou, S.J., Kakitsubata, Y., 2011. Imaging of Paget disease of bone and its musculoskeletal complications: review. *American Journal of Roentgenology*, vol. 196, S64-S75. Doi: 10.2214/AJR.10.7222

Tsuboyama, K., Koyama-Honda, I., Sakamaki, Y., Koike, M., Morishita, H., Mizushima, N., 2016. The ATG conjugation systems are important for degradation of the inner autophagosomal membrane. *Science*, vol. 354, no. 6315, 1036-1041. Doi: 10.1126/science.aaf6136

Usategui-Martin, R., García-Aparicio, J., Corral-Gudino, L., Calero-Paniagua, I., Del Pino-Montes, J., González Sarmiento, R., 2015. Polymorphisms in autophagy genes are associated with paget disease of bone. *PLoS One*, vol. 10, no. 6. Doi: 10.1371/journal.pone.0128984

Vadlamudi, R.K., Joung, I., Strpminger, J.L., Shin, J., 1996. p62, a phosphotyrosine-independent ligand of the SH2 domain of $p56^{lck}$, belongs to a new class of ubiquitin-binding proteins. *The Journal of Biological Chemistry*, vol. 271, no. 34, 20235-20237.

Vallet, M., Ralston, S.H., 2016. Biology and treatment of Paget's disease of bone. *Journal of Cellular Biochemistry*, vol. 117, 289-299. Doi: 10.1002/jcb.25291

Wadsworth, C., Buckley, M., 2014. Proteome degradation in fossils: investigating the longevity of protein survival in ancient bone. *Rapid communications in mass spectrometry*, vol. 28, no. 6, 605-615. Doi: 10.1002/rcm.6821

Xiong, Y., Contento, A.L., Nquyen, P.Q., Bassham, D.C., 2007. Degradation of oxidized proteins by autophagy during oxidative stress in Arabidopsis. *Plant Physiology*, vol. 143, no. 1, 291-299. Doi: 10.11004/pp.106.092106

Appendix:

A. Vector maps

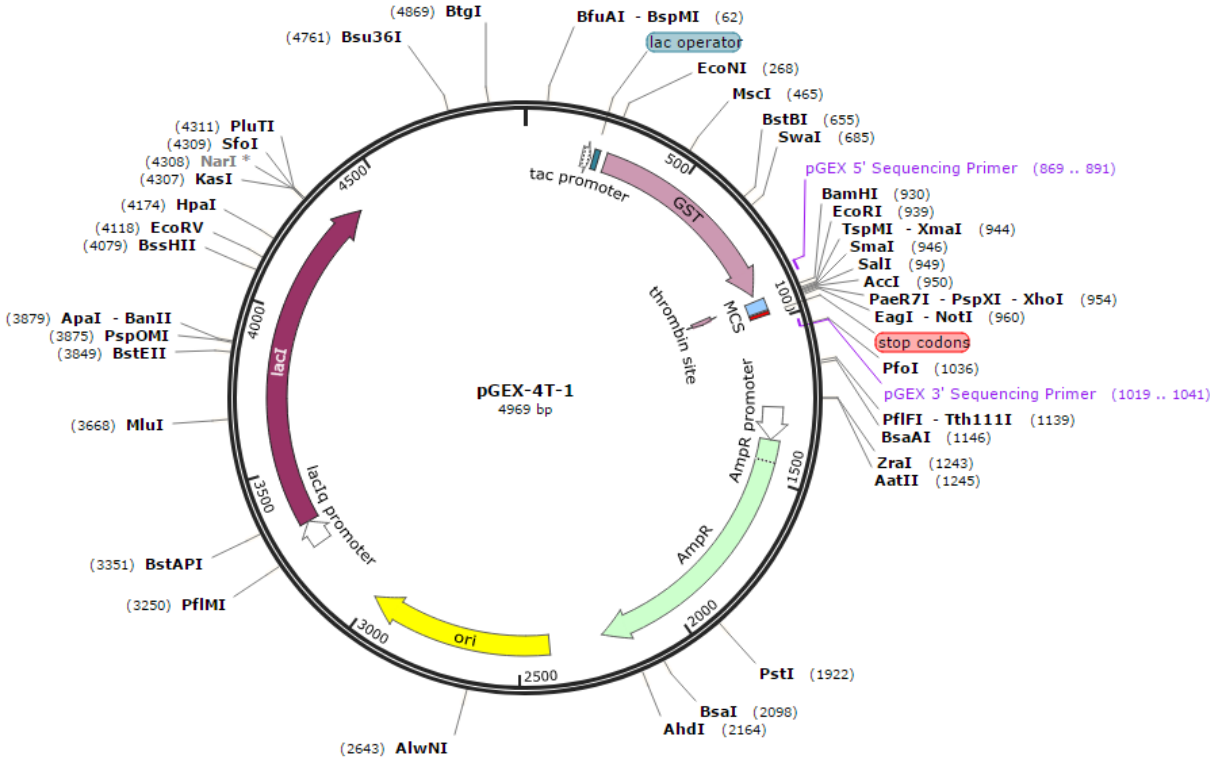


Figure A.1. Empty pGEX-4T1 (Amersham Biosciences).

The plasmids for expression of the full-length wild-type and different mutant SQSTM1/p62 proteins (residues 1–440) as GST fusion proteins (pGEX-4T-1, Amersham Biosciences) were provided, and they were generated by introducing cDNA encoding the related SQSTM1/p62 protein (IMAGE clone 2906264) to the *Eco*RI/*Xho*I restriction sites of the pGEX-4T-1 plasmid in XL10-Gold Ultracompetent Cells (*E. coli*). However, the F406V mutant was produced from the wild-type plasmid by site-directed mutagenesis (QuikChange kit; Stratagene) and subsequently verified by DNA sequencing.

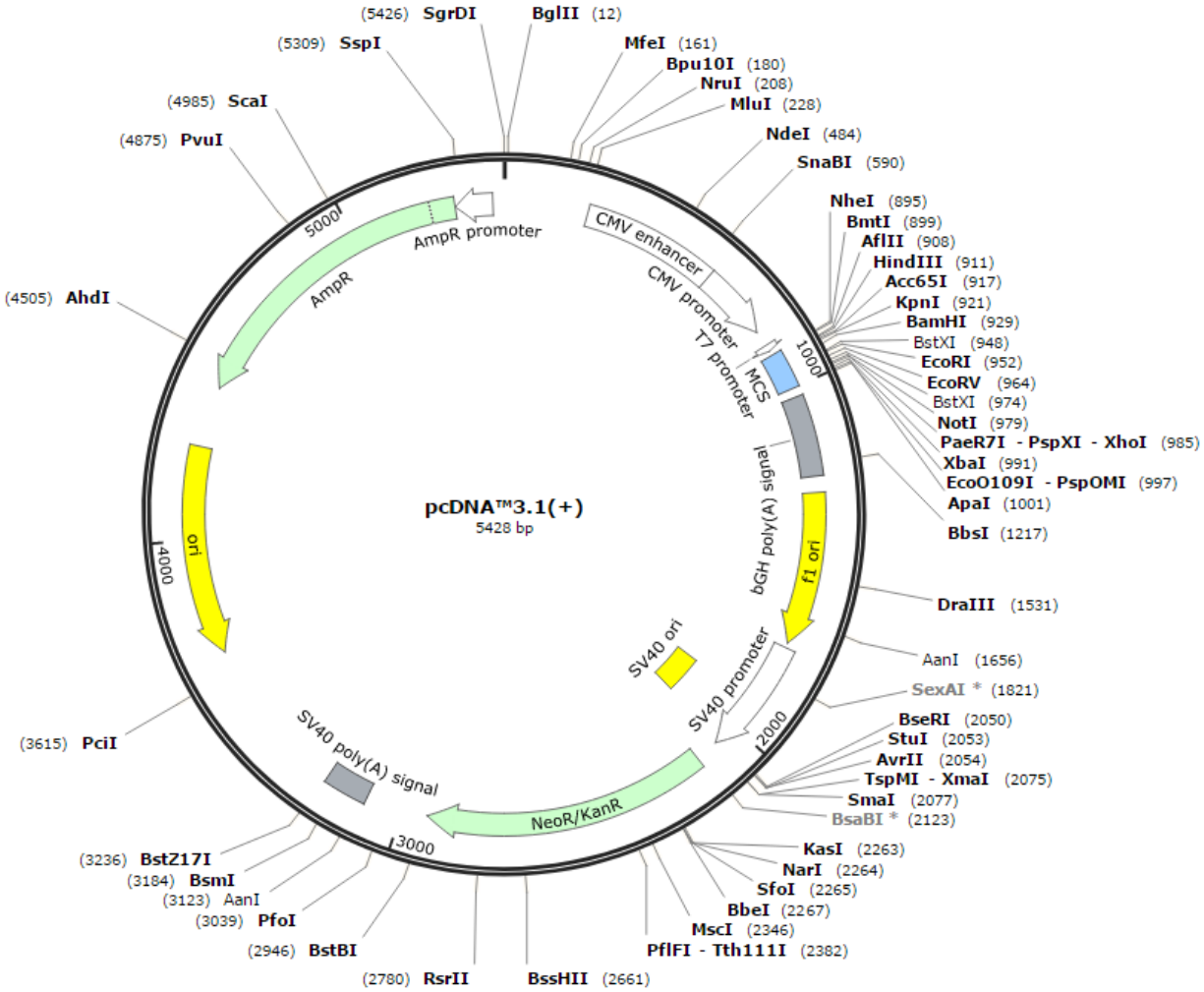


Figure A.2. Empty pDNA3.1 (+) (Invitrogen).

Mammalian expression vectors (pcDNA3.1 construct; Invitrogen) for wild-type and selected PDB-mutant SQSTM1/p62 proteins (His-FLAG tagged) were provided and they were generated by PCR amplification of the related SQSTM1/p62 cDNA, and ligation into the *Not*I restriction site of a pcDNA3.1. However, the F406V mutation (as well as other *SQSTM1* mutations) were again introduced into the wild-type SQSTM1/p62 construct by site-directed mutagenesis and confirmed by DNA sequencing.

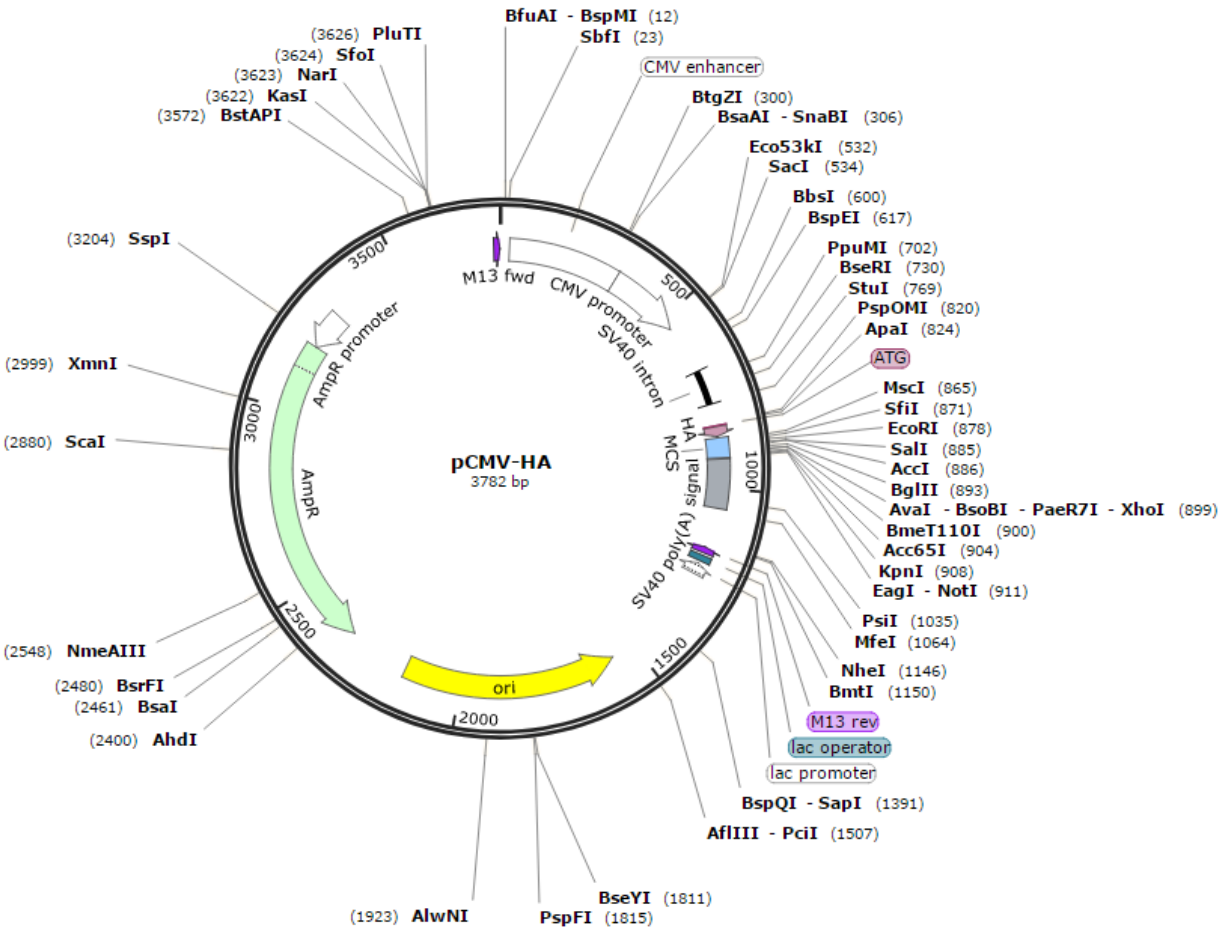


Figure A.3. Empty pcMV-HA.

Vector for expressing an N-terminally HA-tagged protein in mammalian cells. In this case, it was used to express wild type and K38A mutant of TBK1. Both plasmids were provided and they were generated by PCR amplification of the related TBK1 cDNA.

B. Primers

All the primers used during the study were designed following the instructions of QuickChange® Site-Directed Mutagenesis kit (Stratagene).

Figure B.1. Original amino-acid and nucleotide sequence SQSTM1/p62 protein. All the sites of mutations analysed in this study are highlighted in red (P932L; E396X; M404V; F406V; G425R).

```
1    MASLTVKAYL LGKEDAAREI RRFSFCCSPE PEAEAEAAAG PGPCERLLSR 50
51    VAALFPALRP GGFQAHYRDE DGDLVAFSSD EELTMAMSYV KDDIFRIYIK 100
101   EKKECRRDHR PPCAQEAPRN MVHPNVICDG CNGPVVGTRY KCSVCPDYDL 150
151   CSVCEGKGLH RGHTKLAFPS PFGHLSEGFS HSRWLRKVKH GHFGWPGWEM 200
201   GPPGNWSPRP PRAGEARPGP TAESASGPSE DPSVNFLKNV GESVAAALSP 250
251   LGIEVDIDVE HGGKRSRLTP VSPESSSTEE KSSSQPSSCC SDPSKPGGNV 300
301   EGATQSLAEQ MRKIALESEG RPEEQMESDN CSGGDDDWTH LSSKEVDPST 350
351   GELQSLQMPE SEGPSSLDPS QEGPTGLKEA ALYPHLPPEA DPRLIESLSQ 400
401    MLSMGFSDEG GWLTRLLQTK NYDIGAALDT IQYSKHPPPL          440
```

```
atggcgtcgc tcaccgtgaa ggcctacctt ctgggcaagg aggacgcggc gcgcgagatt
cgccgcttca gcttctgctg cagccccgag cctgaggcgg aagccgaggc tgcggcgggt
ccgggaccct gcgagcggct gctgagccgg gtggccgccc tgttccccgc gctgcggcct
ggcggcttcc aggcgcacta ccgcgatgag gacggggact tggttgcctt ttccagtgac
gaggaattga caatggccat gtcctacgtg aaggatgaca tcttccgaat ctacattaaa
gagaaaaaag agtgccggcg ggaccaccgc ccaccgtgtg ctcaggaggc gccccgcaac
atggtgcacc ccaatgtgat ctgcgatggc tgcaatgggc ctgtggtagg aacccgctac
aagtgcagcg tctgcccaga ctacgacttg tgtagcgtct gcgagggaaa gggcttgcac
cgggggcaca ccaagctcgc attccccagc cccttcgggc acctgtctga gggcttctcg
cacagccgct ggctccggaa ggtgaaacac ggacacttcg ggtggccagg atgggaaatg
ggtccaccag gaaactggag cccacgtcct cctcgtgcag gggaggcccg ccctggcccc
acggcagaat cagcttctgg tccatcggag gatccgagtg tgaatttcct gaagaacgtt
ggggagagtg tggcagctgc ccttagccct ctgggcattg aagttgatat cgatgtggag
cacggaggga aaagaagccg cctgaccccc gtctctccag agagttccag cacagaggag
aagagcagct cacagccaag cagctgctgc tctgacccca gcaagccggg tgggaatgtt
gagggcgcca cgcagtctct ggcggagcag atgaggaaga tcgccttgga gtccgagggg
cgccctgagg aacagatgga gtcggataac tgttcaggag gagatgatga ctggacccat
ctgtcttcaa aagaagtgga cccgtctaca ggtgaactcc agtccctaca gatgccagaa
tccgaagggc caagctctct ggacccctcc caggagggac ccacagggct gaaggaagct
gccttgtacc cacatctccc gccagaggct gacccgcggc tgattgagtc cctctcccag
atgctgtcca tgggcttctc tgatgaaggc ggctggctca ccaggctcct gcagaccaag
aactatgaca tcggagcggc tctggacacc atccagtatt caaagcatcc cccgccgttg
tga
```

Table 3. Primers used to generate the different mutated SQSTM1/p62 plasmids from pGEX-4T1-WT-SQSTM1/p62. [Note: All sequences are 5'-3']

Plasmid	Primers		Length (aa)	% mismatch	% GC	Tm (°C)
	For	Rever				
pGEX-4T1-F406V-p62	ccagatgctgtccatgggcgtctctgatgaaggcggc	gccgccttgatcagagacgcccatggacagcatctgg	37	2.70	62.16	86.042
pGEX-4T1-H436X-p62	ccatccagtattcaaagtaacccccgccgttgtgactcg	cgagtcacaacggcgggggttactttgaatactggatgg	39	5.13	48.72	79.03
pGEX-4T1-I431X-p62	ggagcggctctggacacctaacagtattcaaagcatcccc	ggggatgctttgaatactgttaggtgtccagagccgctcc	40	7.5	57.5	80.7
pGEX-4T1-A426X-p62	gaccaagaactatgacatcggataagctctggacaccatccagtattc	gaatactggatggtgtccagagcttatccgatgtcatagttcttggtc	48	6.25	45.83	79.98
pGEX-4T1-N421X-p62	gctcctgcagaccaagtaatatgacatcggagcgg	ccgctccgatgtcatattacttggtctgcaggagc	35	5.71	54.29	78.76
pGEX-4T1-L416X-p62	gcggctggctcaccaggtaactgcagaccaagaac	gttcttggtctgcagttacctggtgagccagccgc	35	8.57	60	78.24
pGEX-4T1-G411X-p62	gggcttctctgatgaaggctaatggctcaccaggctcctgc	gcaggagcctggtgagccagccgccttcatcagagaagccc	41	7.32	58.54	81.72

C. Materials

- **Reagents**
    - **Agar/ampicillin plates:** Luria broth with agar (35 g/L)**;** Select agar (2.5 g/L); Ampicillin (100 mg/ml).
    - **Ammonium persulphate (APS):** 10% APS.
    - **Ampicillin (Fischer):** 100mg/ml; filter sterilised.
    - **BCA reagent:** Purchased from Thermo Scientific; 50 parts of BCA Reagent A with 1 part of BCA Reagent B (50:1; A:B).
    - **Cell freezing medium:** 90 % (v/v) FCS; 10 % (v/v) DMSO.
    - **Cocktail phosphatase inhibitors**
    - **Cocktail protease inhibitors**
    - **Coomassie blue staining solution:** 50 % (v/v) methanol; 20 % (v/v) glacial acetic acid; 0.12 % (w/v) Coomassie Brilliant Blue R-250.
    - **Coomassie blue de-staining solution:** 10 % (v/v) methanol**;** 10 % (v/v) glacial acetic acid.
    - **Bacterial collagenase:** Purchased from SIGMA.
    - **DMEM growth medium:** Dulbecco's Modified Eagle medium (DMEM); 10 % (v/v) FCS; 1 % (v/v) penicillin/streptomycin.
    - **Glutathione Sepharose beads 4B:** Purchased from GE Healthcare.

- **Glycerol 30 %:** Glycerol (0.3 ml/ml); filter sterilised.
- **IPTG solution (Melford):** 200 mM; filter sterilised.
- **LB broth:** Luria broth (25 g/L).
- **Opti-MEM (GIBCO™):** Reduced-serum medium (1X) liquid (Invitrogen), contains A GlutaMAX™- I medium. This includes the dipeptide L-alanyl-L-glutamine substituted on a molar equivalent basis for L- glutamine.
- **Ponceau S staining solution:** 0.1 % (w/v) Ponceau S; 5 % (v/v) acetic acid.
- **TCA (Trichloroacetic acid)**
- **TEMED:** Tetramethylethylenediamine.
- **Triton X-100**
- **Trypsin:** 0.5 g porcine trypsin (Sigma- Aldrich); 0.2 g EDTA·4Na per litre of Hank's Balanced Salt Solution, plus phenol red.

- **Buffers**
  - **Plasmid DNA purification solutions**
    - **P1:** Re-suspension buffer (Tris-EDTA, RNAase added at the time of the experiment).
    - **P2:** Sodium hydroxide (should be closes immediately after use in order to prevent reaction with CO2 in the air, which leads to pH change).
    - **N3:** Neutralization buffer, guanidine hydrochloride/ acetic acid.
    - **PE:** Guanidine hydrochloride/ isopropanol (ethanol added at the time of the experiment).
  - **Mammalian cell culture**
    - **PBS:** Phosphate buffered saline (Dulbecco A) Oxid, each tablet was dissolved in 100 ml $_dH_2O$, autoclaved and left to cool down. The solution has a pH of 7.3 at 25 °C. Each tablet typical formula is:

Component	g/L
NaCl	8
KCl	0.2
Na_2HPO_4	1.15
KH_2PO_4	0.2

- **DPBS:** Dulbecco's Phosphate buffered saline (Sigma), liquid, sterile-filtered, cell culture tested. It has additional $CaCl_2 \cdot 2H_2O$, and $MgCl_2 \cdot 6H_2O$ the typical formula solution is:

Component	g/L
$CaCl_2 \cdot 2H_2O$	0.113
$MgCl_2 \cdot 6H_2O$	0.1
NaCl	8
KCl	0.2
Na_2HPO_4	1.15
KH_2PO_4	0.2

- **RIPA:** 5 M NaCl; 1 M Tris; NP-40; 10 % Sodium deoxycholate; 10 % SDS; pH 8 with HCl.

- **Protein extractions**
  - **Buffer A:** 4 M Guanidine HCl; 20 mM sodium dihydrogen phosphate; 30 mM sodium hydrogen phosphate; pH 7.4 with HCl.
  - **Buffer B:** 4 M Guanidine HCl**;** 20 mM sodium dihydrogen phosphate**;** 30 mM sodium hydrogen phosphate**;** 300 mM EDTA; pH 7.4 with HCl.
  - **Phosphate buffer:** 50 mM phosphate.
  - **Bacterial collagenase digestion buffer:** 50 mM Tris-HCl**;** 5 mM $CaCl_2$**;** 5 mM PMSF (Phenylmethylsulfonylfluoride)**;** pH 7.6 with HCl.

- **SDS PAGE**
  - **Gel application buffer (GAB):** 150 mM Tris (hydroxymethyl) methylamine**;** 8 M Urea**;** 2.5 % (w/v) SDS**;** 20 % (v/v) glycerol**;** 10 % (v/v) 2-βmercaptoethanol**;** 3 % (w/v) DTT (dithiothreitol)**;** 0.1 % (w/v) bromophenol blue**;** pH 6.8 with HCl.
  - **5 % acrylamide resolving gel mixture:** 5 % (v/v) acrylamide**;** 367 mM Tris (hydroxymethyl) methylamine**;** 0.13 % (w/v) SDS**;** APS**;** TEMED**;** pH 8.8 with HCl.
  - **20 % acrylamide resolving gel mixture:** 20 % (v/v) acrylamide**;** 367 mM Tris (hydroxymethyl) methylamine**;** 10 % glycerol**;** 0.13 % (w/v) SDS**;** APS**;** TEMED**;** pH 8.8 with HCl.
  - **Stacking gel buffer:** 0.14 M Tris (hydroxymethyl) methylamine**;** 0.1 % (w/v) SDS; pH 6.8 with HCl.

- **Running buffer:** 25 mM Tris (hydroxymethyl) methylamine**;** 0.1 % (w/v) SDS**;** 186 mM glycine

- **Silver stain solutions:**
  - **Fixing solution:** Ethanol 100 ml**;** Glacial acetic acid 25 ml**;** Water to 250
  - **Sensitising solution:** Ethanol 75 ml**;** Sodium thiosulphate (5 % w/v) 10 ml**;** Sodium acetate 17 g**;** Glutardialdehyde (25 % w/v) 1.25 ml [Note: add just before use]**;** Water to 250 ml.
  - **Silver solution:** Silver nitrate solution (2.5 % w/v) 25 ml**;** Water to 250 ml.
  - **Developing solution**: Sodium carbonate 6.25 g; Formaldehyde (37 % w/v) 0.2 ml [Note: add just before use]; Water to 250 ml.
  - **Stop solution:** EDTA-$Na_2 \cdot 2H_2O$ 3.65 g**;** Water to 250 ml.
- **Western blotting**
  - **Transfer buffer:** 25 mM Tris (hydroxymethyl) methylamine**;** 129 mM glycine; 20 % (v/v) methanol.
  - **Blocking buffer:** 5 % (w/v) Marvel milk powder in TBS.
  - **TBS (Tris buffered saline):** 100 mM Tris (hydroxymethyl) methylamine; 150 mM NaCl; pH 7.5 with HCl.
  - **TBS-Tween 20:** 0.05 % Tween 20 in TBS.
- **Preparation of Control/ Glutathione/ Ubiquitin/ LC3 sepharose beads**
  - **Coupling buffer:** 100 mM Sodium bicarbonate**;** 500 mM Sodium chloride, pH 8.3 with HCl; 1 M Ethanolamine, pH 8 with HCl.
  - **Acetate buffer:** 100 mM Sodium acetate**;** 500 mM NaCl; pH 4 with acetic acid.
  - **Tris buffer:** 100 mM Tris (hydroxymethyl) methylamine; pH 8 with HCl.
  - **Column storage buffer:** 25 mM Tris (hydroxymethyl) methylamine; 1 mM Sodium azide; pH 7.4 with HCl.
  - **TBS-Triton:** 0.1 % (v/v) Triton X-100 in TBS.

- **Antibodies**
  - **Primary antibodies:**
    - Mouse anti HA-HRP was purchased from Roche/UK.
    - Mouse anti-p62 was purchased from BD-Biosciences/UK.
    - Mouse anti-β-actin was purchased from Abcam/UK.
    - Mouse anti-ubiquitin was purchased from Life Science/ UK.
    - Rabbit anti-p62 was purchased from ENZO/UK.

- Rabbit anti-GST-tag was purchased from BETHYL/UK.
- Rabbit anti-vitronectin was purchased from Abcam/UK.
- Rabbit anti-LC3B was purchased from Sigma-Aldrich/UK

- **Secondary antibodies:**
  - Swine anti-mouse immunoglobulins (Solid-Phase Absorbed) was purchased from DAKO/UK.
  - Swine anti-rabbit immunoglobulins (Solid-Phase Absorbed) was purchased from DAKO/UK.
  - Alexaflour488 anti-mouse was purchased from Invitrogen/UK.

- **List of software:**
  - **Reverse Complement:** is a website which converts a DNA sequence into its reverse, complement, or reverse-complement counterpart from The Sequence Manipulation Suite.
  - **Clustal Omega:** is a general purpose multiple sequence alignement programme for DNA from European bioinformatics institute (EBI).
  - **PRISM 7:** is a combination of basic biostatistical, curve fitting, and scientific graphing software from GraphPad.
  - **Huygens:** is an imaging software refers to different Fluorescence Microscope image **processing** packages from Scientific Volume Imaging made for image restoration, interactive analysis, and volume visualization.
  - **Fiji:** is an image processing package-a “batteries-included” distribution of ImageJ, bundling a lot of plugins which facilitate scientific image analysis.

D. Comparison MS results

Table 4. Summary different proteins identified in ancient petrous (SK101) and tooth samples (SK29; SK32).

Protein	Petrous	Tooth
Alpha-2-HS-glycoprotein OS	■	■
Biglycan OS		■
Collagen alpha-1(I) chain OS	■	■
Collagen alpha-1(II) chain OS	■	■
Collagen alpha-1(III) chain OS		■
Collagen alpha-1 (V) chain OS	■	
Collagen alpha-1(X) chain OS		
Collagen alpha-1(XXII) chain OS	■	
Collagen alpha-2(I) chain OS	■	■
Collagen alpha-2(V) chain OS		■
Collagen alpha-2(XI) chain OS	■	■
C-type lectin domain family 11 member A OS	■	
Dentin matrix acidic phosphoprotein 1 OS	■	
Extracellular superoxide dismutase [Cu-Zn] OS		■
Hornerin OS		■
Insulin-like growth factor-binding protein 5 OS	■	
Kininogen-1 OS	■	
Keratin, type I cytoskeletal 9 OS		■
Keratin, type I cytoskeletal 10 OS	■	■
Keratin, type I cytoskeletal 14 OS		■
Keratin, type II cytoskeletal 1 OS	■	■
Keratin, type II cytoskeletal 72 OS	■	
NudC domain-containing protein 2 OS	■	
Osteomodulin OS	■	■
Osteopontin OS	■	
Pigment epithelium-derived factor OS	■	
Periostin OS		■
Prothrombin OS	■	■
Sequestosome-1 OS	■	
Serum albumin OS	■	■
SPARC OS	■	■
Thrombospondin-1 OS	■	
Trypsin-1 OS	■	
Ubiquitin carboxyl-terminal hydrolase 5 OS	■	
Vitronectin OS	■	■